ALFRED WEGENER INSTITUT FÜR POLAR- UND MEERESFORSCHUNG

BREMERHAVEN

ACCLIMATION OF KELP PHOTOSYNTHESIS TO SEASONAL CHANGES IN THE UNDERWATER RADIATION REGIME OF AN ARCTIC FJORD SYSTEM

D I S S E R T A T I O N

ZUR ERLANGUNG DES DOKTORGRADES DER NATURWISSENSCHAFTEN

(Dr. rer. nat.)

FACHBEREICH BIOLOGIE / CHEMIE

UNIVERSITÄT BREMEN

VORGELEGT VON

LENA BREY

Mai 2009

Universität Bremen

Where there’s a will there’s a way.

Table of contents

Abbreviations

%	percent
<	less than
>	greater than
′	arc minute
°	degree
°C	degree Celsius
α	initial linear slope of a P-E curve (dimensionless)
A	antheraxanthin
ANOVA	analysis of variance
Aug.	August
β-Car	*β*-carotene
CAT	catalase
CDOM	chromophoric dissolved organic matter, yellow substance
CFC	chlorofluorocarbon
CH_4	methane
^{3}Chl*	excited triplet chlorophyll
Chl *a*	chlorophyll *a*
Chl *c*	chlorophyll c_1+c_2
cm	centimeter
CO_2	carbon dioxide
CPD	cyclobutane pyrimidine dimer
DNA	desoxyribonucleic acid
DU	Dobson unit
ε	molar extinction coefficient
E	east
E_k	light saturation point of photosynthesis (µmol photons m^{-2} s^{-1})
F_0	minimum chlorophyll fluorescence (dimensionless)
F_m	maximum chlorophyll fluorescence (dimensionless) in dark-acclimated state
F_m'	maximal chlorophyll fluorescence (dimensionless) under a given irradiance
F_t	steady state chlorophyll fluorescence (dimensionless)

F_v	variable chlorophyll fluorescence (dimensionless)
F_v/F_m	optimum quantum yield of photosystem II (dimensionless) in dark-acclimated state
ΔF	difference between F_m' and F_t
$\Delta F/F_m'$	effective quantum yield of PSII (dimensionless) in light-acclimated state
Fig.	figure
Fuc	fucoxanthin
FW	fresh weight (g)
g	gram
h	hour
H_2O_2	hydrogen peroxide
HPLC	high-performance liquid chromatography or high pressure liquid chromatography
H_{sat}	daily period of light-saturation photosynthesis (h)
IR	infrared
K_d	vertical attenuation coefficients of downward irradiance (m^{-1})
kJ	kilojoule
km	kilometre
λ	wavelength (nm)
LHC	light-harvesting pigment-protein complex
LHCF	fucoxanthin-Chl *a*/*c* light-harvesting protein complex
LICF	light-independent carbon fixation
µmol	micromole
m	meter
MAA	mycosporine-like amino acid
min	minute
mL	milliliter
mol	mole
mW	milliwatt
N	north
n	number of independent replicates or measurements
nm	nanometer
nmol	nanomole

NPQ	non-photochemical quenching
$^1O_2$*	singlet oxygen
O_2^-	superoxide anion
O_3	ozone
ODS	ozone depleting substances
PAM	pulse amplitude modulated
PAR	photosynthetically active radiation (µmol photons m^{-2} s^{-1}), λ = 400 - 700 nm
P-E curve	photosynthesis *versus* irradiance curve
PEPCK	phosphoenolpyruvate carboxykinase
PPFD	photosynthetically photon flux density (µmol photons m^{-2} s^{-1})
P_{max}	maximum rate of photosynthesis at light saturation
PQ	photochemical quenching
PS I	photosystem I
PS II	photosystem II
PSU	photosynthetic unit
RC	reaction center
rel.	relative
$rETR_{max}$	maximum relative photosynthetic electron transport rate at light saturation (dimensionless)
ROS	reactive oxygen species
RNA	ribonucleic acid
RUBISCO	ribulose-1,5-bisphosphate-carboxylase/oxygenase
s	second
SD	standard deviation
Sept.	September
SOD	superoxide dismutase
UVAR	ultraviolet A radiation (W m^{-2}), λ = 320 - 400 nm
UVBR	ultraviolet B radiation (W m^{-2}), λ = 280 - 320 nm
UVCR	ultraviolet C radiation (W m^{-2}), λ = 190 - 280 nm
UVR	ultraviolet radiation (W m^{-2}), λ = 280 - 400 nm
V	violaxanthin
VAZ	pool size of violaxanthin, antheraxanthin and zeaxanthin
vol %	volume percent

vs.	*versus*
W	watt
Z	zeaxanthin

Summary

Arctic marine macroalgae are subjected to drastic seasonal changes in environmental conditions, especially in the radiation climate. Perennial kelps (Laminariales, Phaeophyceae) have to endure at least six months of complete darkness and low light conditions during the polar night and periods of sea ice cover. On the other hand, they also have to cope with sudden exposure to high irradiances after the break-up of sea ice in spring. In order to elucidate the physiological bases of macroalgal performance in such extreme environments, the present long-term study (1) monitored the air and water temperatures as well as the irradiances of photosynthetically active radiation (PAR), ultraviolet A radiation (UVAR) and ultraviolet B radiation (UVBR) at the Earth's surface and in the coastal water of Kongsfjorden (Spitsbergen, Norway), covering the variations over seasons and water depths, and (2) evaluated the acclimation status, potential and strategy of four dominant kelp species with respect to the strongly fluctuating radiation regime characteristic for Arctic fjords.

Photosynthetic performance, photosynthetic pigment content and composition as well as the relative content of compounds screening ultraviolet radiation (UVR) were studied in young sporophytes of *Alaria esculenta*, *Laminaria digitata*, *Saccharina latissima* and *Laminaria solidungula*. The algae were collected between 0.5 and 18 m water depth in the field, including the upper and lower distribution limit of perennial Laminariales in Kongsfjorden.

Throughout the study period from May to September 2004, irradiances of PAR and UVR were highest just below the water surface and decreased with increasing water depth. The radiation conditions in the water column were highly variable and strongly depended on seasonal sea ice and snow cover and on the concentration of suspended sediments. Thus, the underwater radiation regime was characterized by extremely low radiation conditions under the sea ice in May, by high underwater irradiances in June, when clear water conditions coincided with high solar radiation, as well as by reduced light availability due to high water turbidity in July and lowered solar altitude angle in August and September.

In all species, photosynthetic characteristics changed significantly in relation to the prevailing radiation conditions at the natural growth sites. In May, low maximum relative electron transport rates ($rETR_{max}$) and light saturation points of photosynthesis (E_k) were accompanied by high photosynthetic efficiencies (α) in all species studied. The algae

acclimated to the strongly increased underwater irradiances in June by an increase in $rETR_{max}$ and E_k concomitantly with a decrease in α. These changes allowed efficient photosynthesis during high light conditions and the increased potential for photochemistry (higher $rETR_{max}$) reduced the susceptibility to photoinhibition and photodamage by excessively absorbed photon energy. With reduced light transmittance through the water column in July and with lowered solar radiation in August and September, the inverse pattern of these photosynthetic parameters was observed. Hence, acclimation to lower irradiances was achieved by an increase in light capture capacity (higher α) and by a decrease of the light saturation point of photosynthesis (lower E_k), thereby remaining photosynthetically productive.

The changes in the photosynthetic characteristics were related to adjustments of the photosynthetic apparatus. The alterations in content and composition of photochemically active and accessory pigments indicate that seaweeds are able to acclimate to higher ambient radiation by decreasing their light-harvesting complexes (LHCs) and, possibly also, by reducing the number of their photosynthetic reaction centers (RCs) in order to avoid absorption of too many photons, which potentially causes damage to the photosynthetic apparatus. In addition, all species developed photoprotective mechanisms when they were exposed to high solar radiation in the field. By an increase in the pool size of the xanthophyll cycle pigments (violaxanthin, antheraxanthin, zeaxanthin) and in the *β*-carotene content in relation to chlorophyll *a*, the algae increased their antioxidative activity and their potential for harmless dissipation of excessively absorbed light energy as heat. In addition, photoprotection against harmful UVB radiation was possibly achieved by the accumulation of UVR-screening substances. In contrast, with reduced light availability from July onwards, the opposite pigment pattern was found, indicating an increase in the light-harvesting antennae, which enables the seaweeds to make best use of low photon flux densities and thereby preventing light limitation of photosynthesis.

Seasonal changes and species-specific differences in the physiological acclimation status of the macroalgae studied were reflected in the susceptibility of photosynthetic efficiency (F_v/F_m) to artificial PAR- and UVR-exposure. In May, *A. esculenta*, *L. digitata* and *S. latissima* were exposed to dim light conditions for more than six months. Under these circumstances, the observed PAR- and UVR-tolerance reflected the genetically fixed ability for dynamic photoinhibition of these species, which was subsequently modified during the study period by acclimation processes to the strongly changing underwater radiation climate. During high radiation conditions in the field all species were able to protect their

photosynthetic apparatus efficiently against high irradiances of PAR and UVR by dynamic photoinhibition. However, the seasonal variations in the PAR- and UVR-tolerance were more pronounced in species from deeper waters compared to shallow-water species and the detrimental effects of PAR and UVR on F_v/F_m were related to the algal zonation pattern at the coastline. Hence, *L. digitata* and especially *A. esculenta* from the upper sublittoral showed highest acclimation potential over a wide range of light intensities and possessed highest capability for photoprotection. In fact, on a seasonal average, the relative content of UVR-absorbing compounds and the proportion of photoprotective *β*-carotene and xanthophyll cycle pigments were inversely proportional to the depth distribution of the species investigated. Thus, *S. latissima* from the mid sublittoral and, in particular, *L. solidungula* from the lower sublittoral exhibited a higher susceptibility to artificial PAR and UVR due to a lower ability to down-regulate photosynthetic activity by protective mechanisms. In September, the harmful effects of high-energy UVB radiation exceeded the acclimation capacities of these species and, thus, photodamage occurred. Low UVR-tolerance, high photosynthetic efficiency, as well as saturation of photosynthesis at low photosynthetically photon flux density (PPFD) were indicative for the strong shade-adaptation of the Arctic endemic *L. solidungula*, which was, therefore, best suited for a life in a habitat characterized by low light availability.

The findings of the present study demonstrate the close relationship between photosynthetic characteristics and pigmentation of the species studied and the seasonal fluctuations in the environmental radiation conditions. The results show to what extent algae are able to protect their photosynthetic apparatus against high irradiances of PAR, UVAR and UVBR and reveal the underlying physiological acclimation strategies, implying that seasonality and life strategy of perennial seaweeds are based on the interaction of genetically fixed adaptation, physiological acclimation and endogenous rhythms. The obtained knowledge of the seasonal acclimation potential of Arctic kelps may serve to evaluate possible consequences of climatic changes for marine Arctic coastal ecosystems in the future.

Zusammenfassung

„Akklimatisierung der Photosynthese von Brauntangen an saisonale Veränderungen der Unterwasser-Strahlungsbedingungen in einem arktischen Fjordsystem“

Marine Makroalgen der arktischen Regionen sind extremen jahreszeitlichen Schwankungen in ihren Umweltbedingungen ausgesetzt, insbesondere in den Strahlungsbedingungen. Während der Polarnacht und unter Meereisbedeckung überdauern perennierende Brauntange (Laminariales, Phaeophyceae) mehr als sechs Monate in völliger Dunkelheit und Schwachlicht, während sie im Frühjahr nach Eisaufbruch stark erhöhten Bestrahlungsstärken ausgesetzt sind.

Das Ziel der vorliegenden Arbeit war es, die Grundlagen der physiologischen Anpassungsprozesse zu erforschen, die den Algen die Fähigkeit verleihen, diesen extremen Lebensraum zu besiedeln. Zu diesem Zweck wurden in einer Langzeitstudie (1) die saisonalen Veränderungen von Luft-, Wassertemperatur und Sonneneinstrahlung dokumentiert. Die einfallende photosynthetisch aktive Strahlung (PAR), Ultraviolett-A-Strahlung (UVA-Strahlung) und Ultraviolett-B-Strahlung (UVB-Strahlung) wurden sowohl auf der Erdoberfläche als auch in unterschiedlichen Wassertiefen im Küstengewässer des Kongsfjords (Spitzbergen, Norwegen) gemessen. (2) Parallel dazu wurden der physiologische Anpassungszustand, das Anpassungspotential sowie die Anpassungsstrategie von vier vorherrschenden Brauntangen im Hinblick auf die starken Schwankungen in den Strahlungsbedingungen charakterisiert.

Die Photosyntheseaktivität, der Gehalt und die Zusammensetzung photosynthetischer Pigmente sowie der relative Gehalt an Substanzen, die ultraviolette Strahlung (UV-Strahlung) absorbieren, wurden in jungen Sporophyten von *Alaria esculenta*, *Laminaria digitata*, *Saccharina latissima* and *Laminaria solidungula* untersucht. Die verschiedenen Arten wurden zwischen 0,5 und 18 m Wassertiefe im Freiland gesammelt, der oberen und unteren Vorkommensgrenze perennierender Laminariales im Kongsfjord entsprechend.

Während des gesamten Untersuchungszeitraumes von Mai bis September 2004 war die Bestrahlungsstärke direkt unter der Wasseroberfläche am höchsten und nahm mit zunehmender Wassertiefe ab. Das Strahlungsklima in der Wassersäule war sehr variabel und

wurde stark durch das saisonabhängige Vorkommen des Meereises bestimmt sowie vom Sedimentgehalt des Wassers. Unter Meereis- und Schneebedeckung im Mai herrschten Schwachlichtbedingungen, während sich der Juni durch hohe Unterwasser-Strahlungsintensitäten auszeichnete, da die Klarwasserphase mit hoher Sonneneinstrahlung zusammenfiel. Im Juli verringerte sich die Lichtverfügbarkeit aufgrund der starken Wassertrübung und im August und September durch einen niedrigeren Sonnenstand.

Alle untersuchten Arten zeigten signifikante Veränderungen in ihren Photosyntheseparametern in Abhängigkeit von den vorherrschenden Lichtbedingungen an ihrem natürlichen Standort. Im Mai zeichneten sich alle Arten durch eine geringe maximale relative Elektronentransportrate ($rETR_{max}$) und einen niedrigen Lichtsättigungspunkt der Photosynthese (E_k) aus sowie durch eine hohe Photosyntheseeffizienz (α). Generell passten sich alle Arten im Juni durch Erhöhung von $rETR_{max}$ und E_k bei gleichzeitiger Verringerung von α an die erhöhten Unterwasser-Strahlungsintensitäten an. Diese physiologischen Veränderungen ermöglichten den Algen eine hohe Photosyntheseleistung in Zeiten hoher Lichtverfügbarkeit. Durch die erhöhte Photosynthesekapazität (höhere $rETR_{max}$-Werte) verringerte sich gleichzeitig die Anfälligkeit für Photoinhibition und Lichtschädigung durch überschüssig absorbierte Lichtenergie. Mit stark reduzierter Lichttransmission des Wasserkörpers im Juli und mit geringerer Sonneneinstrahlung im August und September kam es zur Umkehrung des Photosynthesemusters. Eine Anpassung an die verringerten Lichtintensitäten wurde demnach durch eine Erhöhung der Lichtsammelkapazität (höhere α-Werte) und einer Verringerung des Lichtsättigungspunktes (niedrigere E_k-Werte) erlangt, wodurch die Algen auch im Schwachlicht effizient Photosynthese betreiben konnten.

Die Veränderungen in den photosynthetischen Eigenschaften standen in engem Zusammenhang mit Umstrukturierungen innerhalb des Photosyntheseapparates. Die Veränderungen in der Menge und Zusammensetzung der photochemisch aktiven und akzessorischen Pigmente zeigten, dass sich die Brauntange an höhere Bestrahlungsstärken anpassten, indem sie ihre Lichtsammelkomplexe (LHCs) verkleinerten und möglicherweise auch die Anzahl ihrer photosynthetischen Reaktionszentren (RCs) verringerten, um die Absorption überschüssiger Lichtenergie zu verhindern, welche potentiell zur Schädigung des Photosyntheseapparates führt. Zusätzlich entwickelten alle untersuchten Arten Lichtschutzmechanismen, wenn sie im Freiland hohen Strahlungsintensitäten ausgesetzt waren. Durch einen höheren Gehalt an Xanthophyll-Zyklus-Pigmenten (Violaxanthin, Antheraxanthin, Zeaxanthin) und *β*-Carotin im Verhältnis zu Chlorophyll *a* steigerten die

Algen ihre antioxidative Aktivität und ihre Fähigkeit, überschüssige Lichtenergie in Form von Wärme abzustrahlen. Zusätzlich schützten sich die Algen vor der schädigenden Wirkung energiereicher UVB-Strahlung durch die Anreicherung UV-absorbierender Substanzen. Mit Beginn verringerter Lichtverfügbarkeit im Juli zeigte sich ein entgegengesetztes Pigmentmuster, indikativ für eine Vergrößerung der Lichtsammelantennen, die den Algen ermöglicht, das geringe einfallende Licht optimal zu nutzen und somit eine Lichtlimitierung der Photosynthese zu verhindern.

Die saisonalen Veränderungen und die artspezifischen Unterschiede im physiologischen Anpassungszustand der Algen spiegelten sich in der Empfindlichkeit der Photosyntheseeffizienz (F_v/F_m) gegenüber künstlicher PAR- und UV-Bestrahlung wider. Im Mai waren *A. esculenta*, *L. digitata* und *S. latissima* mehr als sechs Monate lang Schwachlichtbedinungungen ausgesetzt. Aufgrund dieser Voraussetzung reflektierte die beobachtete PAR- und UV-Toleranz die genetisch fixierte Fähigkeit dieser Arten zur dynamischen Photoinhibition, die im Verlaufe der Studie durch Anpassungsprozesse an die stark schwankenden Unterwasserstrahlungsbedingungen modifiziert wurde. In der Zeit hoher Strahlungsintensitäten im Freiland waren alle Arten in der Lage, ihren Photosyntheseapparat effizient vor hoher PAR- und UV-Strahlung durch dynamische Photoinhibition zu schützen. Die saisonalen Schwankungen in der PAR- und UV-Toleranz waren, im Vergleich zu den Flachwasser-Arten, stärker ausgeprägt in Algenarten, die aus größeren Wassertiefen stammten. Die negative Auswirkung der PAR- and UV-Strahlung auf die Photosynthese korrelierte mit der Tiefenzonierung der Algen an der Küstenlinie. Demnach zeigten *L. digitata* und insbesondere *A. esculenta* aus dem oberen Sublitoral das höchste Anpassungsvermögen an eine weite Spanne von Lichtintensitäten und eine besondere Fähigkeit, sich vor Starklicht zu schützen. Tatsächlich waren im saisonalen Durchschnitt der relative Gehalt an UV-absorbierenden Substanzen und der Anteil an *β*-Carotin und Xanthophyll-Zyklus-Pigmenten umgekehrt proportional zur Tiefenverteilung der untersuchten Arten in der Wassersäule. So zeigten *S. latissima* aus dem mittleren Sublitoral und insbesondere *L. solidungula* aus dem unteren Sublitoral eine höhere PAR- und UV-Empfindlichkeit aufgrund einer geringeren Fähigkeit zur Herunterregelung ihrer Photosyntheseaktivität durch Schutzmechanismen. Im September überstieg die schädigende Wirkung der energiereichen UVB-Strahlung die Anpassungskapazität dieser Arten und es kam zur Lichtschädigung. Geringe UV-Toleranz, hohe Photosyntheseeffizienz und Lichtsättigung der Photosynthese bei geringer Photonenflussdichte (PPFD) sind indikativ für

die ausgeprägte Schwachlichtadaptation der arktisch endemischen *L. solidungula*, die daher am besten an einen Lebensraum, der sich durch geringe Lichtverfügbarkeit auszeichnet, angepasst ist.

Die Resultate der vorliegenden Studie demonstrieren den engen Zusammenhang von Photosyntheseparametern und Pigmentierung der untersuchten Arten und den saisonalen Schwankungen im Strahlungsklima. Die Ergebnisse zeigen, in welchem Umfang die Algen in der Lage sind, ihren Photosyntheseapparat gegenüber hoher Weißlicht-, UVA- und UVB-Strahlung zu schützen und zeigen die zugrundeliegenden physiologischen Akklimatisierungsstrategien. Daraus wird ersichtlich, dass Saisonalität und Lebensstrategie dieser perennierenden Makroalgen auf Interaktion von genetisch fixierter Adaptation, physiologischer Anpassung und endogener Rhythmik basieren. Die gewonnenen Erkenntnisse über das saisonale Anpassungspotential arktischer Brauntange können dazu dienen, mögliche Konsequenzen des Klimawandels für marine Küstenökosysteme abzuschätzen.

1. Introduction

1.1. Kelps – ecological role and seasonality

Kelps are perennial marine brown macroalgae, also referred to as seaweeds, of the order Laminariales (Phaeophyceae, Heterokontophyta), forming expanded submarine forests in the sublittoral rocky zones of coastal Arctic and temperate waters (Steneck et al. 2002). These forests provide shelter, habitats, breeding areas, and substrates for an uncountable number of associated auto- and heterotrophic organisms (Kain 1979, Steneck et al. 2002, Bartsch et al. 2008). Additionally, the complex structure of kelp beds significantly influences the coastal oceanographic patterns by wave damping and impedes shoreline erosion (Jackson and Winant 1983). In polar regions, macroalgae are an essential source of dissolved and particulate detritus, with the advantage of providing a year-around carbon source (Amsler et al. 1995). The sporophytic tissue and the seasonally released energy-rich spores of Laminariales supply food for various filter feeders and zooplankton, meso- and macrograzers including amphipods, gastropods, mollusks and echinoderms, which are, in turn, consumed by various predators such as crustaceans, fishes, sea otters, and sea birds (Kain 1979, Steneck et al. 2002, Schiel and Foster 2006, Bartsch et al. 2008). Macroalgal photosynthesis accounts for approximately 5 % of the global primary production and therefore acting as an important carbon sink (Smith 1981).

Laminariales show a marked seasonality of their development. Growth, reproduction and their photosynthetic characteristics strongly depend on environmental factors. For instance, *Laminaria* species in the North Atlantic show a period of rapid growth from January to June and one of slow growth from July to September as summarized by Kain (1979). The seasonal growth dynamics of kelps, for example, are controlled by exogenous factors such as light (i.e. irradiance, spectral composition, photoperiod), temperature, and nutrient availability, and by endogenous factors such as reproductive processes and the use of storage materials, and their interactions (Makarov et al. 1999). Furthermore, in the Laminariales, circannual and circadian endogenous rhythms have been found. Thus, the annual growth patterns of several species of Laminariales are controlled by an endogenous circannual clock synchronized by annual daylength cycles (Lüning 1991, Lüning and Kadel 1993, tom Dieck 1991, Schaeffelke and Lüning 1994). Additionally, growth, mitosis, photosynthetic activity,

and egg release of female gametophytes are under circadian control in several members of the order of the Laminariales, which is distinct from photoperiodic responses such as the induction of new blades and sorus formation as reviewed by Bartsch et al. (2008).

The first data on seasonal changes in the sensitivity to UVR-exposure and in the chlorophyll *a* and total carotenoid content have been previously reported for various Arctic brown, red and green macroalgae, including *S. latissima*, by Aguilera et al. (2002) and Bischof et al. (2002). In addition, the same studies showed a stimulation of photoprotective mechanism, i.e. antioxidative enzyme activities and accumulation of UVR-absorbing mycosporine like amino acids (MAAs), in response to seasonal changes of environmental conditions in different Arctic green and red macroalgal species.

1.2. Light variability in Arctic ecosystems

Subtidal areas of Arctic and cold temperate regions are characterized by pronounced seasonal variations in daylength, light quality and quantity, nutrient concentrations and water temperature (Kain 1979, Lüning 1990). Light is the most rapidly varying environmental factor and of the various abiotic factors changing with the season, only light is clearly related to the geographic latitude and, thus, appears to be the most important factor affecting the seasonality of seaweeds (Kain 1989). Perennial algae in the Arctic have to sustain at least six months of complete darkness and low light conditions due to the polar night and great attenuation of irradiance by sea ice and snow cover (Chapman and Lindley 1980, Gerland et al. 1999). With the sun's return in early spring, the solar elevation increases rapidly. After two months of prevailing twilight conditions, the polar day begins, lasting for four months. From then onwards, solar elevation rapidly decreases again (Svendsen et al. 2002). Thus, at high latitudes, the elevation of the sun is highly variable and, in addition, generally low, e.g. the maximum solar elevation at Kongsfjorden is 34.5° (Sakshaug and Slagstad 1991). Since the incoming light that penetrates the water surface decreases with the solar angle, the underwater radiation conditions are strongly affected by the solar shifts (Kirk 1994). The availability of light is the basic requirement for primary production by photoautotrophic organisms. Hence, at higher latitudes the productivity of the entire ecosystem is highly

susceptible to environmental conditions during the brief period of conditions suitable for primary production.

Of the incident solar radiation, the "visible light" (photosynthetically active radiation, PAR, λ = 400 - 700 nm) is used for photosynthesis. When the solar elevation is higher than 30°, PAR accounts for approximately 45 % of the energy in solar radiation reaching the Earth's surface (Kirk 1994). Ultraviolet radiation (UVR, λ = 280 - 400 nm), and infrared (IR, λ = 700 - 3000 nm) constitute the remaining part of the impinging radiation. According to the Commission Internationale de l'Éclairage (CIE), UVR is defined as UVA radiation (λ = 315 - 400 nm), UVB radiation (λ = 280 - 315 nm), and UVC radiation (λ = 190 - 280 nm). Many photobiologists, however, define UVBR for practical reasons as the wavelength range from 280 to 320 nm owing to the characteristics of the radiation filtering material available (Franklin et al. 2003). UVCR is not a part of the solar spectrum on the Earth's surface, as it is completely absorbed by the stratospheric ozone layer, which also partly absorbs UVBR, while almost not affecting UVAR. The ozone layer comprises the greater part of the stratosphere between altitudes of 10 and 50 km. The highest concentration of ozone is reached between 15 and 30 km above the Earth's surface (Rowland 2006).

1.3. Light-harvesting systems in algae

In photosynthetic eukaryotic cells, the photosynthetic apparatus is organized in the chloroplasts, which contain lipoprotein membranes called thylakoids. The light reactions of photosynthesis and the subsequent transport of protons and electrons through the photosynthetic machinery, resulting in chemical bond energy and reductants, are reactions associated with, or occurring in, the thylakoid membranes (Anderson and Andersson 1988). The light-harvesting pigment-protein complexes (LHCs) are also embedded in the thylakoid membrane. In contrast, the fixation and subsequent biochemical reduction of carbon dioxide (CO_2) to organic carbon compounds occur in the stroma. The accessory LHCs are a diverse group of proteins that bind photochemically inactive pigments, which deliver excitation energy to the photosynthetic reaction centers (RCs) where the excitation energy of light is converted to photochemical energy. In oxygenic photosynthesis two different RCs (RC I and RC II) with significantly different functions and properties act together (Falkowski and

Raven 2007). In contrast to higher plants, the LHCs of algae, associated with PS I or II, are identical with respect to pigmentation and peptide composition (Häder 1999, De Martino et al. 2000). In brown algae the LHCs are highly loaded with xanthophylls and chlorophyll *c* (Chl *c*) and a fucoxanthin-Chl *a*/*c* light-harvesting protein complex (LHCF) is found in brown algae and diatoms (De Martino et al. 2000, Trissl 2003). In the LHCFs of brown algae, chlorophyll *a*, chlorophyll *c*, fucoxanthin, violaxanthin, and *β*-carotene are non-covalently bound to specific proteins (Passaquet et al. 1991, De Martino et al. 2000). These complexes are not directly associated with the reaction center complexes and thus are called peripheral antennae. The excitation energy from the LHCFs is absorbed by a core antenna of PS I or PS II and transferred directly to the reaction centers. The reaction center of PS II contains chlorophyll *a* (Chl *a*) and *β*-carotene (*β*-Car), the core antenna of PS II additionally chlorophyll *c* (Chl *c*) fucoxanthin (Fuc) and violaxanthin (V) (Douady et al. 1993, Alfonso et al. 1994, Falkowski and Raven 2007). The PS I core complex comprises Chl *a* and *β*-Car (Trissl 2003). Thus, Chl *a* und *β*-Car are found in RCs, while Chl *c* and xanthophylls are incorporated in the antennae only (Douady et al. 1993). The concept of the photosynthetic unit (PSU) has much changed during the last decades as many structural details of the RCs, LHCs and their assembly became known. Currently, the term PSU is defined as a structural entity composed of only one type of RC core complex (RC I or RC II) together with its physically associated LHCs (Trissl 2003). However, also other conventions exist (Falkowski et al. 1981).

The photosynthetic apparatus of higher plants, macro- and microalgae is remarkably adaptable to both sudden stress conditions and to long-term changes in light intensity, in order to optimize photosynthesis and minimize damage to the photosystems. By evolutionary adaptation and physiological acclimation processes plants take two approaches to adjust to a changed environment and to counteract seasonal changes in ambient light conditions.

1.4. Inhibition of photosynthesis

Despite of being the energy source for photosynthesis, light can also be harmful to organisms. Excess light can photoinhibit photosynthesis and may cause photooxidative destruction of the photosynthetic apparatus (Powles 1984, Demmig-Adams and Adams III 1992, Osmond 1994). In the field, high irradiances of PAR are generally accompanied by high irradiances of UVR. Although the measurable effects of both wavebands, such as reduced maximum photosynthetic rate and efficiency, are similar, the mechanisms of PAR- and UVR-induced inhibition of photosynthesis are markedly different (Neale et al. 1993).

1.4.1. Photoinhibition induced by PAR

Exposure to high irradiances of PAR may result in an absorption of excitation energy exceeding the requirements of the photosynthetic carbon metabolism (Calvin cycle and photorespiratory C_2 pathway) and consequently resulting in damage of the photosynthetic apparatus (Long et al. 1994, Franklin et al. 2003). Under these conditions, the formation of excited triplet chlorophyll (^{3}Chl*) is facilitated which can interact with ground-state triplet oxygen to produce singlet oxygen ($^1O_2$*) and superoxide radicals (O_2^-) are generated via the Mehler reaction (Foyer et al. 1994). These reactive oxygen species (ROS), including oxygen ions, free radicals, and peroxides, can oxidize pigments, lipids, and proteins, as well as causing DNA and RNA damages (Wise and Naylor 1987, Foyer et al. 1994). The D1 protein in the reaction center of PS II appears to be particularly susceptible to oxidation (Andersson et al. 1992, Franklin et al. 2003). The D1 protein in the thylakoid membrane underlies a permanent turnover that replaces damaged D1 protein by *de novo* synthesis. When the rate of damage exceeds the capacity of the repair cycle of PS II, the function of the reaction center is impaired and photodamage, i.e. chronic photoinhibition, occurs (Aro et al. 1993). However, non-functional D1-containing PS II reaction centers appear to accumulate rather than being rapidly repaired, and to act themselves as efficient quenchers of excitation energy, thereby potentially preventing fully irreversible photooxidative damage to the thylakoid membrane (Krause and Weis 1991, Aro et al. 1993).

1.4.2. Photoinhibition induced by UVR

In contrast to PAR, UVR cannot be regarded as being excessive in a proper sense. UVR exhibits adverse effects on photosynthesis in a more direct way, due to its absorption by biomolecules involved in photosynthetic processes, but also indirectly by the generation of ROS and DNA damage. Within the PAR-region, the action spectrum of photoinhibition runs in parallel to the action spectrum of photosynthesis, and is therefore related to photosynthetic pigment absorption (Jones and Kok 1966). In contrast, inhibition induced by UVBR is related to its absorption by DNA, resulting in the formation of cyclobutane pyrimidine dimers (CPDs) inhibiting genome replication and expression, and by proteins, leading to a loss of specific enzymatic biological functions (Jones and Kok 1966, Strid et al. 1994, Rijstenbil et al. 2000, van de Poll et al. 2001).

Photodestruction of pigments is caused by both high irradiances of PAR and UVR, resulting in a decline in photosynthetic activity (Wood 1987, Strid et al. 1990, Altamirano et al. 2000). Like photoinactivation by PAR, the PS II reaction center is implicated as a primary target of UVBR damage, since UVBR leads to a loss of the D1 and D2 proteins and Cyt b_{559}, as well as to an impairment of the electron transferring plastochinons and the oxygen evolving complex (Iwanzik et al. 1983, Bornman 1989, Renger et al. 1989, Jansen et al. 1996, Mackerness et al. 1996, Babu et al. 1999, Vass et al. 1999). In addition, UVBR might affect the LHC by its functional disconnection from the photosystem, resulting in an impairment of energy transfer to the reaction center (Renger et al. 1989, Lao and Glazer 1996). Besides direct damage to PS II components, destruction of the integrity of the thylakoid membrane and burst of the chloroplast double membrane may result in a reduced photosynthetic activity (Iwanzik et al. 1983, Strid et al. 1994, Malanga and Puntarulo 1995, Lütz et al. 1997). Inhibition of photosynthesis has been also shown to arise from the high susceptibility of carbon assimilation to damage by UVBR due to a reduction in the content and activity of the CO_2-fixating enzyme RUBISCO (Strid et al. 1990, Jordan et al. 1992, Nogués and Baker 1995, Bischof et al. 2000).

1.5. Photoprotective and repair mechanisms

Plants have evolved different mechanisms of avoidance, genetically fixed adaptation, and physiological acclimation to protect themselves against the damaging effects of excessive PAR and harmful UVR. The protection strategies comprise, e.g., non-photochemical quenching, screening, and repair. Carotenoids, e.g. β-carotene and zeaxanthin, do not only act as accessory light-harvesting pigments, they also perform an essential photoprotective role by quenching triplet state chlorophyll molecules and scavenging singlet oxygen and other toxic ROS formed within the chloroplast (Young 1991). However, overexcitation of PS II might be prevented by disconnection of PS II from the LHC decreasing the antenna size of PS II (Sundby and Andersson 1985, Cleland et al. 1986, Demmig-Adams et al. 1989). By increasing the thermal dissipation of harmful excess excitation energy within the antennae seaweeds can remove excessively absorbed energy before ROS formation occurs. This photoprotective thermal energy dissipation arises from the xanthophyll cycle, which is located in the thylakoid membranes in the peripheral antennae of all higher plants, ferns, mosses, and several algal groups. In a light-dependent two-step de-epoxidation, violaxanthin is converted into zeaxanthin via the intermediate antheraxanthin (Fig. 1, Demmig-Adams 1990, Frank et al. 1994). This reaction is catalyzed by the violaxanthin de-epoxidase, whereas a second enzyme, the zeaxanthin epoxidase, reconverts zeaxanthin to antheraxanthin and violaxanthin (Demmig-Adams 1990, Demmig-Adams and Adams III 1992). The regulated process of non-photochemical xanthophyll cycle quenching restricts the energy transfer to PS II, thus down-regulates the PS II activity but also thereby reducing the potential for photodamage of PS II.

Seaweeds also counteract the toxicity of ROS by a highly efficient antioxidative defense system, composed of both non-enzymatic scavenging and quenching of ROS by antioxidants and of enzymatic degradation (Young 1991, Foyer et al. 1994, Aguilera et al. 2002a). However, compared to other algal taxa, antioxidant enzyme activities in brown algae are low (Aguilera et al. 2002a). While Phaeophyceae lack several screening substances, e.g., mycosporine-like amino acids (MAAs) which protect other algal taxa against harmful UVR, they exclusively possess phlorotannins, a class of phenolic compounds (Ragan and Glombitza 1986, Franklin et al. 2003). Phlorotannins have several possible functions in brown algae, including the protection of photosynthetic tissue against UVBR (Pavia et al. 1997, Targett

and Arnold 1998, Schoenwaelder and Wiencke 2000, Schoenwaelder 2002a, b, Clayton et al. 2005, Roleda et al. 2006a).

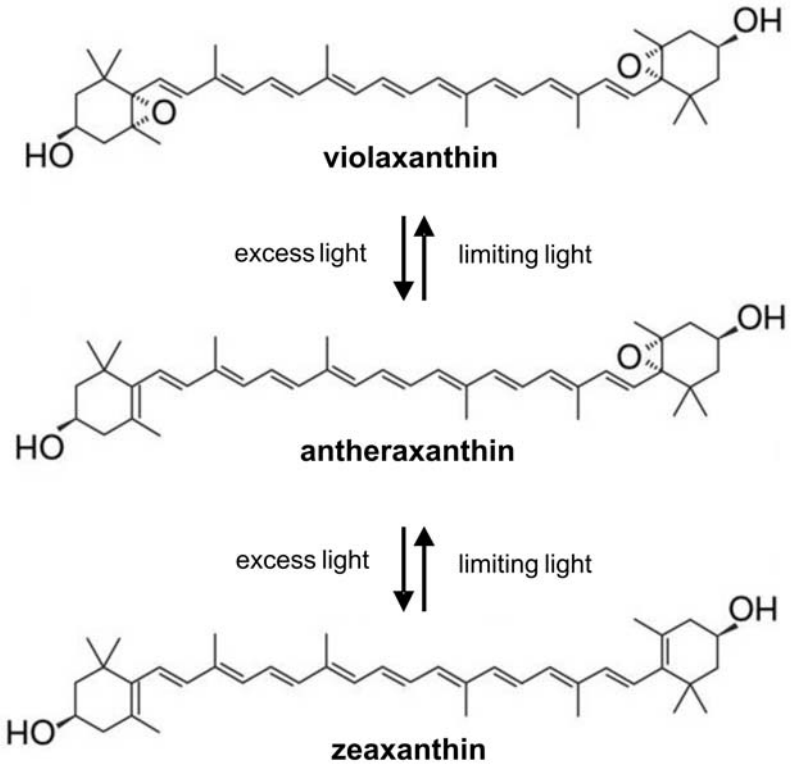

Fig. 1: Structural schema of the xanthophyll cycle, consisting of the di-expoxide violaxanthin, the mono-epoxide antheraxanthin, and the epoxide-free zeaxanthin. De-epoxidation is carried out by the enzyme violaxanthin de-epoxidase and epoxidation by the zeaxanthin epoxidase. Generally, de-epoxidation requires only a few minutes, while the epoxidation process occurs within hours, but can be dramatically slowed by additional environmental stress. Figure modified after Demmig-Adams (1990).

1.6. Recent and future changes in the Arctic ecosystem

Over the last 25 years an increasing rate of global warming has taken place, predominantly due to strongly increased atmospheric concentrations of the greenhouse gases carbon dioxide (CO_2) and methane (CH_4). The global average surface temperature increased by approximately 0.74 °C during the last century. Between 1979 and 1997 a warming of the near surface air temperature in the Arctic of up to 2 °C per decade has been observed (Rigor et al.

2000). The increase in the near surface air temperature was accompanied by a decrease in Arctic sea ice extent during the last decades (Parkinson et al. 1999, Vinnikov et al. 1999, Stroeve et al. 2005, 2007). The length of the frost-free season has increased in most mid- and high-latitude regions of both hemispheres (Solomon et al. 2007). Furthermore, the Arctic Ocean is influenced increasingly by water of the Atlantic origin which becomes increasingly warmer (Morison et al. 2000).

The spectral composition of the Arctic radiation regime has changed during the last decades towards a higher proportion of potentially detrimental UVB radiation (Hassol 2005). Besides others, stratospheric ozone (O_3) is an important factor determining the radiation regime (Arola et al. 2003). The ozone layer has always been undergoing seasonal changes, but during the last decades, severe depletion events have been observed repeatedly, commonly known as "ozone hole", leading to a specific increase in the UVB radiation reaching the Earth's surface. Large losses of stratospheric ozone were first observed in Antarctica and have been later also reported for numerous other regions (Farman et al. 1985, Madronich et al. 1995). A detailed description of changes in stratospheric ozone and UVR measured in Ny-Ålesund (Spitsbergen, Norway) has been given by Dahlback (2002). The destruction of the ozone molecules in the stratosphere is closely linked to elevated concentrations of industrially emitted ozone depleting substances (ODS) such as chlorofluorocarbons (CFCs) and halons (World Meteorological Organization 2007, Harris et al. 2008). The production of ODS was restricted substantially by the Montreal Protocol on Substances that Deplete the Ozone Layer in 1987 and its amendments (World Meteorological Organization 2007). However, there are still many countries that have not signed the convention until today and due to the stability of CFCs it is speculated that the stratospheric ozone depletion will further increase until 2020, dropping from 450 Dobson units (DU) to 130 DU, and may reach a plateau by then (Shindell et al. 1998). A decline in the stratospheric ozone concentration of 10 % results in an increase of irradiance at 297 nm to 50 % and at 303 nm to 25 %, respectively (Roy et al. 1990). High latitudes in early spring are the areas most susceptible to destruction events, since the chemical breakdown of stratospheric ozone requires low temperatures and UVR in addition to CFCs (World Meteorological Organization 2007). The yearly ozone depletion has been most severe in Antarctica, where colder and more stable stratospheric temperatures are found. However, stratospheric ozone depletion up to 60 % over the Kongsfjord area has been recorded (Müller et al. 1997, Rex et al. 1997, 2006, SCOUT-O3 2005). These ozone losses were greater than observed in Antarctica in 1985 and

were linked to extremely low stratospheric temperatures. However, more recent studies showed that in the northern mid-latitudes and in the Arctic the chlorine concentration of the stratosphere peaked already in the late 1990s and that the total ozone at northern mid-latitudes has increased for more than a decade. Interestingly, this trend change in total ozone was not attributed to the small decrease in ODS and better explained by changes in dynamical processes (Weatherhead and Andersen 2006, Harris et al. 2008). A cooling of the stratosphere is an expected result of increasing concentrations of greenhouse gases in the atmosphere (Shindell et al. 1998, Harris et al. 2008). A progressing global warming could thus accentuate such periods of major ozone losses. The current rise in tropospheric temperatures leads to a decrease of stratospheric temperature, and thereby increases the risk for ozone depletion in the Arctic (McKenzie et al. 2007). Coldest Arctic winters have become significantly colder, and hence are more conducive to ozone depletion by anthropogenic halogens (Rex et al. 2006). In addition, sulfate aerosols, which are released to the stratosphere by volcanic eruptions, might strongly enhance the chemical loss of polar ozone, especially in the Arctic, as observed after the eruption of Mount Pinatubo in 1991 (Tilmes et al. 2008).

Nevertheless, there is great uncertainty of modeling future ozone losses and relating those to climate changes (Baldwin et al. 2007, McKenzie et al. 2007, Schiermeier 2007, Harris et al. 2008).

1.7. Thesis outline

This long-term study was motivated by the work of Aguilera et al. (2002) and Bischof et al. (2002) and aimed to investigate the seasonal patterns of Arctic kelp photosynthesis, pigmentation, accumulation of sunscreen substances, and susceptibility of photosynthesis to PAR, UVAR and UVBR with respect to changes in environmental conditions, especially in the radiation climate, over season and water depth.

Most information on algal physiology has been so far obtained in laboratory short-term studies by the use of cultivated algal material. However, studying the seasonality of Arctic species principally depends on field studies, since the very complex variations in abiotic conditions cannot be mimicked in the laboratory by the variability of light only. Former field studies on algal seasonality have mainly focused on seasonal growth and

photosynthetic activity of sporophytes, whereas seasonal changes in pigmentation, particularly in the xanthophyll cycle pigments, were less investigated and often based on chlorophyll *a* measurements only.

In order to assess the acclimation potential and strategy of four dominant Arctic brown macroalgae (Laminariales, Phaeophyceae) in relation to the strong seasonal fluctuations in the radiation regime, photosynthetic pigment content and composition as well as various photosynthetic parameters were studied in detail, providing information on alterations of the photosynthetic apparatus. To investigate the stimulation of protective mechanisms, changes in the accumulation of xanthophyll cycle pigments (violaxanthin, antheraxanthin, and zeaxanthin) and UVR-screening compounds were studied and the potential for photoprotection was tested by different artificial radiation treatments.

To characterize macroalgal acclimation processes, the following research questions were considered:

- How do underwater irradiances of PAR, UVAR and UVBR in Kongsfjorden vary between seasons and water depths?
- How do seaweeds adjust their light-harvesting antennae to the ambient light fields at their natural growth site?
- To what extent do macroalgae alter their photosynthetic characteristics in relation to environmental radiation conditions?
- Are all species studied able to develop photoprotective mechanisms (i.e. accumulation of UVR-absorbing compounds and xanthophyll cycle pigments) when they are exposed to high solar radiation in the field?
- To what extend are they able to protect their photosynthetic apparatus against high irradiances of PAR, UVAR and UVBR by dynamic photoinhibition?
- Do species-specific differences exist in acclimation strategy and potential and how do they look like?

2. Material and methods

2.1. Study area, sampling sites and species studied

Kongsfjorden is a 20 km long fjord in the Arctic, located on the west coast of Svalbard at 79° N, 12° E (Fig. 2, Svendsen et al. 2002). It is influenced by Atlantic and Arctic water masses. The North Atlantic Current provides relatively warm and salty water to the West Spitsbergen Current, whereby Kongsfjorden becomes rather sub-Arctic (Svendsen et al. 2002). Kongsfjorden is a glacial fjord system displaying characteristics specific to Arctic fjords as well as features common to broad fjords. The latter relates to the water temperature and the freshwater supply, showing pronounced seasonal variations, to dominant wind directions, and to the corresponding impact on stratification and circulation, which varies profoundly during the year. Another common feature relates to the rotational dynamics that have an important impact on fjord dynamics in wide and stratified fjords such as Kongsfjorden. The specific Arctic features of the fjord are related to the way how freshwater is supplied to the fjord. The active glacier system provides freshwater throughout the year and has a significant impact on circulation and mixing processes (Svendsen et al. 2002).

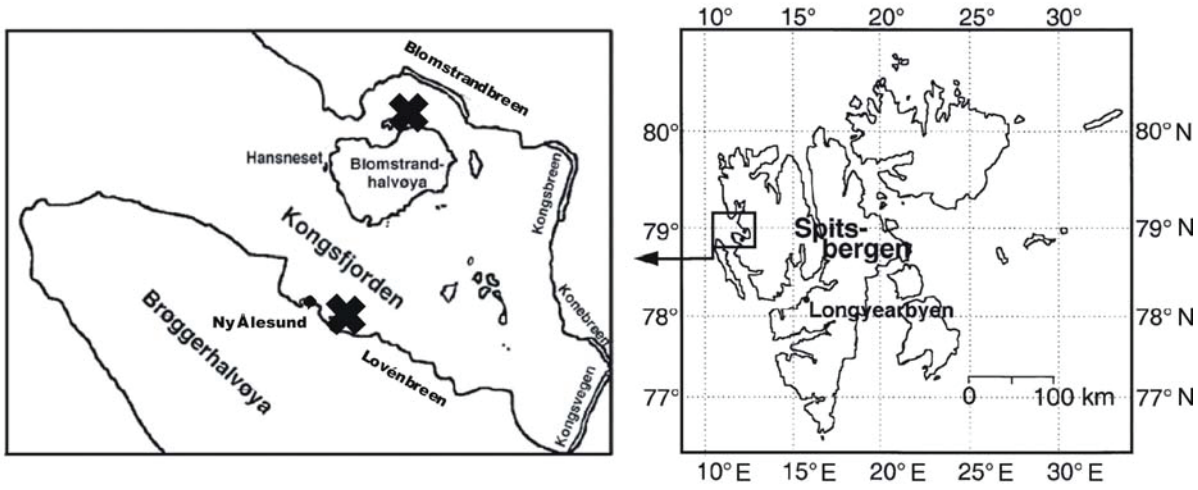

Fig. 2: Maps of Spitsbergen (Svalbard, Norway), black crosses indicate the locations of the sampling sites of seaweeds in Kongsfjorden. Figure modified after Hanelt et al. (2001).

Kongsfjorden is similar to other fjords along the western coast of Spitsbergen with regard to the Atlantic, glacial, and advection influences (Svendsen et al. 2002). The primary production rates and the benthic macrofauna of Kongsfjorden are also broadly representative for other fjords of West Spitsbergen (Eilertsen et al. 1989, Kendall and Aschan 1993). However, one unique attribute of Kongsfjorden is that it harbours both boreal and Arctic flora and fauna (Hop et al. 2002). Thus, the marine flora of Kongsfjorden has an intermediate position between that of East Greenland, with a higher number of Arctic species, and that of northern Norway, with a higher number of cold temperate species (Wiencke et al. 2004a).

The pelagic ecosystem of Kongsfjorden is thought to be mainly influenced by oceanographic conditions (Atlantic *vs.* Arctic), whereas the benthic ecosystem might be more affected by hydrography, glacial runoff and sedimentation. Since the influx of Atlantic waters and the melting of glaciers are closely linked to climate variability, Kongsfjorden is assumed to be a sensitive indicator of climate change phenomena. (For a detailed overview of the ecosystem Kongsfjorden see Hop et al. 2002, Svendsen et al. 2002).

The study sites were located in the inner part of the fjord (i.e. in the transitional zone between inner and middle zone as defined by Hop et al. 2002), which is of relatively shallow water and strongly influenced by glacial activity (< 100 m) (Fig. 2, Svendsen et al. 2002). Four marine perennial brown algal species were investigated. *Laminaria solidungula* inhabits only the inner part of Kongsfjorden, indicating its strong adaptation to Arctic conditions (Hop et al. 2002). This species is considered to be endemic to the Arctic even though there is a minor occurrence of it outside the Arctic region (e.g. on the coast of Newfoundland, but only in deep water). *Alaria esculenta* and *Saccharina latissima* (Lane et al. 2006, formerly *Laminaria saccharina*) are Arctic cold temperate amphioceanic species inhabiting the Arctic Ocean, the North Atlantic and the North Pacific. The northern distribution limit of *A. esculenta* is the Arctic Ocean while the southern distribution limits in the Atlantic are northern France (Europe) and New Hampshire (North America), and in the Pacific South Alaska (North America) and Vladivostok (North Asia) (Lüning 1990). *S. latissima* penetrates even further into the Arctic Ocean, reaching at least 80° N along the coasts of Greenland. To the south, its distributional limit is along the coast of Portugal (Lüning 1990). *Laminaria digitata* is an Arctic cold temperate North Atlantic species that is distributed between the Arctic and the coast of northern France (Europe) and New Hampshire (North America). This species does not occur in the North Pacific (Lüning 1990).

Table 1: Species studied, water depths of sampling in Kongsfjorden, geographical coordinates of the collecting sites, and dates of sampling during the study period in 2004.

Species	Sampling depth (m)	Collecting site	Sampling date
Alaria esculenta (Linnaeus) Greville	0.5 - 2	79° 0.027` N, 12° 0.511` E	28 May, 2 June, 15 July, 16 Aug., 13 Sept.
Laminaria digitata (Hudson) Lamouroux	0.5 - 2	79° 0.027` N, 12° 0.511` E	28 May, 2 June, 15 July, 16 Aug., 13 Sept.
*Saccharina latissima** (Linnaeus) Lane, Mayes, Druehl and Saunders	4	78° 55.204` N, 11° 59.809` E	26 May, 10 June, 12 July, 10 Aug., 8 Sept.
Laminaria solidungula Agardh	18	78° 55.359` N, 11° 59.702` E	26 May, 10 June, 12 July, 10 Aug., 8 Sept.

* formerly *Laminaria saccharina* (Linnaeus) Lamouroux

2.2. Transport and preparation of algal material

Juvenile kelp sporophytes with blade lengths of 10 - 20 cm were sampled between 26 May and 13 September 2004 in Kongsfjorden by SCUBA diving according to their natural depth distribution (Table 1). Under water, specimens were put in black bags to avoid exposure to high irradiances during transportation to the laboratory. From each sporophyte one disc of tissue (Ø 2.5 cm) was cut from the basal part of the blade above the meristem. For characterization of changes in photosynthetic efficiency the pieces of tissue were kept in dim white light (10 µmol m^{-2} s^{-1}) overnight before they were subjected to different radiation treatments described below. Samples for pigment analysis were immediately frozen in liquid nitrogen and kept at - 80 °C until analysis.

2.3. Temperature and radiation measurements

Air temperature was determined 2 m above the ground by the Baseline Surface Radiation Network (BSRN) station run by the AWIPEV Arctic Research Base in Ny-Ålesund (Spitsbergen, Norway). The water temperature of Kongsfjorden was measured in the seawater, which was pumped directly from the fjord into the flow through system of the experimental setup in the laboratory.

Photosynthetically active radiation was measured with a cosine-corrected flat-head quantum sensor LI-190 SA connected to a LI-1000 datalogger (LI-COR Biosciences, Lincoln, Nebraska, USA). The instrument was installed on the roof of the observatory of the AWIPEV Arctic Research Base. Continuous measurements of UVR were performed using a 32-channel spectroradiometer (isiUV, L3, isiTec GmbH, Bremerhaven, Germany) adjacent to the PAR datalogger. Irradiances below 290 nm were not detectable and integrals over the wavelength ranges 290 - 320 nm and 320 - 400 nm were used to calculate the irradiances and daily dose of UVBR and UVAR, respectively.

Whenever feasible, underwater radiation measurements were conducted directly at the different sampling sites of the algae. In total, 22 depths profiles of underwater irradiances were recorded on calm days with low wave action and stable light conditions around noon. Spectra of underwater radiation (λ = 280 - 700 nm) were recorded with an underwater spectroradiometer with a cosine-corrected 2π UV-VIS quantum sensor (Ramses ACC, TriOS, Oldenburg, Germany). Mean values of three spectra were used to calculate the vertical attenuation coefficient (K_d) of downward irradiance according to Kirk (1994):

$$K_d = \ln (E_{d(z1)}/E_{d(z2)}) \bullet (z_2-z_1)^{-1} \quad (2.1)$$

where $E_{d(z1)}$ and $E_{d(z2)}$ are the respective irradiances at depths z_1 and z_2. The vertical attenuation coefficients (K_d) for PAR, UVAR, and UVBR were calculated using integrals of underwater irradiances over the wavelength ranges 400 - 700 nm, 320 - 400 nm, and 310 - 320 nm, respectively. Irradiances below 310 nm were below the detection limit. Maximum irradiances at the different growth sites were determined for each month by using the maximum values of surface PAR, UVAR and UVBR and the appropriate minimum K_d values measured at the respective growth site and month. Average underwater irradiances at the

growth sites were calculated from the average irradiances of surface PAR, UVAR and UVBR and the appropriate averaged K_d values measured at the respective growth site and month. Under sea ice, underwater PAR was measured with a cosine-corrected flat-head underwater sensor connected to a LI-1000 datalogger (LI-192 SA, LI-COR Biosciences, Lincoln, Nebraska, USA).

Corresponding 1 % depths for PAR, UVAR, and UVBR were calculated using integrals of underwater irradiances over the wavelength ranges 400 - 700 nm, 320 - 400 nm and 310 - 320 nm, respectively. To follow the relative changes in the underwater UVBR during sea ice break-up, erythemally weighted irradiance ($UVBR_{ery}$) was measured continuously with an ELUV-14 datalogger (El Naggar et al. 1995). The spectral sensitivity of the datalogger resembles the standard CIE erythemal action spectrum after (McKinley and Diffey 1987).

In the laboratory, artificial PAR was measured with a cosine-corrected flat-head LI-190 SA quantum sensor connected to a LI-1000 datalogger. UVAR and UVBR in the experimental setup were measured with a Solar Light PMA 2100 radiometer (Solar Light Co. Inc., Philadelphia, USA) equipped with an UVAR (PMA 2110) and an UVBR (PMA 2106) broad-band quantum sensor. To avoid overestimation of UVBR due to sensitivity of the UVBR sensor to wavelengths of the UVAR-region, irradiances were measured with a quartz glass filter (WG320, Schott Glass Technologies, Duryea, Pennsylvania, USA) on top of the UVBR sensor, cutting off wavelengths below 320 nm. Thereby measured irradiances of UVA radiation were subsequently subtracted from the irradiances measured without the filter.

2.4. Determination of photosynthetic parameters

Photosynthetic activity was determined by measuring the *in vivo* chlorophyll fluorescence of photosystem II (PS II) with a pulse-amplitude modulated fluorometer (PAM 2000, Walz, Effeltrich, Germany) equipped with a leaf distance clip. The general principle of this method is reviewed by Krause and Weis (1991) and Schreiber et al. (1994). The quantum energy absorbed by a chlorophyll *a* molecule raises an electron from the ground state to an excited state. In the process of de-excitation of a chlorophyll *a* molecule a small proportion (0.6 - 3 % *in vivo*) of the excitation energy is dissipated as red fluorescence (Barber et al. 1989). The

indicator function of chlorophyll fluorescence arises from the fact that fluorescence emission is complementary to alternative pathways of de-excitation which are primarily photochemistry (photochemical quenching, PQ) and heat dissipation (non-photochemical quenching, NPQ). Owing to this competition, the fluorescence yield is highest when the photochemistry and heat dissipation are lowest. Therefore, changes in the fluorescence yield reflect changes in photochemical efficiency and heat dissipation. The optimum quantum yield of PS II is a commonly used parameter in stress research and was determined as the ratio of variable to maximum fluorescence (F_v/F_m) in temporarily dark-acclimated plants according to Hanelt (1998) and Bischof et al. (1999). It indicates the efficiency of energy transfer from the antennae systems to the reaction centers. After application of a 5 s far-red pulse (30 µmol m^{-2} s^{-1}, λ = 735 nm), which selectively excites photosystem I (PS I) and thus completely oxidize the electron transport chain, the algal tissue pieces were darkened for 5 min. Subsequently, pulsed dim red light (0.3 µmol m^{-2} s^{-1}, λ = 650 nm) was applied to measure the minimum fluorescence (F_0, all reaction centers of PS II are oxidized), followed by a short pulse of saturating white light (0.8 s, 8000 µmol m^{-2} s^{-1}) to measure the maximum fluorescence (F_m, all reaction centers of PS II are reduced and photochemical quenching is zero). The variable fluorescence (F_v) was determined as:

$$F_v = F_m - F_0 \tag{2.2}$$

Thus, the optimum quantum yield of PS II is given by:

$$F_v/F_m = (F_m - F_0)/F_m \tag{2.3}$$

The maximum values for the optimum quantum yield vary in the different algal groups due to differences in the composition of the photosynthetic apparatus. For Phaeophyta maximum F_v/F_m values from 0.7 to 0.8 can be recorded in unstressed adult plants (Büchel and Wilhelm 1993).

To determine seasonal variations in the photosynthetic status of the seaweeds, photosynthesis *vs.* irradiance curves (P-E curves) were measured directly after each sampling of the algae as described by Bischof et al. (1998a). Samples were irradiated with stepwise increasing irradiances of actinic red light (10.1 - 244.7 µmol m^{-2} s^{-1}, λ = 650 nm). Starting with the lowest irradiance, the steady state fluorescence (F_t) was measured after stabilization

of the fluorescence level. Upon the application of a saturating white light flash in the presence of actinic light, the maximal fluorescence of the light-acclimated plant tissue (F_m') was obtained, followed by 5 s darkness to measure the minimal fluorescence of the light-incubated plant (F_0'). Every 30 s the actinic irradiance was further increased and the respective F_t, F_m' and F_0'were determined. The effective quantum yield ($\Delta F/F_m'$) reflects the actual light utilization during illumination of samples and was calculated for each irradiance using following equation after Genty et al. (1989):

$$\Delta F/F_m' = (F_m' - F_t)/ F_m' \quad (2.4)$$

The recorded P-E curves were used to estimate the maximum relative electron transport rate ($rETR_{max}$) as a measure of photosynthetic capacity, the initial slope (α) as an indicator of photosynthetic efficiency at sub-saturating irradiance and the saturating irradiance (E_k) of photosynthesis, i.e. the light intensity at which the initial slope of the P-E curve intercepts the horizontal asymptote of $rETR_{max}$.

The relative electron transport rate (rETR) for each irradiance was calculated by multiplying $\Delta F/F_m'$ by the respective photosynthetically photon flux density (PPFD) of actinic irradiance as described by Schreiber et al. (1994):

$$rETR = \Delta F/F_m' \bullet PPFD \quad (2.5)$$

The obtained relative electron transport rates were plotted against the respective irradiances of actinic light and $rETR_{max}$, α, and E_k were calculated using the modeling equation by Eilers and Peeters (1988).

2.5. Experimental setup for chlorophyll fluorescence measurements

During the study period, laboratory experiments were conducted to study radiation effects on macroalgal photosynthesis and to test for seasonal changes in the sensitivity of photosynthetic efficiency to PAR and UVR. The capability for photoprotection was investigated by measuring photoinhibition and recovery of the optimum quantum yield of photosynthesis

(F_v/F_m) in field-collected seaweeds after transferring them to controlled irradiances of PAR, UVAR and UVBR.

Artificial radiation of approximately 180 µmol m^{-2} s^{-1} PAR, 4 W m^{-2} UVAR, and 0.4 W m^{-2} UVBR, was produced by four white light fluorescence tubes (Osram L58W/950, Germany) and one UVA-340 fluorescence tube (Q-Panel, Cleveland, USA). Three different radiation treatments were obtained by the use of different filter foils: (1) P-treatment (PAR, λ = 400 - 700 nm) using Ultraphan 400 (Digefra GmbH, Munich, Germany), (2) PA-treatment (PAR + UVAR, λ = 320 - 700 nm) using Folarnorm 320 (Folex GmbH, Dreieich, Germany), and (3) PAB-treatment (PAR + UVAR + UVBR, λ = 280 - 700 nm) using Ultraphan 295 (Digefra GmbH, Munich, Germany). The spectral transmission of the three different filters used is shown in Figure 3.

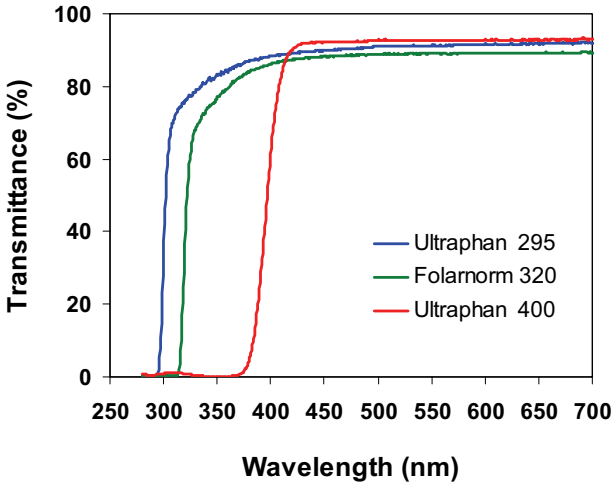

Fig. 3: Transmission spectra of the filter foils Ultraphan 295 (blue curve), Folarnorm (green curve) and Ultraphan 400 (red curve) used in the laboratory experiment to create three different light treatments.

The algal material was exposed in flow through systems for 4 hours to the different radiation conditions and was subsequently allowed to recover for 20 hours in dim white light (10 µmol m^{-2} s^{-1} PAR). The optimum quantum yield of photosynthesis (F_v/F_m) was determined just before and after 1, 2, and 4 hours of exposure as well as after 1, 2, 4, 6, and 20 hours of recovery. Running seawater, pumped directly from the fjord, kept the water temperature constant during the experiment.

2.6. Analysis of photosynthetic pigments and UVR-absorbing compounds

To assess seasonal changes in the amount of photoprotective pigments and alterations of the photosynthetic apparatus, pigments were extracted, after each sampling, from untreated frozen blades of sporophytes by incubation for 12 hours in *N,N*-dimethylformamide (DMF) at 4 °C in darkness under a nitrogen atmosphere. This extraction procedure was repeated once. Subsequently, the extracts were pooled and centrifuged for 5 min at 10,000 g and 4 °C before further analysis by spectrophotometry or and high-performance liquid chromatography (HPLC).

2.6.1. Spectrophotometric measurements

To evaluate the presence of UVR-absorbing compounds, absorption spectra of the DMF extracts were recorded in the 260 - 750 nm wavelength range using a U-3310 UV-VIS Spectrophotometer (HITACHI, Japan). For better comparison, the spectra were normalised to the absorption maximum of Chl *a* at 664 nm. With regard to the potential photoprotective role of screening the photosynthetic apparatus from harmful UVR, the absorption maximum at 273 nm was related to the Chl *a* absorption peak at 664 nm, yielding the relative content of UVR-absorbing compounds ($Abs_{273/664}$).

2.6.2. HPLC

Photosynthetic pigments were separated by high-performance liquid chromatography (HPLC) using a Waters HPLC system (Eschborn, Germany) consisting of a 600E multisolvent delivery system with system controller, a 117 plus autosampler, and a 996 photodiode array detector. Separation was performed at a constant temperature of 20 °C on a LiChrosphere® RP-18 column (5 µm, 4 x 125 mm, Agilent Technologies France, Massy, France) after passing a LiChrosphere® RP-18 guard column (5 µm, 4 x 4 mm, Merck, Darmstadt, Germany), according to the protocol listed in Table 2. Total analysis time was 19 minutes. Between runs the column was equilibrated for 45 minutes with 90 % methanol.

Table 2: Binary gradient for HPLC analysis of photosynthetic pigments. Solvent A = 75 vol % acetonitrile, 15 vol % methanol, 10 vol % tetrahydrofuran, solvent B = 0.13 M ammonium acetate, 0.05 M tetrabutyl ammonium acetate.

Time (min)	Flow rate (mL min^{-1})	A (vol %)	B (vol %)
0.01	1.5	85	15
5.00	2.0	100	0
17.00	2.0	100	0
19.00	1.5	85	15

Pigments were identified by comparison of their retention times and spectral properties with those of pigment standards. They were quantified by their peak areas, which were previously calibrated against external standards. Calibration was done with known quantities of pure pigments: chlorophyll *a* (Chl *a*) was isolated from *Delesseria salicifolia* Reinsch and *Polysiphonia urceolata* (Lightfoot ex Dillwyn) Greville, chlorophyll c_1+c_2 (Chl *c*) and fucoxanthin (Fuc) from *L. solidungula*, *β*-carotene (*β*-Car) from *Delesseria lancifolia* (Hooker) Agardh, violaxanthin (V) from *Ulva compressa* Linnaeus, antheraxanthin (A) from *D. lancifolia*, and zeaxanthin (Z) from *P. urceolata*. In contrast to other marine red algae, *D. lancifolia* exhibits a more complex carotenoid pattern including violaxanthin, antheraxanthin and zeaxanthin (Marquardt and Hanelt 2004). The pigments were isolated from pigment extracts of the respective algal species by HPLC. The purity of the pigments was checked spectroscopically and by HPLC.

The contents of Chl *a* and Chl *c* were calculated from absorbance values in 90 % acetone, contents of carotenoids were calculated from absorbance values in ethanol, except for the content of fucoxanthin, which was determined from absorbance values in acetone, using the pigment-specific molar extinction coefficients (ε) for the respective solvent listed in Table 3. The pool size of the xanthophyll cycle pigments (VAZ) was calculated as the sum of the contents of the xanthophylls violaxanthin (V), antheraxanthin (A), and zeaxanthin (Z). Pigment contents are expressed in nanomoles per gram fresh weight (nmol/g FW).

Table 3: Pigment-specific molar extinction coefficients (ε) for the respective solvents at the wavelengths indicated, used to calculate the pigment contents.

Pigment	Molar extinction coefficient* ($L\ mol^{-1}\ cm^{-1}$)	Solvent	Wavelength (nm)
chlorophyll *a*	78.75×10^3	90 % acetone	663
chlorophyll *c*	26×10^3	90 % acetone	631
fucoxanthin	109×10^3	acetone	443
β-carotene	141×10^3	ethanol	453
violaxanthin	153×10^3	ethanol	443
antheraxanthin	137×10^3	ethanol	446
zeaxanthin	145×10^3	ethanol	450

* according to Strain (1938), Isler et al. (1956), Davies (1965), Hager and Meyer-Bertenrath (1966), Jeffrey (1972), Jeffrey and Humphrey (1975), Haugan and Liaaen-Jensen (1989)

2.7. Data treatment and statistical analysis

All values of $rETR_{max}$, E_k, α, F_v/F_m, pigment contents, pigment ratios, and absorbance ratios are expressed as mean values and standard deviations calculated from single measurements of four individual plants (n = 4) if not otherwise stated.

To test for differences between species and for the effect of different sampling dates (acclimation status) on the pigment contents, pigment ratios, absorbance ratios, $rETR_{max}$, E_k, and α, the data were tested for statistical significance of means by one-way analysis of variances (ANOVA). Prior to analysis, data were tested for homogeneity of variances (Cochran´s test). Heteroscedastic data were ranked or analyzed by the non-parametric Kuskal-Wallis test (as indicated in the text). Post-hoc comparisons were performed with Tukey´s honestly significantly different test (Tukey´s HSD).

The F_v/F_m initial values of unexposed algae (0 h exposure) were set to 100 % to allow a better comparison among different species. To test for the effects of different radiation treatments, sampling dates, and their interaction on the photoinhibitory response and recovery of the algae, data were analyzed by two-way ANOVA followed by a Tukey´s HSD. Prior to analysis, percentage data were arcsine transformed to assure normal distribution. The data of

S. latissima after 4 hours of exposure were additionally square-root transformed. All data were tested for homogeneity of variances (Cochran´s test). Even though the Cochran´s test revealed heterogeneous variances for the data of *A. esculenta* and *S. latissima* after 20 h of recovery, also these data were analyzed by two-way ANOVA, since ANOVA is sufficient robust to resist this violation when variance is partitioned in several sources (month, irradiation, month x irradiation, and error), and when the design is balanced, i.e. the same number of replicates for each treatment (Underwood 1997). Significance level was set at $\alpha < 0.05$ (Sokal and Rohlf 1981), except for testing for homogeneity of variances by a Crochan´s test when $\alpha < 0.01$ was used (McGuinness 2002). Statistical analysis were done using StatisticaTM 6.0 software package.

To test for correlations between photosynthetic parameters, underwater irradiances, pigment contents and ratios, a correlation coefficient (r) was determined using the Microsoft Excel software tool KORREL (Pearson). For this purpose, the underwater PAR measured at 0.5 and 2 m water depths at the sampling site of *A. esculenta* and *L. digitata* was averaged. The Pearson correlation indicates the strength of a linear relationship between two variables, its value alone may not be sufficient to evaluate this relationship, especially in the case where the assumption of normality is incorrect. Thus, the data were additionally subjected to an individual examination.

3. Results

3.1. Seasonal variations of abiotic factors

3.1.1. Air temperatures and surface radiation conditions

During the study period from 26 May to 14 September 2004 the weather was fairly unstable, as reflected in strong variations of the daily dose of UVBR, UVAR and PAR reaching the Earth's surface (Fig. 4b - d). Between the end of May and the beginning of July, the surface irradiances were high compared to those in August and September.

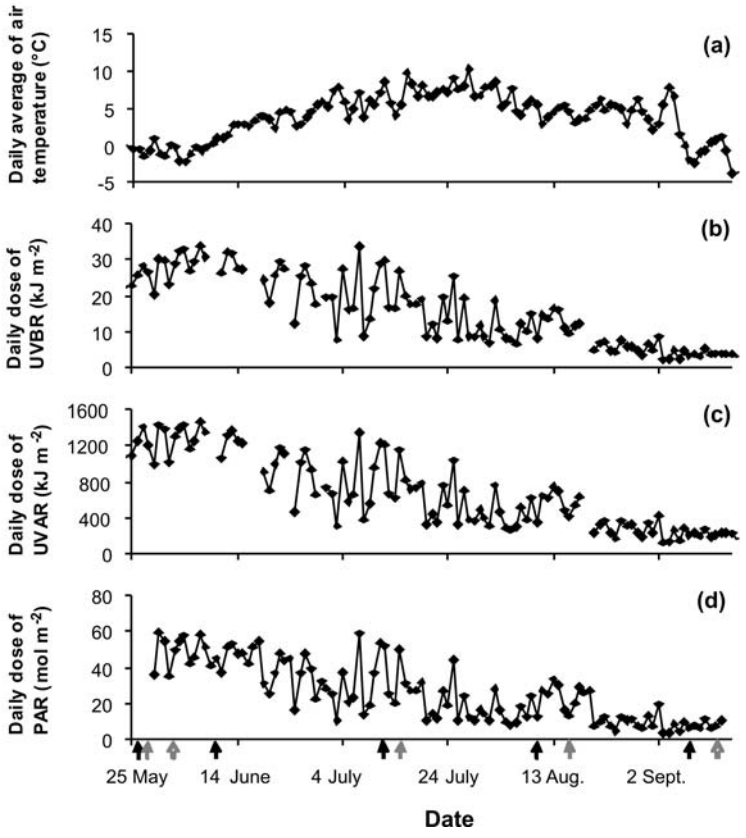

Fig. 4: Air temperature and Earth's surface radiation during the course of the season 2004. (a) Daily average of air temperature, (b) daily dose of UVBR, (c) daily dose of UVAR, (d) daily dose of PAR. Arrows indicate sampling dates of macroalgae and subsequent conduction of irradiation experiments: *A. esculenta* and *L. digitata* were sampled on 28 May, 2 June, 15 July 16 August, 13 September (grey arrows), *S. latissima* and *L. solidungula* were collected on 26 May, 10 June, 12 July, 10 August, 8 September (black arrows). Missing data in the daily dose of UVBR and UVAR are due to malfunction of the temperature stabilisation of the spectroradiometer.

Daily doses of PAR, UVAR and UVBR were highest in early July, whereas maximum irradiances of PAR and UVAR were measured in June and of UVBR in July (Table 4). From September on, irradiances of PAR and UVAR were temporarily below the detection limit of the measuring instruments, while UVBR was for the first time temporarily not detectable in August.

High variability and strong seasonality were also found in air temperature (Fig. 4a). The daily average of temperature varied between -2.4 and +10.4 °C. In May, the air temperature was around the freezing point and increased from mid-June on to its maximum by the end of July. Generally, air temperatures were high in July and August before decreasing again in September (Table 4).

Table 4: Maximum and minimum values of abiotic parameters throughout the study period from 26 May to 14 September 2004. Dates related to minimum irradiances indicate the first time, when irradiances were temporarily below the detection limit of the measuring instruments. The 1 % water depth indicates the depth at which irradiances are reduced to 1 % of those just below the water surface.

Abiotic parameter	Maximum	Date	Minimum	Date
Temperature $_{air}$	10.4 °C	28 July	-2.4 °C	9 Sept.
Temperature $_{water}$	6.9 °C	13 July	2.0 °C	27 May
Irradiance $_{PAR}$	1498 µmol $m^{-2}s^{-1}$	12 June	below detection limit	13 Sept.
Irradiance $_{UVAR}$	32.98 W m^{-2}	7 June	below detection limit	4 Sept.
Irradiance $_{UVBR}$	0.90 W m^{-2}	2 July	below detection limit	5 Aug.
1% depth $_{PAR}$	23.4 m	14 May	5.1 m	21 July
1% depth $_{UVAR}$	23.8 m	14 May	2.7 m	10 July
1% depth $_{UVBR}$	13.6 m	31 May	1.3 m	10 July

3.1.2. Water temperatures and radiation conditions in Kongsfjorden

Throughout the seasons the water temperature of Kongsfjorden varied between approximately 2 and 7 °C. The average water temperature was lowest in May and increased during June to its maximum in mid-July (Table 4, 5). Water temperatures were high in July and August and decreased again towards the end of the study period in September.

Table 5: Seasonal changes in the seawater temperature (monthly mean ± SD) of Kongsfjorden during the study period from 26 May to 14 September 2004.

Month	May	June	July	August	September
Water temperature (°C)	2.3 ± 0.2	3.7 ± 1.2	6.5 ± 0.4	5.7 ± 1.2	4.3 ± 1.7

Underwater irradiances at the algal growth sites were also highly variable, since they depend additionally on atmospheric conditions, on ice cover and on optical characteristics of the water body (Table 6). A sea ice layer of 1.3 m and 1 m, with a snow layer of about 5 cm, covered the sampling site of *S. latissima* until 27 May 2004 and that of *A. esculenta* and *L. digitata* until 29 May 2004, respectively. Underwater light measurements on 14 May 2004 revealed that under this condition, only 2 % and 3 % of the surface PAR reached a water depth of 4 m (sampling site of *S. latissima*) and of 2 m (growth site of *A. esculenta* and *L. digitata*), respectively.

The monitoring of erythemally weighted UVBR ($UVBR_{ery}$), directly at the growth site of *S. latissima*, revealed the fast and pronounced changes in underwater irradiances during the time of sea ice break-up (Fig. 5). The sea ice break-up on 28 May 2004 coincided with high incident UVB radiation and resulted in a sudden 15-fold increase of underwater UVBR at 4 m water depth compared to the previous days. Irregular variations in the daily fluctuation of $UVBR_{ery}$ values, e.g. on 30 May 2004, are presumably caused by drift ice.

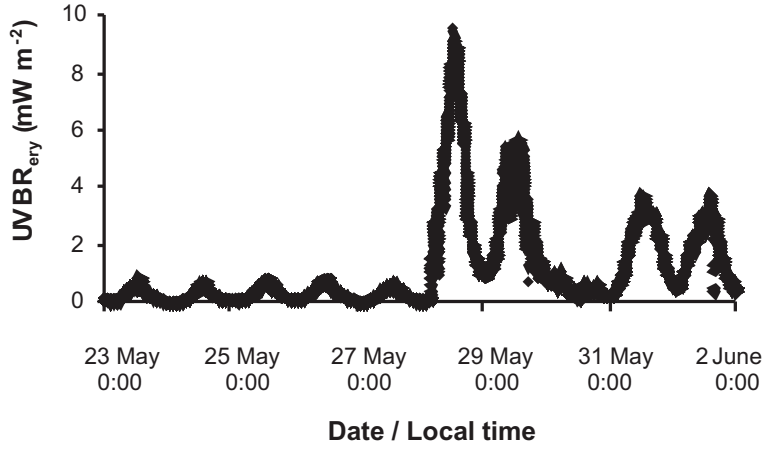

Fig. 5: Changes in the underwater radiation during the time around the sea ice break-up. Erythema-weighted UVBR ($UVBR_{ery}$) measured at a water depth of 4 m, at the sampling site of *S. latissima*.

The seasonal changes in the vertical attenuation coefficient of downward irradiance (K_d) of the water column above the sampling site of *S. latissima* are shown in Figure 6. Maximum light transmittance of the water body was observed in May, indicated by minimal K_d values of 0.20 m^{-1} for PAR, 0.19 m^{-1} for UVAR, and 0.34 m^{-1} for UVBR. Subsequently, the transmittance of the water column decreased and was lowest in July, when maximal K_d values of about 0.91 m^{-1} for PAR, 1.71 m^{-1} for UVAR, and 3.58 m^{-1} for UVBR were measured. Later on, the transmittance increased again, as reflected in lowered K_d values in August and September. The resulting maximum and minimum values for the 1 % depth for PAR, UVAR and UVBR are listed in Table 4.

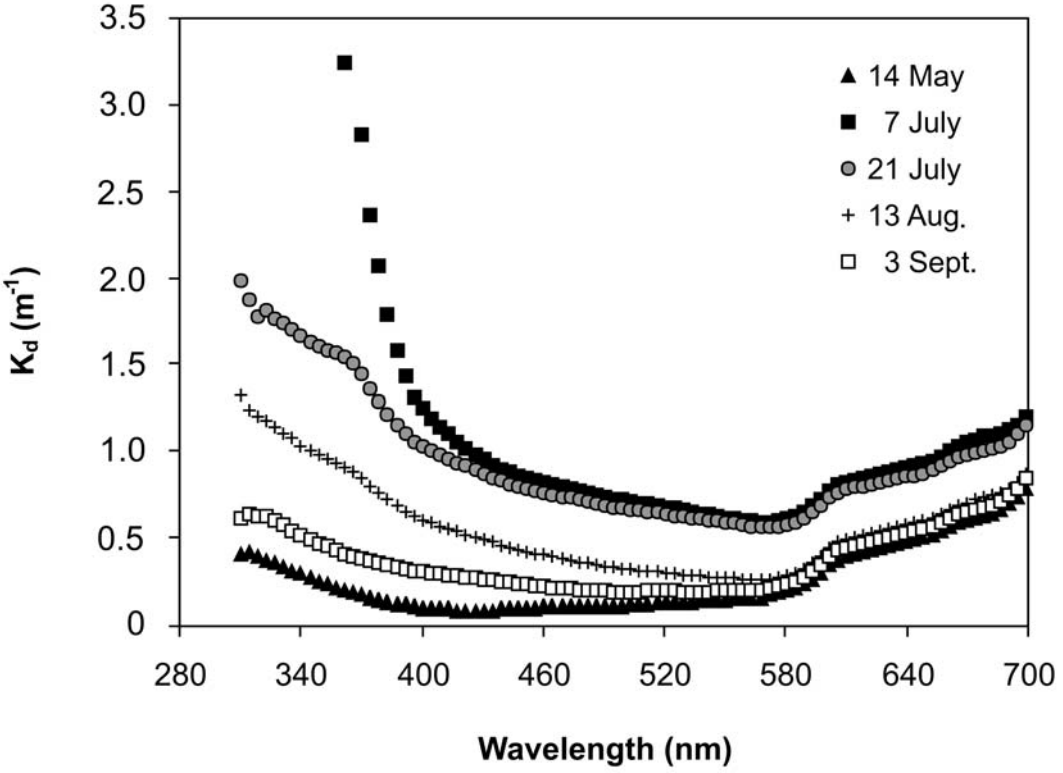

Fig. 6: Seasonal variation in the vertical attenuation coefficient (K_d) of downward irradiance calculated from spectral radiometric measurements (mean, n = 3) during the study period in 2004 at the sampling site of *S. latissima*.

At the growth sites of *A. esculenta*, *L. digitata* and *S. latissima*, underwater radiation was lowest under sea ice cover in May. At all algal growth sites, the underwater irradiances of PAR, UVAR and UVBR were highest in early June, directly after the sea ice break-up, except for the growth site of *L. solidungula* which was not covered by sea ice and exposed to

highest PAR in May (Table 6). Generally, radiation conditions were highest at the sampling site of *A. esculenta* and *L. digitata* in 0.5 to 2 m depth and lowest at that of *L. solidungula* in 18 m depth, where no UVBR was detected.

Table 6: Seasonal changes in the underwater irradiances at different sampling sites between 29 May and 14 September 2004. Maximum underwater irradiances (max.) were calculated from the maximum value of Earth's surface PAR, UVAR and UVBR and the appropriate minimum K_d value measured at the respective growth site and month. Average underwater irradiances (av.) were calculated from the average irradiances of surface PAR, UVAR and UVBR and the appropriate monthly mean of K_d values measured at the respective growth site.

Species	Depth		May	June	July	August	September
		Underwater PAR (µmol m^{-2} s^{-1})					
A. esculenta / *L. digitata*	0.5 m	max.	n.d.	1289.06	930.28	722.98	484.48
		av.	n.d.	426.19	204.54	135.36	72.89
	2.0 m	max.	32.56*	821.40	308.51	277.77	222.23
		av.	n.d.	271.57	64.12	50.96	33.43
S. latissima	4.0 m	max.	21.51*	592.97	74.02	202.66	208.79
		av.	n.d.	196.05	15.27	26.39	27.29
L. solidungula	18.0 m	max.	42.24	23.14	b.d.l.	10.63	7.46
		av.	16.66	7.65	b.d.l.	0.10	1.12
		Underwater UVAR (W m^{-2})					
A. esculenta / *L. digitata*	0.5 m	max.	n.d.	29.73	13.48	13.10	7.55
		av.	n.d.	11.71	3.57	2.90	1.58
	2.0 m	max.	n.d.	21.78	1.37	3.17	1.61
		av.	n.d.	8.58	0.32	0.62	0.34
S. latissima	4.0 m	max.	n.d.	15.24	0.14	1.46	2.50
		av.	n.d.	6.00	0.02	0.25	0.41
L. solidungula	18.0 m	max.	0.91	1.02	b.d.l.	0.03	0.01
		av.	0.45	0.40	b.d.l.	b.d.l.	b.d.l.
		Underwater UVBR (W m^{-2})					
A. esculenta / *L. digitata*	0.5 m	max.	n.d.	0.76	0.36	0.40	0.33
		av.	n.d.	0.26	0.05	0.05	0.02
	2.0 m	max.	n.d.	0.46	0.02	0.06	0.04
		av.	n.d.	0.16	b.d.l.	0.01	b.d.l.
S. latissima	4.0 m	max.	n.d.	0.18	b.d.l.	0.02	0.05
		av.	n.d.	0.06	b.d.l.	b.d.l.	b.d.l.
L. solidungula	18.0 m	max.	b.d.l.	b.d.l.	b.d.l.	b.d.l.	b.d.l.
		av.	b.d.l.	b.d.l.	b.d.l.	b.d.l.	b.d.l.

* Under the sea ice, PAR was measured with a LI-COR datalogger at noon.
b.d.l. = below detection limit, < 0.01
n.d. = not determined

3.2. Photosynthetic performance

3.2.1. Light saturation point of photosynthesis (E_k)

In all species studied, saturating irradiances of photosynthesis (E_k) varied significantly between months (Fig. 7), whereas seasonal variations of E_k were smallest in *L. solidungula*.

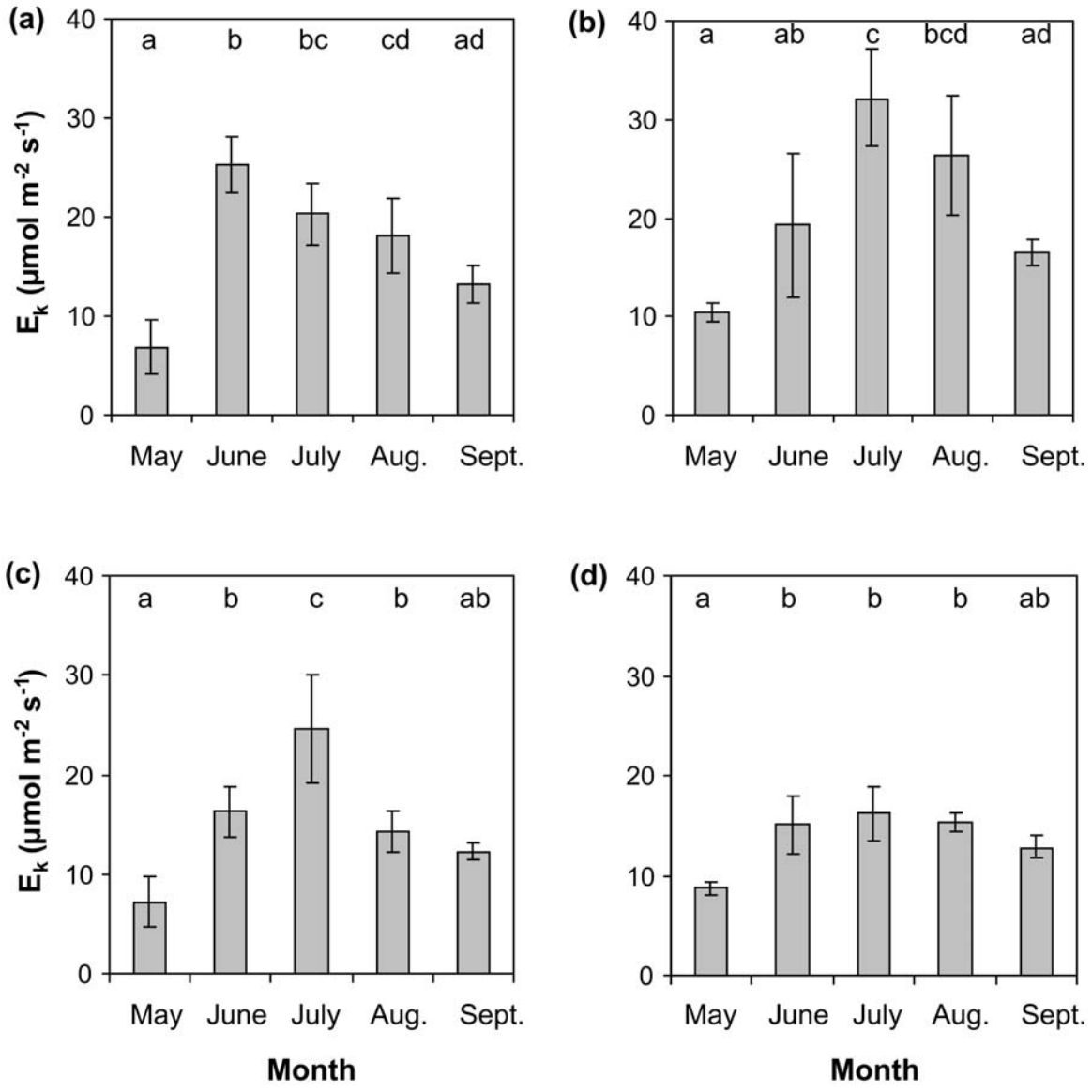

Fig. 7: Seasonal changes of the light saturation point of photosynthesis (E_k, µmol photons m^{-2} s^{-1}, mean ± SD, n = 4) in (a) *A. esculenta*, (b) *L. digitata*, (c) *S. latissima*, and (d) *L. solidungula*. Different lower case letters indicate significant differences in E_k between months in one species.

The light saturation points in *L. digitata* ranged from 11 to 32 µmol photons m^{-2} s^{-1}, in *A. esculenta* and *S. latissima* from 7 to 25 µmol photons m^{-2} s^{-1}, and in *L. solidungula* from 9 to 16 µmol photons m^{-2} s^{-1}.

All species showed similar minimum E_k values in May. Later on, E_k significantly increased to a maximum in July in all species, except for *A. esculenta* showing a maximum in June (ANOVA, *A. esculenta*, *S. latissima*, *L. solidungula*: $p < 0.001$, *L. digitata*: $p < 0.05$), and subsequently decreased again in August and September. Hence, the E_k of *A. esculenta*, *L. digitata* and *S. latissima* increased approximately three-times, while that of *L. solidungula* increased only two-times. Throughout the study period, highest E_k values were found in *L. digitata*, except for June when *A. esculenta* revealed a higher E_k value. The photosynthesis of *L. solidungula* was constantly light-saturated at relatively low irradiances compared to the other species.

3.2.2. Maximum relative electron transport rate ($rETR_{max}$)

The relative maximal electron transport rates of photosynthesis ($rETR_{max}$), as a measure of photosynthetic capacity, changed significantly in all species studied throughout the months (Fig. 8). In *A. esculenta* $rETR_{max}$ varied between 5 and 14 relative units, in *L. digitata* between 9 and 17 relative units, in *S. latissima* between 5 and 17 relative units, and in *L. solidungula* between 7 and 14 relative units.

Generally, the seasonal pattern of the $rETR_{max}$ values was quite similar to that of the E_k values, in that in all species $rETR_{max}$ was lowest in May and continuously increased during summer. However, in *A. esculenta* and *L. digitata* $rETR_{max}$ values were maximal in August and remained relatively high until the end of the study period. The maximum $rETR_{max}$ values in *A. esculenta* and *L. digitata* were three-times and two-times higher than the corresponding minimum values, respectively (ANOVA, *A. esculenta*: $p < 0.001$, *L. digitata*: $p < 0.05$). In *S. latissima* and *L. solidungula*, the highest $rETR_{max}$ values in July correspond to a three- and twofold increase in $rETR_{max}$, respectively, before a stepwise decrease was observed (ANOVA, $p < 0.001$). At any time of the study period, $rETR_{max}$ values were highest in *L. digitata*.

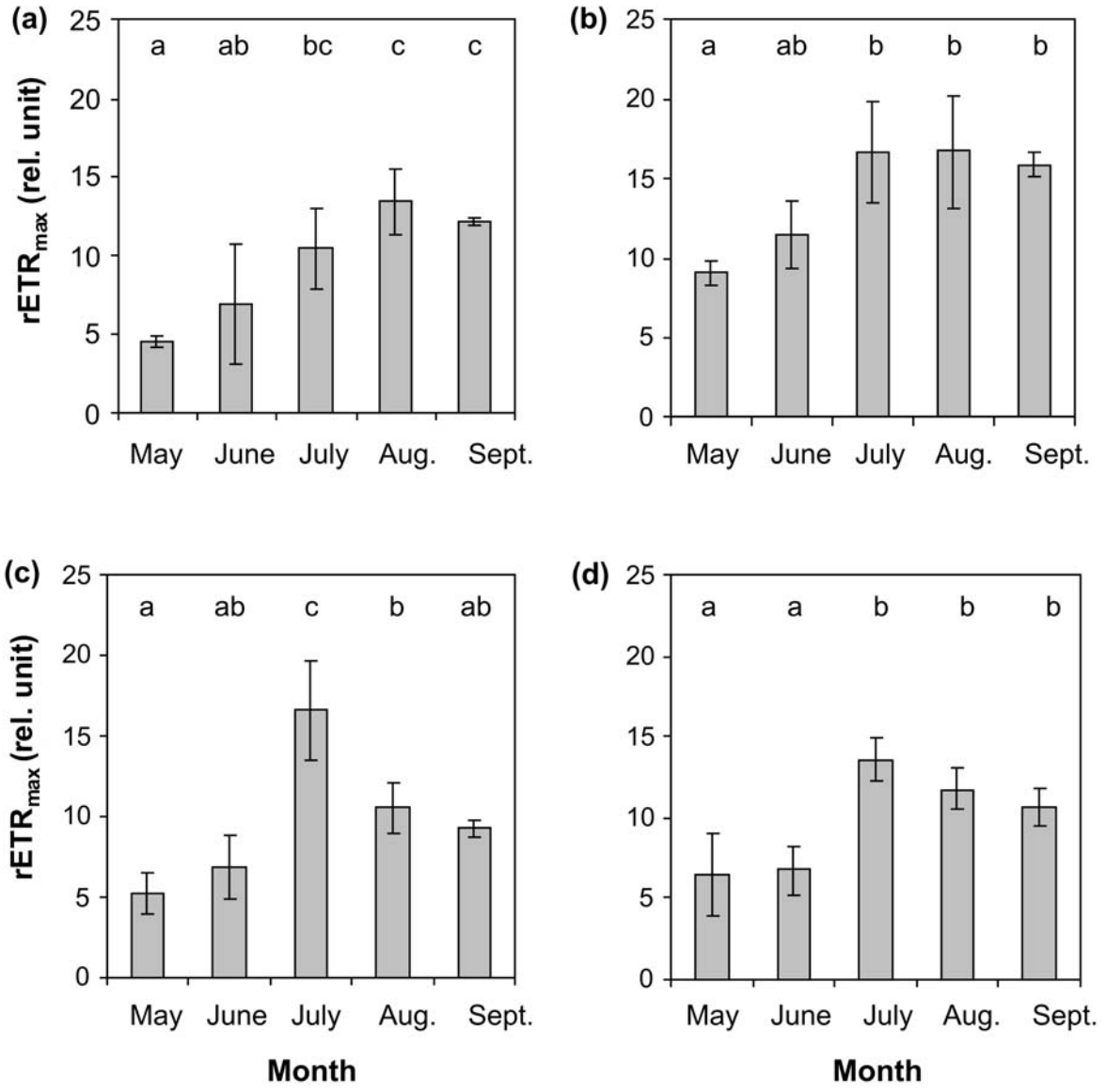

Fig. 8: Seasonal changes of the maximum relative photosynthetic electron transport rate of ($rETR_{max}$, relative unit, mean ± SD, n = 4) in (a) *A. esculenta*, (b) *L. digitata*, (c) *S. latissima*, and (d) *L. solidungula*. Different lower case letters indicate significant differences in $rETR_{max}$ between months in one species.

3.2.3. Photosynthetic efficiency at sub-saturating irradiances (α)

The photosynthetic efficiency at sub-saturating irradiances (α) differs significantly in all species between months (Fig. 9). In *A. esculenta* the values of α ranged from 0.29 to 0.93 relative units, in *L. digitata* from 0.52 to 0.96 relative units, in *S. latissima* from 0.41 to 0.79 relative units, and in *L. solidungula* from 0.45 to 0.85 relative units.

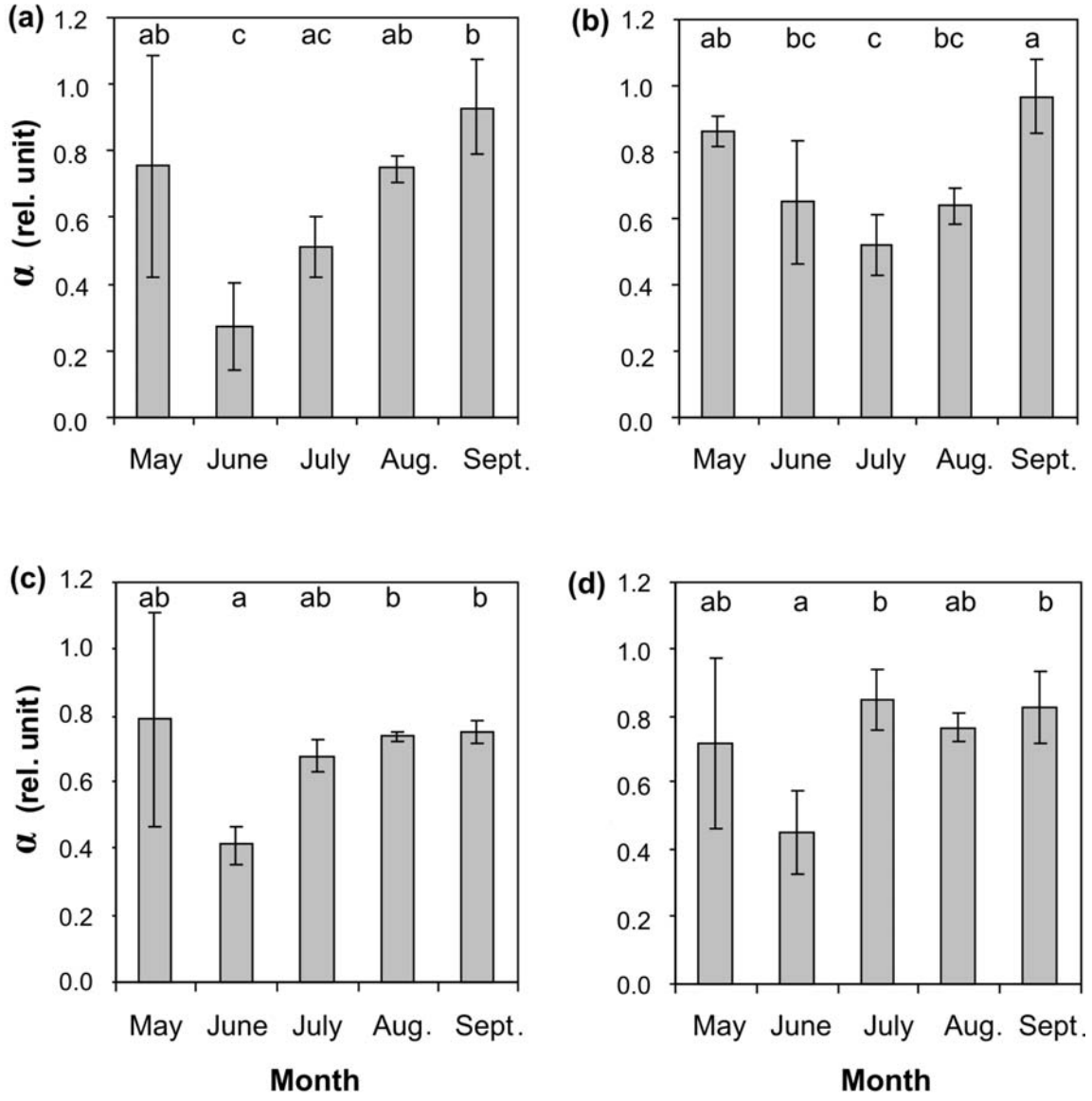

Fig. 9: Seasonal changes of the photosynthetic efficiency at sub-saturating irradiance (α, relative unit, mean ± SD, n = 4) in (a) *A. esculenta*, (b) *L. digitata*, (c) *S. latissima*, and (d) *L. solidungula*. Different lower case letters indicate significant differences in α between months in one species.

Generally, the seasonal pattern of α was inverse to that of E_k. Thus, the photosynthetic efficiency at sub-saturating irradiances was maximal in May and September and minimal in June or July, except for *L. solidungula* displaying a maximum in July. In *S. latissima* and *L. solidungula* a two-fold increase between the minimum value, which was observed already in June, and the respective maximum value was found (ANOVA, *S. latissima*, *L. solidungula*: $p < 0.05$). In *A. esculenta* and *L. digitata*, the maximum α value measured in September was more than three-times and two-times higher than the corresponding minimum value,

respectively (ANOVA, *A. esculenta*, *L. digitata*: $p < 0.001$). The seasonal variation in the photosynthetic efficiency at sub-saturating irradiances was most pronounced in *A. esculenta*. On a seasonal average, *L. digitata* and *L. solidungula* showed highest photosynthetic efficiency under low light conditions.

3.2.4. Susceptibility of the optimum quantum yield (F_v/F_m) to PAR and UVR

Before irradiation, the F_v/F_m initial values of all species ranged between 0.60 and 0.79 throughout the study period, only in June a lower F_v/F_m value of 0.50 was found in *S. latissima* (Table 7).

Table 7: Initial values of optimum quantum yield of photosynthesis (F_v/F_m, relative unit, mean ± SD, n = 12) measured throughout the season in the four species studied directly before exposure experiment was conducted.

	F_v/F_m initial (rel. unit)			
Month	*A. esculenta*	*L. digitata*	*S. latissima*	*L. solidungula*
May	0.77 ± 0.02	0.79 ± 0.01	0.71 ± 0.02	0.71 ± 0.02
June	0.60 ± 0.07	0.75 ± 0.02	0.50 ± 0.06	0.65 ± 0.05
July	0.63 ± 0.06	0.65 ± 0.06	0.68 ± 0.02	0.73 ± 0.01
August	0.65 ± 0.05	0.65 ± 0.05	0.70 ± 0.02	0.67 ± 0.05
September	0.65 ± 0.08	0.73 ± 0.02	0.73 ± 0.01	0.74 ± 0.03

Sensitivity of photosynthesis to artificial radiation varied significantly in all species between months, especially in species from deeper water (Fig. 10a - t). Throughout the study period, 4 h exposure to PAR alone resulted in all species in a strong inhibition of photosynthetic efficiency between 67 and 80 % (F_v/F_m = 0.12 - 0.23) of the initial values. Generally, additional UVAR, and in particular UVBR, caused a faster and stronger reduction in F_v/F_m and a delay in recovery. In all species, the seasonal variations in the degree of photoinhibition were relatively small compared to the remarkable variations in the capacity for recovery.

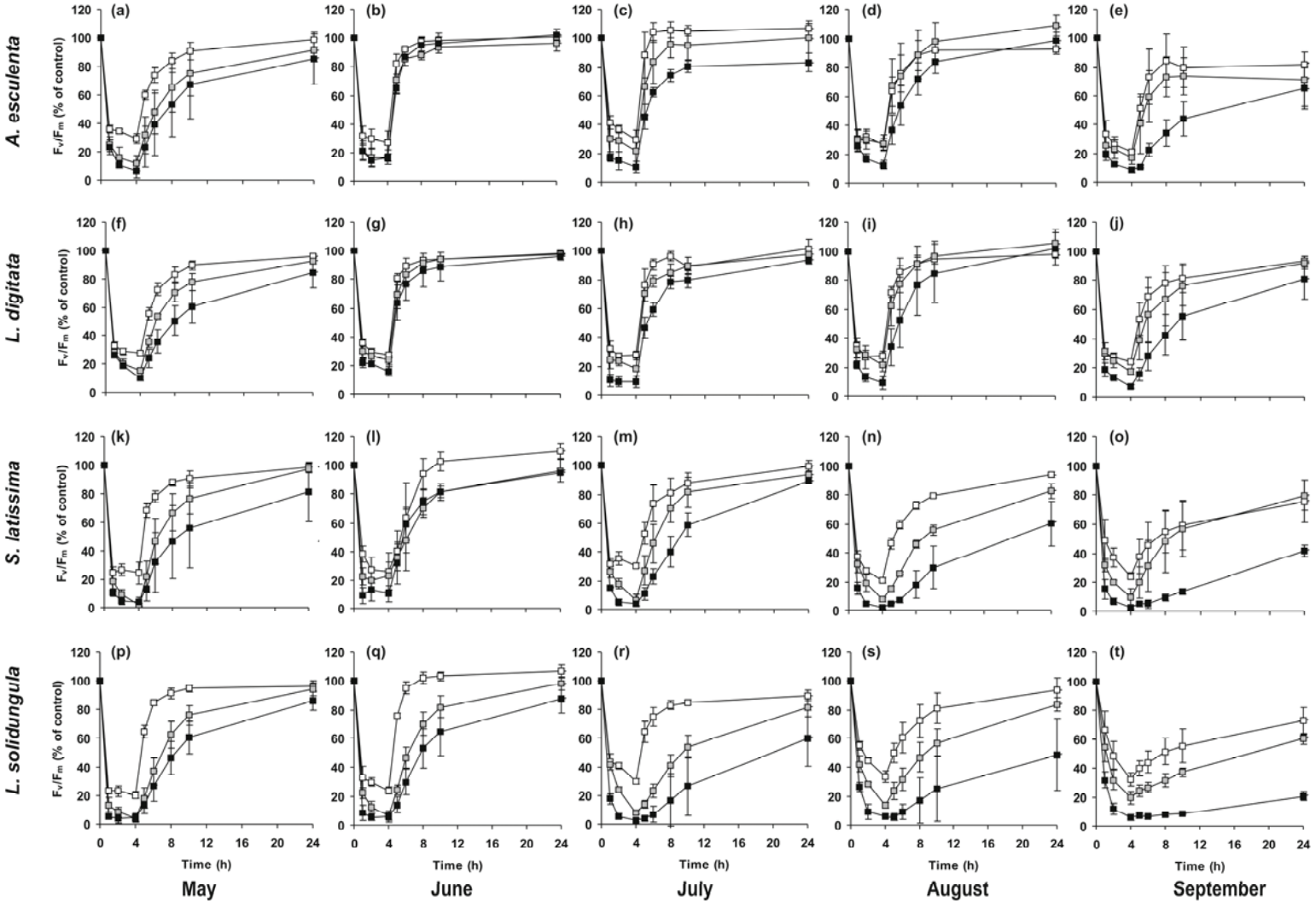

Fig. 10: Seasonal changes in the photosynthetic response of *A. esculenta* (a - e), *L. digitata* (f - j), *S. latissima* (k - o) and *L. solidungula* (p - t) to artificial radiation. Changes in optimum quantum yield of photosynthesis (F_v/F_m expressed as per cent of the respective initial value, mean ± SD, n = 4) during 4 h of exposure to different radiation treatments (PAR = white squares, PAR + UVAR = grey squares, PAR + UVAR + UVBR = black squares) and subsequent recovery for 20 h in dim white light.

Table 8: Results of two-way ANOVA for main effects and interaction between different radiation conditions (P = PAR, PA = PAR + UVAR, PAB = PAR + UVAR + UVBR) and sampling dates on photosynthetic efficiency (F_v/F_m) after 4 h of exposure and 20 h of recovery. On the right site of the table, the radiation-dependent differences in F_v/F_m after exposure and recovery are listed for the individual months. Significant p-values at $\alpha = 0.05$ and significant differences between radiation treatments are given in bold. df = degrees of freedom, F = F-ratio, p = p-value

Species	Source of variation	After exposure			After recovery			Month	After exposure	After recovery
		df	F	p	df	F	p			
A. esculenta	Month (A)	4	5.1	**0.002**	4	15.7	**<0.001**	May	**P ≠ PA, PAB**; PA = PAB	P = PA = PAB
	Irradiation (B)	2	52.7	**<0.001**	2	5.2	**0.009**	June	P = PA = PAB	P = PA = PAB
	A x B	8	2.9	**0.011**	8	3.3	**0.005**	July	**P ≠ PAB**; PA = P, PAB	**P ≠ PAB**; PA = P, PAB
								Aug.	**P, PA ≠ PAB**; P = PA	P = PA = PAB
								Sept.	**P ≠ PAB**; PA = P, PAB	P = PA = PAB
L. digitata	Month (A)	4	6.8	**<0.001**	4	8.3	**<0.001**	May	**P ≠ PA, PAB**; PA = PAB	P = PA = PAB
	Irradiation (B)	2	150.9	**<0.001**	2	3.6	**0.037**	June	**P ≠ PAB**; PA = P, PAB	P = PA = PAB
	A x B	8	2.3	**0.037**	8	1.6	0.163	July	**P ≠ PA ≠ PAB**	P = PA = PAB
								Aug.	**P, PA ≠ PAB**; P = PA	P = PA = PAB
								Sept.	**P, PA ≠ PAB**; P = PA	P = PA = PAB
S. latissima	Month (A)	4	8.2	**<0.001**	4	31.3	**<0.001**	May	**P ≠ PA, PAB**; PA = PAB	P = PA = PAB
	Irradiation (B)	2	85.5	**<0.001**	2	35.8	**<0.001**	June	P = PA = PAB	**P ≠ PA, PAB**; PA = PAB
	A x B	8	3.7	**0.002**	8	2.9	**0.011**	July	**P ≠ PA, PAB**; PA = PAB	P = PA = PAB
								Aug.	**P ≠ PAB**; PA = P, PAB	**P ≠ PAB**; PA = P, PAB
								Sept.	**P ≠ PAB**; PA = P, PAB	**P ≠ PAB**, PA; P = PA
L. solidungula	Month (A)	4	15.7	**<0.001**	4	40.9	**<0.001**	May	**P ≠ PA, PAB**; PA = PAB	P = PA = PAB
	Irradiation (B)	2	219.7	**<0.001**	2	52.5	**<0.001**	June	**P ≠ PA, PAB**; PA = PAB	**P ≠ PAB**; PA = P, PAB
	A x B	8	4.0	**0.001**	8	2.5	0.023	July	**P ≠ PA, PAB**; PA = PAB	**P ≠ PAB**; PA = P, PAB
								Aug.	**P ≠ PA ≠ PAB**	**P, PA ≠ PAB**; P = PA
								Sept.	**P ≠ PA ≠ PAB**	**P, PA ≠ PAB**; P = PA

Main effects and interaction of different radiation conditions and sampling dates (i.e. acclimation statuses) on F_v/F_m are shown in Table 8. The results of the Cochran´s tests of heteroscedastic data, which were used for two-way analysis of variances, are given in Table 9. In all four species, the two factors tested had significant effects on the degree of photoinhibition and recovery of F_v/F_m. The interaction effect between irradiance and month was also significant in all species, except for *L. digitata* and *S. latissima* after the recovery period (Table 8).

Table 9: Results of the Cochran´s tests of the heteroscedastic data of *A. esculenta* and *S. latissima* after 20 h of recovery. df = degree of freedom, C = Cochran C, p = p-value

Species	df	C	p
A. esculenta	14	0.194	0.008
S. latissima	14	0.292	< 0.001

A. esculenta and *L. digitata* showed a very dynamic photosynthetic response and relatively small seasonal variations compared to the species sampled in deeper water (Fig. 10a - e). Throughout the study period, recovery in dim light was fastest and most efficient in this two species. In May, the degree of photoinhibition in *A. esculenta* and *L. digitata* was significantly higher in samples exposed to additional UVR than to PAR alone (Fig. 10a, f, Table 8, two-way ANOVA, $p \leq 0.001$) and recovery proceeded slower and less efficiently, e.g., F_v/F_m in PAB-treated samples was restored to only 85 % of the respective initial value (Fig. 10a, f). In June, after sea ice break-up, effects of UVR on photoinhibition and recovery were minimal and the recovery in all radiation treatments increased remarkably (Fig. 10b, g, Table 8). PAR-exposed algae sampled in July, recovered fastest and most efficiently and the initial F_v/F_m values were restored to more than 100 % after 20 h of recovery in dim white light (Fig. 10c, h). Simultaneously, UVR effects on the recovery increased again, e.g. PAB-treated samples of both species recovered slower, leading in *A. esculenta* to an incomplete recovery of only 83 % of the initial F_v/F_m value. In August, recovery from PAR-exposure decreased in both species (Fig. 10d, i) and in September, photosynthetic efficiency of *A. esculenta* and *L. digitata* responded most sensitive to irradiation (Fig. 10e, j). Recovery from photoinhibition was slow and incomplete in all radiation treatments, especially in PAB. Thus,

by the end of the recovery period initial F_v/F_m values of *A. esculenta* were only partly restored to approximately 82, 71 and 65 % after P-, PA- and PAB-exposure, respectively. P-, PA- and PAB-treated *L. digitata* recovered to 93, 92 and 81 %, respectively. Nevertheless, throughout the study period no significant UVR-effect on F_v/F_m persists after 20 h of recovery in these species, except for *A. esculenta* sampled in July, when exposure to PAB resulted in a significant lower degree of recovery compared to P and PA (Table 8).

In *S. latissima*, the sensitivity of F_v/F_m towards PAR and UVR varied widely during the study period (Fig. 10k - o). Photosynthetic efficiency of *S. latissima* was stronger inhibited by PAR, UVAR, and especially UVBR, and recovery was slower compared to the species from shallow water. In *S. latissima* sampled in May, additional UVAR and UVBR resulted in a significantly higher degree of photoinhibition than irradiation with PAR alone (Fig. 10k, Table 8, two-way ANOVA, $p < 0.001$). The recovery in PAB-treated samples to 81 % of the initial F_v/F_m value was incomplete, but did not differ significantly from PAR- and PA- treated samples (Table 8). Similar to *A. esculenta* and *L. digitata*, minimal UVR-effects on F_v/F_m were found after the sea ice break-up in June (Fig. 10l). After 4 h exposure no significant differences were observed between the radiation treatments (Table 8). Recovery proceeded fastest and most efficiently, especially from PAB. After the recovery period, the F_v/F_m value in PAR-exposed samples even exceeded the initial value. From July onwards a stepwise increase in the susceptibility of F_v/F_m towards PAR, UVAR and UVBR was observed, reflected in decreasing recovery rates (Fig. 10m). In contrast to *A. esculenta* and *L. digitata*, incomplete recovery in all three radiation treatments occurred in *S. latissima* already in August (Fig. 10n). In September, the recovery was slow and photosynthetic efficiency recovered to only 76, 80, and 42 % in P-, PA-, and PAB-treated samples, respectively (Fig. 10o). In *S. latissima*, significant UVR-effects on F_v/F_m persist after 20 h of recovery in June, August and September (Table 8).

The Arctic endemic species *L. solidungula* was most sensitive to PAR and UVR, because it showed the lowest recovery rates, and exhibited the strongest seasonal variations in the photosynthetic response (Fig. 10p - t). In May, the response of PS II to artificial irradiation (Fig. 10p) was similar to that of *S. latissima* and did not vary much between May and June, so that a significantly higher degree of photoinhibition due to UVAR- and UVBR-exposure also persists in June (Fig. 10q, Table 8, two-way ANOVA, $p < 0.001$). Despite of this, slightly increased recovery rates in all three radiation treatments resulted in recovery of initial F_v/F_m values to more than 100 % in PAR-exposed samples. In contrast to the other

three species, the photosynthetic response of *L. solidungula* became already less dynamic from July onwards and the vulnerability for PAR and UVR continuously increased. A stepwise decline in recovery rates in all radiation treatments, especially in PAB, was observed. Similar to the other three species studied, *L. solidungula* showed the lowest degree of photoinhibition in all three radiation treatments in September and failed to recover efficiently, resulting in an incomplete recovery of 73, 60, and 21 % after P-, PA-, and PAB-exposure, respectively. Only in *L. solidungula*, F_v/F_m was significantly stronger inhibited by additional UVA and UVB radiation throughout the whole study period (two-way ANOVA, $p < 0.001$, except for September, when PA *vs.* PAR $p < 0.05$) and never recovered completely from PAB-exposure. In contrast to the species from shallow water, significant irradiation-dependent differences in F_v/F_m persisted even after 20 h during all months, except for May (Table 8).

3.3. Photosynthetic pigments and UVR-absorbing compounds

3.3.1. Content and composition of photosynthetic pigments

The photosynthetic pigment content and composition varied significantly in all species throughout the seasons. In *A. esculenta* the Chl *a* content ranged from 369 to 688 nmol/g FW, in *L. digitata* from 184 to 360 nmol/g FW. In these two species, highest Chl *a* content was found in May, when the water was still covered by sea ice (Fig. 11a). After sea ice break-up, the Chl *a* content decreased drastically in *A. esculenta*, and gradually in *L. digitata*. In July, in both species the Chl *a* content was reduced to approximately 50 %. This minimum value was significantly lower compared to the respective maximum value in May (ANOVA, $p < 0.05$). The Chl *a* content strongly increased again in August, reaching in *A. esculenta* almost the value of May, and was, despite of a slight decrease, still high in September. In *S. latissima*, the Chl *a* content varied between 156 and 349 nmol/g FW and in *L. solidungula* between 180 and 393 nmol/g FW. In contrast to the two species from shallow water, the Chl *a* content in *S. latissima* and *L. solidungula* was relatively low in May and reached a minimum already in June (Fig. 11a). In these species, the Chl *a* content tends to increase already in July. In August and September, maximum Chl *a* levels were measured in

S. latissima and *L. solidungula*, respectively, corresponding to a significant increase by approximately 50 % compared to the appropriate minimum values in June (ANOVA, $p < 0.001$).

The seasonal changes in the molar ratios of Chl *c*/Chl *a* were quite similar to changes in the total Chl *a* content in all species (Fig. 11b). However, in *A. esculenta* the Chl *c*/Chl *a* ratio only slightly decreased between May and June, and maximum ratios in *A. esculenta* and *L. digitata* were observed in September. In *A. esculenta* and *L. digitata* the lowest ratio was found in July, which was, in *A. esculenta*, significantly lower compared to May (ANOVA, $p < 0.05$). In August an increase in the Chl *c*/Chl *a* ratio was observed in both species, as well as an approximately 30 % higher ratio in September compared to July (ANOVA, $p < 0.001$). In *S. latissima* and *L. solidungula* the Chl *c*/Chl *a* ratios declined to a minimum already in June and significantly increased from July onwards by approximately 40 % and 30 % to a maximum in August and September, respectively (ANOVA, $p < 0.001$). The observed increase of the ratio in July was more pronounced in *L. solidungula*.

In *S. latissima* and *L. solidungula* Fuc/Chl *a* followed the pattern of Chl *c*/Chl *a* whereas changes in Fuc/Chl *a* ratios did not follow any clear seasonal pattern in *A. esculenta* and *L. digitata* (Fig. 11c). Nevertheless, Fuc/Chl *a* ratios were also in these species highest in August and September, but only significantly in *A. esculenta* (ANOVA, $p < 0.001$).

In general, the ratios of *β*-Car/Chl *a* (Fig. 11d) and of VAZ/Chl *a* (Fig. 11e) exhibited a reverse seasonal pattern to that of the total Chl *a* content. Thus, in *A. esculenta* and *L. digitata*, *β*-Car/Chl *a* and VAZ/Chl *a* ratios were lowest under sea ice cover in May and increased in June, except for *β*-Car/Chl *a* in *A. esculenta.* In July, the maximum ratios were significantly higher than the ratios in May (*β*-Car/Chl *a*: ANOVA, $p < 0.05$, VAZ/Chl *a*: ANOVA, $p < 0.001$ in *A. esculenta* and $p < 0.05$ in *L. digitata*), corresponding to an increase in VAZ/Chl *a* of approximately 140 and 150 % in *A. esculenta* and *L. digitata*, respectively. Lower ratios were measured in August and September. In *S. latissima* and *L. solidungula* maximum *β*-Car/Chl *a* and VAZ/Chl *a* ratios were measured in June, except for *β*-Car/Chl *a* in *S. latissima* which was highest in July. Minimum values were detected in August and September. In both macroalgae, the maximum VAZ/Chl *a* was nearly 180 % higher than the corresponding minimum ratio. Hence, minimum and maximum values of *β*-Car/Chl *a* and VAZ/Chl *a* differ significantly (ANOVA, $p < 0.05$).

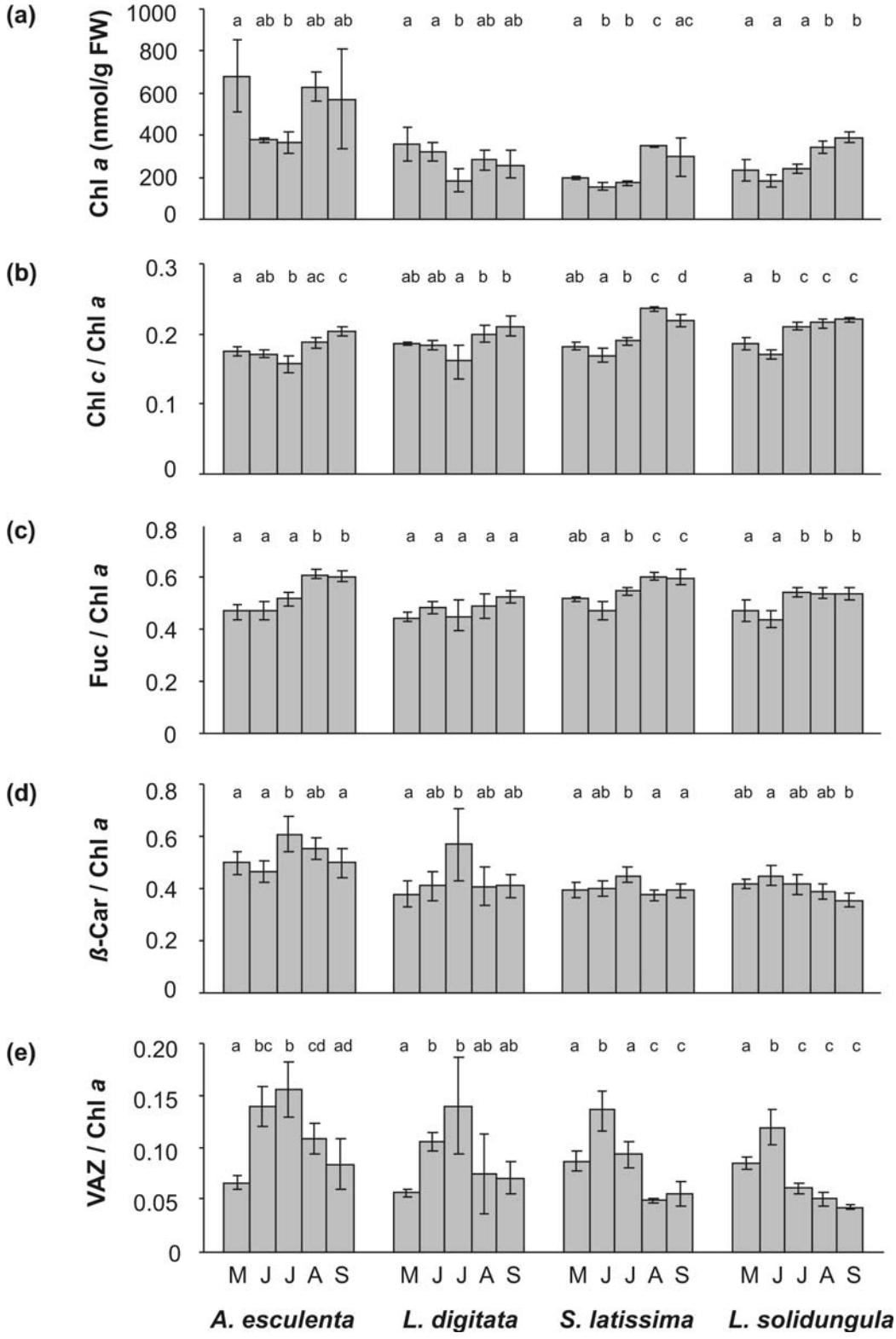

Fig. 11: Seasonal variation in the pigmentation of *A. esculenta*, *L. digitata*, *S. latissima* and *L. solidungula*: (a) chlorophyll *a* content (nmol/g FW, mean ± SD, n = 4), ratio of (b) chlorophyll *c* to chlorophyll *a* (dimensionless, mean ± SD, n = 4), (c) fucoxanthin to chlorophyll *a* (dimensionless, mean ± SD, n = 4), (d) *β*-carotene to chlorophyll *a* (dimensionless, mean ± SD, n = 4), (e) sum of violaxanthin, antheraxanthin and zeaxanthin to chlorophyll *a* (dimensionless, mean ± SD, n = 4). Different lower case letters indicate significant differences in absorbance ratios between months in one species. M J J A S = May, June, July, August, September

Altogether, in all species studied, the main light-harvesting pigments Chl *a*, Chl *c* and Fuc account to more than 90 % of the total pigment content (Table 10). The proportion of photoprotective pigments on the total pigment content was highest in *A. esculenta*, followed by *L. digitata*, *S. latissima*, and finally *L. solidungula*.

Table 10: Proportion of individual pigments on the total pigment content in *A. esculenta*, *L. digitata*, *S. latissima*, and *L. solidungula*, on a seasonal average (mean ± SD, n = 4).

	Proportion of pigment on the total pigment content (%)			
Pigment	*A. esculenta*	*L. digitata*	*S. latissima*	*L. solidungula*
Chl *a*	53.5 ± 2.3	55.5 ± 1.4	53.6 ± 1.4	55.1 ± 1.1
Chl *c*	9.6 ± 0.8	10.5 ± 1.1	10.7 ± 1.2	11.1 ± 1.0
Fuc	28.3 ± 2.5	26.6 ± 1.2	29.1 ± 2.2	27.7 ± 2.0
β-Car	2.8 ± 0.3	2.4 ± 0.4	2.2 ± 0.2	2.2 ± 0.2
VAZ	5.8 ± 2.1	5.0 ± 1.8	4.5 ± 2.0	4.0 ± 1.8

Chl *a* = chlorophyll *a*, Chl *c* = chlorophyll *c*, Fuc = fucoxanthin, *β*-Car = *β*-carotene, VAZ = sum of violaxanthin, antheraxanthin, and zeaxanthin

3.3.2. Content of UVR-absorbing compounds

Absorption spectra of tissue extracts of all species are exemplarily illustrated for samples from July (Fig. 12). All species exhibited absorption maxima at 664 nm and at approximately 430 nm, characteristic for Chl *a*, as well as a broad absorption band from approximately 330 to 500 nm caused by carotenoids and Chl *c*. Strong absorption below 300 nm indicated the presents of substances contributing to the absorption in the UVBR-range and was measured in A. *esculenta*, *L. digitata* and *S. latissima* but not in *L. solidungula*.

Significant seasonal changes in the ratios of the absorption peaks at 273 nm and 664 nm ($Abs_{273/664}$) were found in all species, except in *L. digitata* (Fig. 13). During the study period, absorption ratios $Abs_{273/664}$ ranged from 1.1 to 2.1 in A. *esculenta*, from 1.8 to 2.4 in *L. digitata*, from 1.4 to 1.9 in *S. latissima*, und from 0.5 to 0.7 in *L. solidungula*.

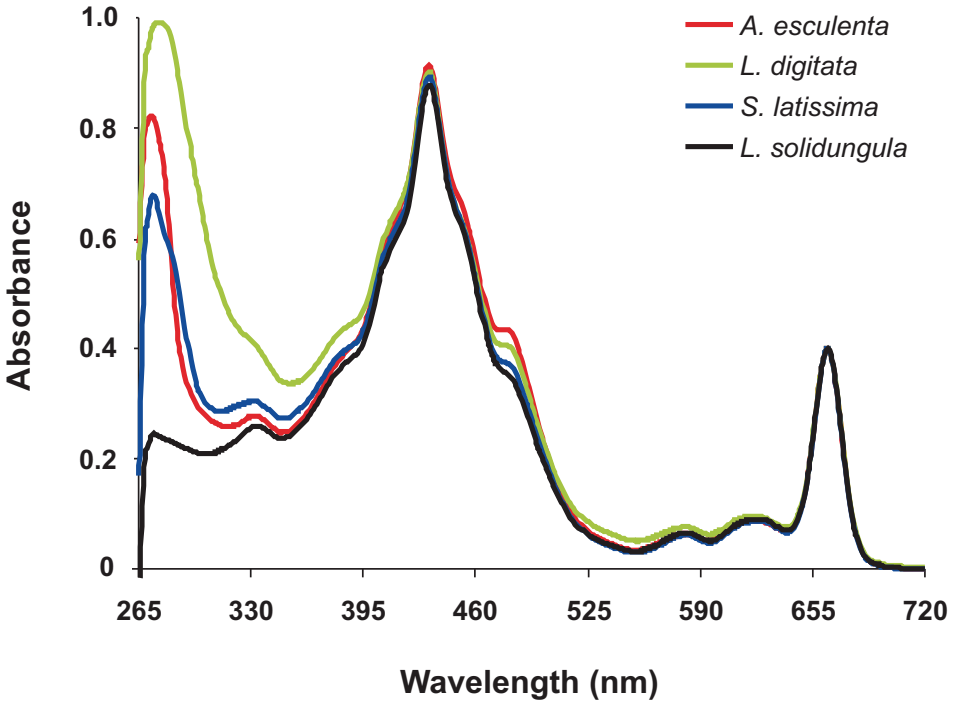

Fig. 12: Absorption spectra of DMF tissue extracts from *A. esculenta* (red curve), *L. digitata* (green curve), *S. latissima* (blue curve), and *L. solidungula* (black curve) sampled in July (mean, n = 4). Spectra are standardized to the absorption maximum of chlorophyll *a* at 664 nm.

In *A. esculenta*, *S. latissima*, and *L. solidungula*, the $Abs_{273/664}$ ratios were lowest in May and increased significantly after sea ice break up and during summer. In *A. esculenta* a maximum $Abs_{273/664}$ ratio was observed in August, corresponding to an increase of approximately 90 % compared to May (ANOVA, $p < 0.05$). In *S. latissima* and *L. solidungula* the $Abs_{273/664}$ ratios increased by approximately 40 and 30 %, respectively to a significantly higher maximal value in June (ANOVA, $p < 0.05$) and subsequently decreased again. Nevertheless, at any time of the study period, the $Abs_{273/664}$ ratio in *L. solidungula* was two- to four-times lower compared to that of the other three species, resulting in a significant lower $Abs_{273/664}$ ratio on a seasonal average (Kruskal-Wallis-Test, $p < 0.001$).

No seasonal pattern of $Abs_{273/664}$ ratios was found in *L. digitata*. This species revealed relatively high $Abs_{273/664}$ ratio throughout the sampling period without significant differences. On a seasonal average, the highest $Abs_{273/664}$ ratio was found in *L. digitata*, followed by *A. esculenta*, *S. latissima*, and *L. solidungula*.

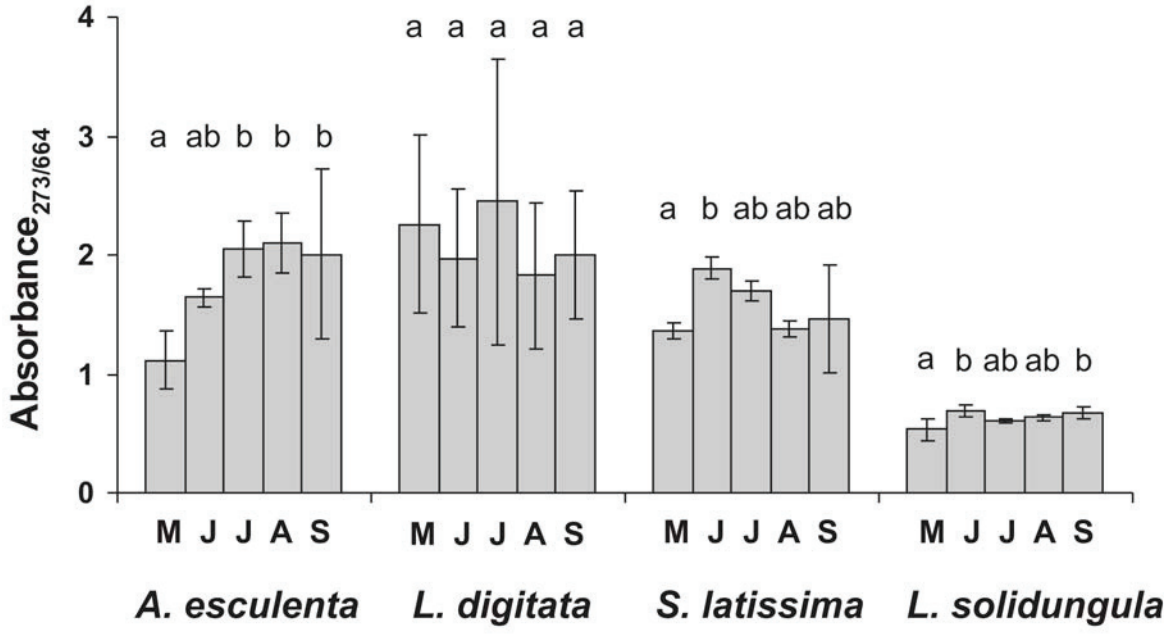

Fig. 13: Seasonal changes in UVR-absorbing compounds in tissue extracts from *A. esculenta*, *L. digitata*, *S. latissima*, and *L. solidungula*. The absorption maximum in the UVR-region at 273 nm was normalised to the absorption maximum of chlorophyll *a* at 664 nm (mean ± SD, n = 4). Different lower case letters indicate significant differences in absorption ratios between months in one species. M J J A S = May, June, July, August, September

3.4. Relationship between physiological parameters and environmental conditions

Correlation coefficient for the parameter measured, are given in Table 11, indicating the extent to which two parameters did or did not vary together. The correlation coefficient reaches values between -1 and +1 and indicates the strength and direction of a linear relationship between two variables. If two variables tend to vary together, then the correlation coefficient will be positive. On the other hand, if one of the variables tends to rise when the other one declines, then the correlation coefficient between the two variables will be negative. The closer the coefficient is to either -1 or +1, the stronger is the correlation between the variables. However, correlation does not imply causation and, hence, cannot indicate a causal relation.

Table 11: Correlation coefficients (r) after Pearson, indicating the strength and direction of a linear relationship between two variables. PAR = monthly mean of ambient PAR at the respective growth site, temperature = seawater temperature, F_v/F_m recovery = F_v/F_m (%) in PAR-exposed samples after 20 h of recovery, F_v/F_m inhibition = F_v/F_m (%) after 4 h exposure to PAR+UVAR+UVBR, $Abs_{273/664}$ was used as a measure of the relative content of UVR-absorbing compounds.

	Correlation coefficient (r)			
Variables	*A. esculenta*	*L. digitata*	*S. latissima*	*L. solidungula*
α *vs.* PAR	- 0.91*	- 0.50*	- 0.95	- 0.43
$rETR_{max}$ *vs.* temperature	0.78	0.94	0.93	0.94
VAZ/Chl *a vs.* PAR	0.62*	0.47*	0.80	0.62
α *vs.* (Chl *c* + Fuc)/Chl *a*	0.70	0.59	0.66	0.91
F_v/F_m recovery *vs.* VAZ/Chl *a*	0.63	0.82	0.82	0.84
F_v/F_m recovery *vs.* α	- 0.75	- 0.96	- 0.67	- 0.79
F_v/F_m recovery *vs.* Chl *c*/Chl *a*	- 0.99	- 0.90	- 0.72	- 0.83
F_v/F_m inhibition *vs.* $Abs_{273/664}$	0.29	- 0.14	0.54	0.85

* As monthly mean of underwater PAR at the growth site of *A. esculenta* and *L. digitata*, the average of the respective mean values at 0.5 and 2 m water depths was used.

4. Methodological considerations

4.1. Measurements of seawater temperature

Throughout the seasons the water temperature of Kongsfjorden was measured in the seawater pumped directly from a water depth of 1.5 m into the flow through system of the experimental setup in the laboratory. Despite the short distance between fjord and laboratory, warming or cooling of the water could not be excluded, when passing the pipeline. However, the fact that the stratification of different water masses was not taken into account, might had an even more severe effect on the temperature measured. Therefore, the measured temperatures given in Table 5 are approximation values of the actual water temperatures at the respective growths sites. A detailed description of temperature gradients between seasons and different water depths is given by Svendsen et al. (2002).

4.2. Experimental radiation conditions

A critical point of most laboratory studies is the emission of artificial light sources which hardly meets the natural solar spectrum. In the field, high UVR levels are always accompanied by high levels of PAR, which is barely the case in laboratory radiation treatments but most important for realistic ecological plant experiments. In the laboratory relatively high levels of artificial PAR were generated by four daylight fluorescence tubes (Osram L58W/950, Germany). Ultraviolet radiation was produced by a special fluorescent lamp (UVA-340, Q-Panel, Cleveland, USA), emitting a spectrum similar to that of sunlight at wavelengths below 340 nm, with no emission below the natural solar cut-off at 295 nm (Bischof et al. 1998b). The resulting PAR/UVAR/UVBR ratio of 100/2.2/0.2 did not entirely match the natural solar ratio of 100/10/0.6 at the Earth's surface (Franklin and Forster 1997). Compared with a natural ratio of 100/2.75/0.06, which was measured in the field at a water depth of 0.5 m in June, the artificial ratio of PAR/UVAR was similar to the natural one, whereas artificial UVBR was overrepresented and thus rather represents a future scenario of solar radiation with an increased proportion of UVBR.

While being aware of these restrictions, the laboratory experiments were useful to study seasonal changes in the acclimation status and the potential for dynamic photoinhibition of the algae. Preliminary experiments ensured that the irradiances chosen for the experimental setup were high enough to cause inhibition of photosynthetic activity in all species studied and were, at the same time, low enough to allow recovery, so that variations in these parameters could be studied throughout the season. Moreover, the light intensities were realistic since they occurred during summer in shallow waters in the field (Table 6).

4.3. Pulse amplitude modulated fluorescence measurements

Employing pulse amplitude modulated (PAM) fluorometry photosynthetic activity is very quickly to measure *in vivo*. Over a wide range of physiological conditions, fluorescence parameters are directly proportional to the quantum yield of non-cyclic electron transport (Genty et al. 1989). However, fluorescence values may be misinterpreted, since differences between photosynthetic oxygen production or carbon fixation and fluorescence parameters have been found in algae (Hanelt and Nultsch 1995, Schofield et al. 1995). The fluorescence ratio F_v/F_m is not well suited to reflect changes in the photosynthetic capacity as determined by oxygen measurements, because changes in the saturation level of fluence rate response curves are not well correlated with changes in the variable fluorescence (Hanelt and Nultsch 1995, Hanelt et al. 1995). In contrast, photosynthetic efficiency (i.e. non-saturated photosynthetic rate) is strongly correlated with F_v/F_m, therefore, fluorescence measurements are a powerful tool for the investigation of radiation stress of the energy converting photosynthetic apparatus in photoinhibition experiments (Hanelt et al. 1992, Dring et al. 1996). Moreover, a positive linear or curvilinear relationship between photosynthetic rates measured by oxygen electrodes and those measured as electron transport rates by PAM fluorometry (determined from P-E curves) have been demonstrated in studies on *Ulva* species (Chlorophyta) and seagrasses (Beer et al. 1998, 2000). Also in brown macroalgae, PAM fluorometry can be used to accurately measure relative photosynthetic electron transport rates, since rETR and rates of photosynthetic O_2 evolution are linearly related, as long as the effective quantum yield of PS II ($\Delta F/F_m'$) is > 0.1 (Beer and Axelsson 2004). Thus, the maximum relative photosynthetic electron transport rate ($rETR_{max}$) measured by PAM

fluorometry and the maximum rate of photosynthesis (P_{max}) measured by oxygen evolution, may both serve as an indicator for photosynthetic capacity. However, it should be noted that by plotting P-E curves as rETR *vs.* incident irradiance, correct values of α are obtained while $rETR_{max}$ and E_k might be overestimated (Saroussi and Beer 2007). However, the focus of the present study was on the relative changes of these photosynthetic parameters during the seasons. Nevertheless, even if fluorescence data indicate acclimation to environmental or experimental conditions, this does not inevitably imply that the experimental individuals are unaffected, since, e.g., UVR-exposure may exert effects on growth rate and reproduction success, which are not necessarily reflected neither by changes in the fluorescence signal nor in measurements of photosynthesis at all (Ding et al. 1996).

4.4. Xanthophyll cycle pigments

Even though the contents of the three pigments violaxanthin, antheraxanthin and zeaxanthin contributing to the xanthophyll cycle were measured individually, stating the pool size of these pigments (VAZ) was more meaningful in order to represent the acclimation status of the algae. That is because the interconversion of these pigments requires only minutes and might have taken place during the transportation of the collected seaweeds to the laboratory.

5. General discussion

5.1. Seasonal environmental changes

5.1.1. Factors determining the underwater radiation regime

In the Arctic, benthic communities are subjected to extreme seasonal environmental changes, particularly to strongly fluctuating light intensities due to seasonal variations in solar elevation and daylength (Sakshaug and Slagstad 1991, Gross et al. 2001, Hanelt et al. 2001, Svendsen et al. 2002, Rysgaard et al. 2008, Sejr et al. 2008). On the west coast of Spitsbergen (79° N, 12° E), the sun stays below the horizon from 25 October to 17 February and the

midnight sun period lasts from 18 April to 23 August (Svendsen et al. 2002). The strong fluctuations of solar radiation at the Earth's surface during the summer season (Fig. 4b - d) are caused by a number of factors such as surface albedo due to snow and ice-covered surroundings, atmospheric absorption and scattering by gas molecules, aerosols, clouds and fog (Kirk 1994, Ørbæk et al. 1999, Svendsen et al. 2002). The comparison of spectroradiometric measurements and data derived from TOMS (total ozone mapping spectrometer) and ozone probes revealed that the irradiance of UVBR reaching the Earth's surface at the Kongsfjorden area strictly depends on the actual ozone concentration in the atmosphere above (Gross et al. 2001, Hanelt et al. 2001). Consequently, the seasonal depletion of the stratospheric ozone layer is an important factor controlling the underwater UVBR intensity.

In aquatic ecosystems, the radiation regime depends, beside on atmospheric conditions, also on the transmission across the air-water interface, on the tidal cycle, and on the optical properties of the water column (Kirk 1994, Hanelt et al. 2001). Wind conditions and wave actions influence the reflectance of the incident light by the water surface (Kirk 1994). In Arctic spring, the underwater light climate is controlled by the presence/absence and structure of sea ice and snow covering the fjord. The yearly variations of the ice conditions inside Kongsfjorden are described by Mehlum (1991) and Ito and Kudoh (1997). The photosynthetically active radiation measured under the sea ice was only 3 % of surface PAR after passing a 1.3 m thick ice cover and a 5 cm snow layer. A comparable attenuation of PAR was also reported by Hanelt et al. (2001) under similar ice and snow conditions in Kongsfjorden in 1998. The findings of the present study are also in line with data on the spectral distribution of light beneath the sea ice in the Arctic Ocean, published by Maykut and Grenfell (1975), reporting vertical attenuation coefficients (K_d) for sea ice of 1.5 m^{-1} for PAR. Approximately 20 % of incident PAR is able to pass through a 1 m thick layer of sea ice, which shows a maximum transmittance in the wavelength range of 450 to 550 nm. Only 1 % of surface radiation is transmitted when the ice is covered by snow to about 30 cm due to higher attenuation of PAR by snow (K_d = 16 - 45 m^{-1}) (Palmisano et al. 1987).

The residual light that penetrates the water surface is controlled by the inherent optical properties of the water body, which are governed by scattering and absorption by water molecules, chromophoric dissolved organic matter (CDOM, yellow substance), organic particles (e.g. phytoplankton), and inorganic sediments. In the present study, UV radiation (λ < 400 nm) and red light (λ > 600 nm) were attenuated most strongly (Fig. 6),

corresponding to the spectral data of Hanelt et al. (2001). While photosynthetic pigments of the phytoplankton contribute to the attenuation of PAR, the light attenuation in the blue and UVR-region is mainly cause by dissolved organic matter (Jerlov 1976, Kirk 1994, Tedetti and Sémperé 2006). However, due to the low run-off of organic material from the sparse vegetation on land, the concentration of CDOM is typically low in the Arctic, even in coastal waters. Hence, in Kongsfjorden, the content of mineral sediment particles is the main factor controlling the penetration of both, PAR and UVR, into the water column (Fig. 6, Svendsen et al. 2002). Suspended particulated matter (organic and inorganic) enters the fjord via terrestrial run-off and glacial meltwater with direct consequences for the spectral composition of the underwater radiation regime and the extent of the euphotic zone. The freshwater, running into Kongsfjorden, mainly derives from ice- and snowmelt, glacier ablation, summer rainfall and ice calving (Svendsen et al. 2002). The total annual freshwater discharge into the fjord has been estimated at 1370 x 10^6 m^3 (Svendsen et al. 2002). At the sampling site of *A. esculenta* and *L. digitata*, the main source of turbid freshwater inflow was the nearby calving front of the glacier Blomstrandbreen, while the sampling sites of *S. latissima* and *L. solidungula* were mainly affected by the glacial run-off from Lovénbreen (Fig. 2). For the Lovénbreen and the neighboring Pedersenbreen, an annual run-off of 42 x 10^6 m^3 was calculated (Svendsen et al. 2002). Environmental gradients in sedimentation along the length and the depth of the fjord show marked seasonality and were described by Svendsen et al. (2002). The particles exported by the glaciers are mainly trapped in the inner part of the fjord. A peak of sediment concentration is found close to the glacier front with a sediment accumulation rate of 20,000 g m^{-2} $year^{-1}$ which decreases towards the central part of the fjord by one order of magnitude (1800 - 3800 g m^{-2} $year^{-1}$) and by another order of magnitude (200 g m^{-2} $year^{-1}$) towards the outer fjord. The vertical distribution of sediments is characterized by subsurface maxima in 10 to 20 m depths. In April, the sediment accumulation rates begin to increase and reach a maximum in July, since the main freshwater input to the fjord occurs in the summer season. By the mid of September, the process is almost completed (Svendsen et al. 2002).

5.1.2. Light history of the algae

The species *A. esculenta*, *L. digitata* and *S. latissima* experienced lowest underwater radiation under the sea ice shield in May due to the strong attenuation by ice and snow, despite of clearest water conditions, as reflected in lowest K_d values and in a similar PAR and UVAR transmittance (Table 4). At Kongsfjorden the sea ice usually breaks up between April and early June within a few days (Mehlum 1991, Gerland et al. 1999), coinciding with maximum daylength, high solar radiation, high albedo due to snow and ice covered surroundings, and high transmittance of the water column characteristic for this time of the year (Chapman and Lindley 1980, Dunton and Schell 1986, Dunton 1990, Ørbæk et al. 1999, Hanelt et al. 2001, Bischof et al. 2002, Borum et al. 2002). Consequently, *A. esculenta*, *L. digitata* and *S. latissima* had to cope with suddenly strongly increased underwater irradiances after the sea ice break-up at the end of May (Fig. 5, Table 6). With rising air and water temperatures in June and July (Fig. 4a, Table 5) turbid freshwater was discharged into the fjord and, therefore, transmittance of the water column strongly decreased to a minimum in early July (Fig 6). Hence, despite of high solar radiation, *S. latissima* and *L. solidungula* at 4 and 18 m water depth faced low light conditions in July due to strong attenuation of the water column above (Table 6). In contrast, the sampling site of *A. esculenta* and *L. digitata* between 0.5 and 2 m depth remained exposed to relatively high irradiances of PAR, while UVAR and especially UVBR strongly decreased in July because of the wavelength-selective attenuation by particulate matter (Table 6, Svendsen et al. 2002). This specific attenuation by particles was also the reason why the sampling site of *L. solidungula* was permanently protected against UVB radiation (Table 6). After the melting of snow around the fjord, the freshwater influx continuously decreased. However, the resulting increase in water transparency (Fig. 6) was counteracted by decreasing solar radiation due to the gradually decreasing solar zenith angle in August and September (Fig. 4b - d). Since daylengths are shorter underwater, macroalgae sampled in September were already exposed to conditions characteristic for autumn (Lüning and Dring 1979, Gómez et al. 1997, Kain 2006).

5.1.3. Seasonal changes in abiotic factors at different geographic regions

The observed seasonal fluctuations in the underwater radiation regime are comparable with studies from other polar regions, for instance from the Alaskan and Canadian High Arctic (Chapman and Lindley 1980, Dunton and Schell 1986, Dunton 1990) and from Antarctica (Drew and Hastings 1992, Kirst and Wiencke 1995). Thus, Arctic and Antarctic waters are generally characterized by darkness and low light conditions prevailing during winter and spring under the sea ice. After the ice break-up in spring or summer, radiation penetrates to considerable depths until water transparency decrease in summer by the development of plankton blooms and turbid meltwater in coastal areas. However, the length of the open water period differs between regions. An important difference between Arctic and Antarctic waters is the fact that other abiotic factors such as salinity, temperature and nutrients remain almost constant in Antarctic waters, i.e. low temperatures and high nutrient concentrations persist throughout the year (Drew and Hasting 1992, Kirst and Wiencke 1995, Weykam 1996, Peters et al. 2005).

The strong depletion of available inorganic nutrients during the summer months is a feature that Arctic waters have in common with cold temperate waters (Chapman and Craigie 1977, Chapman and Lindley 1980, Wheeler and North 1981, Dunton et al. 1982, Conolly and Drew 1985, Kain 1989, Lüning 1990, Makarov et al. 1999, Aguilera et al. 2002b). However, compared to polar regions, seasonal changes in seawater temperature are greater in cold temperate regions where temperatures in summer and autumn are much higher (Lüning 1971, Drew 1983, Kain 1989, Hanelt et al. 2002). At the poleward distribution limits of seaweeds, at 77° S and 80° N, respectively, the annual solar radiation is 30 to 50 % less than in temperate and tropical regions due to the lower solar elevation (Kondratyev 1954). Even though lower latitudes are generally characterized by higher solar irradiances and the absence of sea ice, the annual underwater quantum budget might be lower compared to Arctic waters, e.g. in the North Sea near Helgoland (German Bight) the total annual photon flux density of PAR received at 8 m water depth was 71 mol m^{-2} $year^{-1}$, whereas in the Canadian High Arctic near Igloolik an annual quantum budget of 590 m^{-2} $year^{-1}$ was measured at the same water depth (Lüning and Dring 1979, Chapman and Lindley 1980). This enormous difference is accounted for by differences in the water transparency. Also the water column of Kongsfjorden exhibits a higher irradiance transmittance compared to cold temperate coastal

waters around Helgoland due to substantially lower amounts of CDOM (Lüning and Dring 1979, Dring et al. 2001, Hanelt et al. 2001). Altogether, the seasonal changes in underwater radiation are less pronounced in cold temperate regions but the seasonal pattern is similar to that of Arctic regions (Lüning 1971).

The strong seasonal fluctuations in ambient conditions were mirrored in changes of the photosynthetic characteristics and pigmentation of the seaweeds studied, illuminating the seasonal physiology and acclimation potential of the species.

5.2. Acclimation of macroalgae to seasonal changes in environmental conditions

Alterations of the photosynthetic apparatus and physiological processes, reflected in changes in photosynthetic characteristics and pigmentation, enable the algae to remain productive despite of widely changing ambient conditions. Acclimation of seaweeds was observed in laboratory and field experiments in response to changes in light quantity and quality (Brinkhuis 1977, Rosenberg and Ramus 1982, Lewey and Gorham 1984, Dring 1986, Henley and Ramus 1989, Fillit 1995, Bischof et al. 2002), water temperature (Davison et al. 1991, Wiencke et al. 1993, Machalek et al. 1996), nutrient levels (Stengel and Dring 1998), and daylength (Gómez et al. 1995, Gómez and Wiencke 1997, Lüder et al. 2001).

Photoacclimation involves coordinated changes in the composition and functioning of the photosynthetic apparatus in response to variations in irradiance. Several strategies of photoacclimation are based on changes in the composition and abundance of photoprotective and light-harvesting pigments and associated proteins, in the abundances and ratios of PS I and PS II reaction centers, of other catalysts within the electron transport chain and elements of the carbon metabolism (Sukenik et al. 1987, Falkowski and LaRoche 1991, Silva et al. 1998, Raven and Geider 2003, Falkowski and Raven 2007). However, since irradiances in the field are fluctuating and photoacclimation takes time, the photosynthetic characteristics and pigments measured are continually changing and in principle never entirely matching the instantaneous irradiance. Thus, the occasionally observed time lag between e.g. highest E_k or maximum photoprotective pigment content and maximum underwater irradiances may reflect

acclimation to lower incident irradiance that reached the habitat earlier. This might be particularly relevant for samples of *A. esculenta* and *L. digitata* in June, because they were collected only four days after the sea ice break-up, while *S. latissima* was exposed to high ambient light for 14 days before collection.

5.2.1. Seasonal changes in photosynthetic characteristics

The relative maximum electron transport rates ($rETR_{max}$) measured are within the range of 2 to 38 relative units reported for Arctic and Antarctic macroalgae (Beer et al. 1998, Lüder et al. 2001, Bischof et al. 2002, Runcie and Riddle 2006). Due to thermal acclimation, Arctic species might reach photosynthetic capacities comparable to conspecifics from cold temperate regions (Davison et al. 1991). However, the only directly comparable data on $rETR_{max}$ were measured in *S. latissima* from the English Cannel (France) at a seawater temperature of 8 °C in winter and amounted to 36 relavite units (Gévaert et al. 2002).

The photosynthetic efficiencies at sub-saturating irradiance (α), estimated from PAM recorded P-E curves, are not easy to compare with other studies, since apart from the present study, most data available are based on measurements of oxygen production and thus given in dissimilar units. However, the α values are in line with those reported for *S. latissima* from the English Channel (France) ranging from 0.38 to 0.53 relative units (Gévaert et al. 2002).

In general, light saturating points of photosynthesis (E_k) are low in Arctic species. The measured irradiances for photosynthetic saturation are similar to those reported for various polar macroalgae ranging from 4 to 60 µmol photons m^{-2} s^{-1} (Wiencke et al. 1993, Gómez et al. 1995, Gómez and Wiencke 1997, Gómez 2001, Bischof et al. 2002, Runcie and Riddle 2006). For *L. digitata*, *S. latissima* and *L. solidungula* also higher E_k values are found in the literature (King and Schramm 1976, Dunton and Jodwalis 1988, Borum et al. 2002). However, different measuring methods were used and the seaweeds were exposed to considerably higher irradiances, suggesting that the algae had not the same acclimation state as in the present study (Dunton and Schell 1986, Borum et al. 2002). Furthermore, it has been shown that the use of different P-E curve modeling equations significantly influences the outcome of the values, e.g., calculated P_{max} and α values may differ up to 24 % by the use of different fit procedures (Frenette et al. 1993, Aalderink and Jovin 1997).

Generally, all species studied acclimated to changes in environmental conditions by increasing E_k and $rETR_{max}$ and decreasing α during the period of higher light intensities after the sea ice break-up in May (Table 6, Fig. 7, 8, 9). These changes allow efficient photosynthesis during high light conditions and the increased photosynthetic capacity reduces the susceptibility to photoinhibition and photodamage by decreasing the amount of excess energy (Park et al. 1996, Savitch et al. 2000). With reduced light transmittance through the water column in midsummer and lowered solar radiation by the end of summer, an inverse pattern of these photosynthetic parameters was observed. Thus, all species acclimated to lower irradiances by increasing their ability to capture photons (higher α) and reaching saturation of photosynthesis at lower irradiance (lower E_k), thereby remaining productive.

The results are in accordance with the photoacclimation theory of algae and higher plants and agree with field and laboratory studies showing that macroalgae, which are acclimated to high light intensities, usually have higher maximum photosynthetic capacities (P_{max}, $rETR_{max}$), higher photosynthetic saturation points (E_k), and lower photosynthetic efficiencies (α) compared to low light acclimated algae (Hsiao 1990, Machalek et al. 1996, Bischof et al. 1999, Gévaert et al. 2002, Raven and Geider 2003, Runcie and Riddle 2006).

On its own, the light saturation point of photosynthesis (E_k) is not a convenient indicator of the photoacclimational status. This is, because E_k equals photosynthetic capacity (P_{max}, $rETR_{max}$) divided by photosynthetic efficiency at sub-saturating irradiances (α), and hence, any environmental factor which reduces the maximum photosynthetic capacity to a greater extend than it affects α, will reduce E_k (Kirk 1994). For example, a lower temperature lowers E_k by diminishing the photosynthetic capacity without affecting α. This is because the rates of dark respiration and carboxylation decrease with decreasing temperature (Kirk 1994). Thus, from lower E_k values alone cannot be concluded that the light-harvesting capability has increased. Rather, the ratio of the light-harvesting capability to the carboxylation rate has increased by elevated pigment content and/or by a depletion of a surplus of carboxylation capacity.

Since measurements of photosynthetic parameters were carried out at the prevailing water temperature at the respective time, it is not possible to determine whether photoacclimation or thermal acclimation accounted for changes in E_k. The observed seasonal variations of E_k were most likely caused by an interaction of both, since in all species studied, a negative correlation between α and ambient PAR implies that α was strongly effected by underwater irradiance (Table 11). This finding is in accordance with the photoacclimation response

reported for *S. latissima* (Machalek et al. 1996). In contrast, the correlation between $rETR_{max}$ and ambient light was weak, which is in line with the postulated light-independence of the photosynthetic capacity (P_{max}) in *S. latissima* (Machalek et al. 1996). However, changes in $rETR_{max}$ were positively correlated with the seawater temperature, rather than with the monthly mean of PAR (Table 11). Such metabolic effects of temperature on the photosynthetic capacity have been previously reported by Davison et al. (1991) and Wiencke et al. (1993) and it was shown that temperature plays a role in controlling carboxylation processes since PEPCK and RUBISCO activities were positively correlated with variations in water temperature in *L. hyperborea* (Küppers and Weidner 1980). However, this finding contrasts studies which have shown, that low-temperature grown plants of *S. latissima* compensate for the reduction in the activity of individual enzyme molecules by increasing the content of Calvin cycle enzymes (Davison 1987, 1991, Davison and Davison 1987, Davison et al. 1991, Machalek et al. 1996). Finally, the photosynthetic capacity might also underlie a programmed seasonal pattern, triggered by photoperiod as shown in the brown alga *Desmarestia menziesii* and the red alga *Palmaria decipiens* (Gómez and Wiencke 1997, Lüder et al. 2001).

The observed changes in the photosynthetic characteristics were associated with changes in pigment composition of the photosynthetic apparatus.

5.2.2. Seasonal changes in photosynthetic pigments and UVR-absorbing compounds

Generally, all species studied, acclimated to changes in environmental conditions by reducing their amounts of photochemically active and accessory pigments (i.e. Chl *a*, Chl *c*, Fuc) as well as their ratio of accessory pigments to chlorophyll *a* during the period of high underwater irradiances (Fig. 11a - c). Thus, after the sea ice break-up in May, the algae might have reduced their energy costs by reducing excessive amounts of light-harvesting pigments and/or protected their photosynthetic apparatus from photodamage due to absorption of too many photons by reducing their light capture ability. Analogous, with reduced light availability in summer, these pigment contents and ratios increased again, enabling the plants

to make best use of low photon flux densities and thus preventing light limitation of photosynthesis. Hence, the photoacclimation strategy of the species studied, involves alterations of the number and/or the size of the photosynthetic units (PSUs). Chlorophyll *a* is present in both, in the reaction centers (RCs) and in the light-harvesting complexes (LHCs) of the algae (Douady et al. 1993, Trissl 2003). Thus, higher Chl *a* contents under sea ice in May and at the end of the sampling period indicate an increase in the RCs and/or in the size of the antennae (Falkowski and Owens 1980, Falkowski et al. 1981). Beside Chl *a*, Chl *c* and Fuc are the primary light-harvesting pigments in brown algae. These pigments occur only in the antennae (Passaquet et al. 1991, Douady et al. 1993, De Martino et al. 2000, Trissl 2003). Since the size of a PSU is indicated by the number of light-absorbing pigment molecules contributing excitation energy to a reaction center, i.e. by the ratio of antennae to reaction center or simply by the ratio of accessory pigments to Chl *a*, the marked increase in the Chl *c*/Chl *a* and Fuc/Chl *a* ratios during low light conditions is indicative for an increase in the PSU size (Mauzerall and Greenbaum 1989, Trissl 2003, Falkowski and Raven 2007). The observed increase of Chl *c* and Fuc in relation to Chl *a* during lower ambient light results in an increase in the functional absorption cross-section and therefore in the amount of photons that can potentially be absorbed by each LHC (Falkowski and LaRoche 1991, Falkowski and Raven 2007).

In contrast, the seasonal changes in the pool size of the photoprotective xanthophyll cycle pigments (VAZ) and *β*-carotene (*β*-Car) in relation to chlorophyll *a* as well as the relative content of UVR-absorbing compounds showed the opposite trend (Fig. 11d, e, Fig. 13). The strategy of photoprotection the kelps employed include an increase in the absorption of photons by pigments that dissipate the absorbed energy as heat instead of transferring it to the reaction center Chl *a*, thereby lowering the absorption cross-section of PS II (Demmig-Adams 1990, Demmig-Adams and Adams III 1992, Falkowski and LaRoche 1991, Olaizola et al. 1994). In the reaction centers, *β*-carotene is located next to the chlorophyll *a* dimer and acts as a direct quencher of ^{3}Chl*, thereby avoiding energy transfer to triplet oxygen. Illumination promotes the formation of zeaxanthin, likewise an effective direct quencher of ^{3}Chl*, via *de novo* synthesis and rapid enzymatic de-epoxidation of violaxanthin via the xanthophyll cycle (Fig. 1, Demmig-Adams 1990, Frank et al. 1994). An increase in heat dissipation by the interconversion of the three xanthophylls violaxanthin, antheraxanthin and zeaxanthin within the xanthophyll cycle, was shown for green and brown algae (Uhrmacher et al. 1995, Schofield et al. 1998, Rodrigues et al. 2002). Thus, zeaxanthin and *β*-carotene

may prevent the photosynthetic apparatus against photodamage by non-photochemical quenching of excess excitation energy and by their antioxidative activity (Niyogi 1999, Müller et al. 2001, Franklin et al. 2003). In addition, photoprotection against harmful UVB radiation was achieved by the accumulation of UVR-screening substances.

Beside radiation conditions also nutrient levels have been shown to affect the pigment content, e.g. Chl *a* content in fucoid *Ascophyllum nodosum* increases under nitrogen enrichment (Stengel and Dring 1998). However, even though low pigment contents coincided with nutrient depletion, the effect of nutrient levels on algal pigmentation is probably neglectable for the species studied here. This is, because Gordillo et al. (2006) reported that *A. esculenta* and *L. solidungula* from Kongsfjorden responded to nutrient enrichment in summer with a significant decrease in their Chl *a* content (µg/g FW), while nutrient enrichment had no significant effect on the Chl *a* content of *S. latissima* and on the carotenoids/Chl *a* ratios of all three species (Gordillo et al. 2006).

Hence, the observed seasonal changes in algal pigmentation follow the classical view of photoacclimation responses in microalgae, macroalgae and higher plants (Falkowski and Owens 1980, Falkowski et al. 1981, Anderson 1986, Demmig-Adams 1990, Thayer and Björkman 1990, Falkowski and LaRoche 1991, Anderson et al. 1995, Horton et al. 1996, Häder and Figueroa 1997, Raven and Geider 2003). The findings agree with laboratory and field studies on seaweeds of the three taxonomic classes, where low light availability was generally reflected in higher contents of the major light-harvesting pigments as well as in higher ratios of accessory pigments/Chl *a* (Ramus et al. 1976a, 1977, Rosenberg and Ramus 1982, Lewey and Gorham 1984, Dring 1986, Henley and Ramus 1989, Fillit 1995). In contrast, acclimation to higher irradiances of PAR and UVR generally resulted in an increase of the pool size of the xanthophyll cycle pigments (VAZ) in relation to Chl *a* and in an accumulation of UVR-absorbing compounds (Aguirre von Wobeser et al. 2000, Colombo-Pallotta et al. 2006).

However, the low Chl *a* content in *S. latissima*, found under dim light conditions in May, is possibly a result of pigment "dilution" caused by rapid growth, since it is in line with the seasonal growth rhythms of this species (Lewey and Gorham 1984, Henley and Dunton 1995). Arctic *S. latissima* from the Alaskan Beaufort Sea, where the ice cover usually persists until June, exhibits maximum growth rates between late April and late July (Dunton 1985). The higher Chl *a* and total pigment content in shallow-water *A. esculenta*, compared to the other three species (Fig. 11a), is due to morphological differences between the thallus

structures, since *A. esculenta* possesses a higher proportion of photosynthetically active cortical cells. The surprising fact, that *L. solidungula* growing under extreme low light conditions does not contain significantly more light-harvesting pigments than the other three species might be explained by a lower proportion of photosynthetic tissue per unit biomass. This is, because *L. solidungula* had the thickest thallus of the species studied. Nevertheless, also exceptions to the acclimation theory are found in the literature, e.g. acclimation to lower irradiances does not necessarily include an increase in pigment content (Rodrigues et al. 2000, Runcie and Riddle 2006). Also Henley and Dunton (1995) did not find any obvious qualitative or quantitative difference in the pigmentation between *L. solidungula* and *S. latissima* that would suggest different light-harvesting efficiencies. Raven (1984) and Markager (1993) showed that an increment in the number of photons absorbed under very low light conditions would not necessarily compensate for the costs of the synthesis of additional pigments. Only for optically thin algae, an increase in pigments will result in a net increase in photosynthesis at low light intensities, whereas in optically thick algae, e.g. in optically opaque *L. solidungula*, the chlorophyll will be heterogeneously light exposed and thus unequally efficient (Ramus et al. 1976b). As reported by Enríquez et al. (1994), an increase in thallus thickness might be more effective to increase light capture than is an increase in pigment content. This is because with increasing thallus thickness, pigments can be distributed more effectively, avoiding packing and self shading, and thereby increasing the absorption cross-section. Additionally, multiple scattering within the thallus increases the effective path length and, hence, the absorption of photons (Ramus 1978, 1990). The price paid for a thallus structure as a light-collecting strategy is higher respiration and slower growth, as respiration is directly related to frond structure (Markager and Sand-Jensen 1992). Thus, *L. solidungula* might optimize its light absorption at low light intensities not by increasing the pigment content but by absorbing light more efficiently, as suggested by Rodrigues et al. (2000). They found that the deep water *Laminaria abyssalis* contained only half of the pigment content per thallus area compared with the intertidal *L. digitata*, whereas dark respiration rate and thallus thickness were similar. At the same time, photosynthetic efficiency on a Chl *a* basis was higher in *L. abyssalis*. Hence, the photosynthetic apparatus of *L. abyssalis* was, under saturating light, as efficient as *L. digitata*, and under limiting light even more efficient.

The UVR-absorbing substances found in the species studied, showed absorption characteristics of phlorotannins, a class of phenolic compounds found exclusively in brown

algae (Ragan and Glombitza 1986). Phlorotannins has been shown to serve as UVBR-screening substances, e.g., in *A. nodosum* and *Macrocystis integrifolia* as well as in zoospores of Arctic *Saccorhiza dermatodea*, *A. esculenta* and *L. digitata* (Pavia et al. 1997, Pavia and Brock 2000, Swanson and Druehl 2002, Roleda et al. 2006a). Isolated phlorotannins from *A. nodosum* and *Fucus gardneri* extracted in 80 % methanol exhibited a peak at 265 nm and 268 nm, respectively (Pavia et al. 1997, Henry and van Alstyne 2004). The shift in the absorption maximum to 273 nm in the present study might be caused by the use of a different solvent (DMF *vs.* methanol). However, if the strong absorption below 300 nm really belongs to the absorption by phlorotannins or if it is caused, e.g., by absorption of nucleic acids or proteins remains to be proven.

5.2.3. Mechanisms of acclimation

The underlying mechanisms of acclimation are widely unknown, but it can be assumed that in all species studied, higher $rETR_{max}$ values were achieved by an increase in the turnover rate of the PSUs, which is favored in light and predominantly regulated on the level of membrane-associated electron-transport chain components and the cellular concentration and/or activity of RUBISCO (Sukenik et al. 1987, Davison et al. 1991). Changes in α resulted from alterations in the number or size of the PSUs, or a combination of both (Falkowski and LaRoche 1991), as indicated by a positive correlation between α and the Chl *a* content, as well as between α and the (Chl *c* + Fuc)/Chl *a* ratio (Table 11). In *Macrocystis pyrifera* (Laminariales), the expression of the fucoxanthin-Chl *a*/*c* light-harvesting protein complex (LHCF) genes and the rate of transcription have been shown to be modulated by the light intensity and quality (Apt et al. 1995). The positive relationship between VAZ/Chl *a* ratios and the respective monthly mean of underwater PAR, suggests an induction of the biosynthesis of the xanthophyll cycle pigments by PAR (Table 11). This is consistent with the reported specific stimulation of *β*,*β*-carotenoid synthesis, the three xanthophylls of the xanthophyll cycle and *β*-carotene are all *β*,*β*-carotenoids, in response to high photon flux density (Jones and Porter 1986, Demmig-Adams 1990, Demmig-Adams and Adams III 1992). Analogous, the accumulation of UVR-absorbing compounds in *A. esculenta* and *S. latissima* (Fig. 13) during high irradiances of UVR in the field might result from an induction

of the biosynthesis of phlorotannins, as reported for *A. nodosum, S. latissima* and *M. integrifolia* after 2 to 8 weeks in response to UVBR-exposure and in the latter also to UVAR-exposure (Pavia et al. 1997, Swanson and Druehl 2002, Swanson and Fox 2007). Increases in the number and size of physodes in UVR-exposed zoospores of *A. esculenta*, *L. digitata* and *S. latissima*, but not in *L. solidungula*, have been reported by Wiencke et al. (2004b), indicating as well an induction of phlorotannin biosynthesis by UVR. Generally, in all eukaryotic photosynthetic cells, the photosynthetic genes are encoded in both, in the nucleus and in the chloroplast (Falkowski et al. 1981). Basically, the gene expression and thereby the amount of synthesized protein is controlled by the rate of transcription, by post-transcriptional processing of the messenger RNA, and at the level of translation (Falkowski and Raven 2007). The expression of genes encoding chloroplast components have been shown to be regulated by external factors including light and temperature (Pfannschmidt et al. 1999, 2001, Quail 2002). However, in higher plants, the mechanisms regulating chloroplast composition and facilitating acclimation are very complex and the biochemistry of irradiance-signal transduction into pigment composition is largely unknown (Anderson et al. 1995).

5.2.4. Comparison of algal acclimation responses found with those of other field studies

The same seasonal patterns of photosynthetic characteristics and pigmentation were found in long-term studies on field-collected Arctic brown macroalgae. In *S. latissima*, *Saccorhiza dermatodea* and *Desmarestia aculeata*, $rETR_{max}$ increased in parallel to increasing light availability upon the sea ice break-up in early summer, while during this period the Chl *a* content decreased (Bischof et al. 2002, Aguilera et al. 2002b). As in the present study, this acclimation was reversible as soon as light availability decreased by the end of summer. However, in contrast to the present study, no recovery of the Chl *a* content was reported for *S. latissima* during lowered irradiances in late summer (Aguilera et al. 2002b). This discrepancy might be explained by interannual differences in environmental radiation conditions and the use of different sporophyte life stages, because the pigment content has been shown to vary with the thallus age (Hanelt et al. 1997a, Campbell et al. 1999).

Similarly, the deep water species *Phyllariopsis purpurascens* from the Strait of Gibraltar (Southern Spain), a warm temperate member of the Laminariales, exhibited an increase in net oxygen production, indicating photosynthetic capacity, from April to June in parallel to an increment in the photon flux density, while the Chl *a* content decreased (Flores-Moya et al. 1995). This is also the pattern observed in cold temperate *Sargassum muticum* from the English Channel (Lewey and Gorham 1984).

In accordance to the present findings, a comparison between a spring and winter population of young sporophytes of cold temperate *S. latissima*, collected from the eastern English Channel (France), revealed higher $rETR_{max}$ and E_k values in response to higher irradiance in spring (Gévaert et al. 2002). In addition, the plants minimized the susceptibility of their photosynthetic apparatus to photoinhibition and destruction by higher VAZ/Chl *a* ratios during higher irradiance in spring. Analogous, *S. latissima* acclimated to low light availability in winter by developing more efficient light-harvesting complexes, as revealed by higher Chl *c*/Chl *a* and Fuc/Chl *a* ratios. However, in contrast to the present study, α values remained almost unchanged and the Chl *a* content was higher during high light conditions in spring.

A similar seasonal pattern of gross photosynthesis (measured as O_2 evolution per time, expressed on an area basis) was observed in cold temperate *L. digitata*, *S. latissima* and *L. hyperborea* from the North Sea (Lüning 1971, Drew 1983). Photosynthetic rates, adjusted to ambient seawater temperature and irradiances, strongly increased in spring and reached a maximum in summer. Subsequently, the photosynthetic rates begin to decrease slowly during autumn and were lowest in winter. The photosynthetic efficiencies (α) were also relatively high in spring and decreased in summer, but different from the present study, this occurred despite of increasing chlorophyll *a* contents (Drew 1983). The changes in net photosynthesis were related to the daylength and to metabolic effects of temperature. However, since high water temperature and high underwater irradiance are positively correlated, it cannot be excluded that alterations of the P-E curves were caused by acclimation to irradiance.

In Greenlandic *S. latissima* and in the Laminariales *Ecklonia radiata* and *Undaria pinnatifida* from South Australia, the seasonal patterns of E_k and α were in principle the same, i.e. low E_k and high α during high underwater radiation in spring and summer compared to low light conditions under sea ice and during autumn and winter (Campbell et al. 1999, Borum et al. 2002, Fairhead and Cheshire 2004). Higher Chl *a*, Chl *c*, and Fuc contents were attributed to lower underwater irradiances, and in *E. radiata*, the concentration

of UVR-absorbing substances changed seasonally and was significantly related to UVR and PAR flux densities at the algal growth site (Wood 1987). However the seasonal trends of the Chl *c*/Chl *a* and Fuc/Chl *a* ratios in *E. radiata* and *U. pinnatifida* partly contrasted with the photoacclimation theory (Falkowski and LaRoche 1991). Different from the present study, highest photosynthetic capacities (P_{max} measured as oxygen evolution per time expressed on a dry weight basis) were measured during low irradiances in the field and were related to high Chl *a* contents. This is, because an increase in Chl *a* content is consistent with an increased number of PSUs and the maximum potential rate of photosynthesis, in return, is directly related to the number of functional PSUs (Falkowski and Raven 2007). However, a reverse seasonal trend of P_{max} and α was observed in juvenile *U. pinnatifida*, when the data were expressed on a Chl *a* basis (Campbell et al. 1999).

The comparison of acclimation strategies between different species and conspecifics from other geographic regions shows that acclimation processes are very diverse and seem to depend not only on the species-specific life strategy but also on ecotypic differentiation (Bartsch et al. 2008).

5.2.5. Seasonal changes in the susceptibility of the optimum quantum yield (F_v/F_m) to artificial PAR and UVR

During the seasons, differences in the acclimational status of the species studied became manifested in their photosynthetic performance when subjected to artificial radiation treatments applied in the laboratory.

The reduction in photosynthetic efficiency during exposure to high irradiances and the subsequent recovery in dim light are typically based on two different types of photoinhibition. The dynamic photoinhibition (now also referred to as "photoprotection") is characterized by the quickly reversible down regulation of PS II as a mechanism to protect the photosynthetic apparatus against excessively absorbed light energy by thermal dissipation (Powles 1984, Osmond 1994). It is often found in high light adapted organisms. In contrast, shade-adapted organisms suffer chronic photoinhibition (now also referred to as "photoinactivation") by damage of antenna components or due to photodegradation of the D1 protein in PS II causing a decrease also in the photosynthetic capacity (Powles 1984, Krause

1988, Krause and Weis 1991, Critchley and Russell 1994, Osmond 1994, Franklin and Forster 1997, Häder and Figueroa 1997).

The exposure experiments indicate that photoinhibition is predominantly caused by white light, whereas UVR rather slows down the recovery process. These results are in line with the findings by Hanelt et al. (1997b) and Bischof et al. (1999). Within the brown algae studied, two different responses were observed in the process of acclimation of photosynthetic efficiency to higher irradiances in the field. Firstly, the degree of inhibition observed in the artificial radiation treatments became smaller, and secondly, recovery proceeded faster and more efficiently (Fig. 10), which is in accordance with previous studies by Bischof et al. (1998a, 1999) and Hanelt (1998).

Generally, the seasonal changes in the photosynthetic efficiency, measured as F_v/F_m under controlled irradiances of PAR, UVAR and UVBR, indicate changes in the acclimation status of the species as a result of acclimation to the actual intensities at the respective growth site. Thus, the strongly increased tolerance of the species against artificial PAR- and UVR-exposure observed in June, pointing to an efficient acclimation to higher underwater irradiances of PAR and UVR after the sea ice break-up by photoprotective mechanisms (Fig. 10). The stepwise decline in recovery rates between July and September reflects increasing sensitivity of the photosynthetic apparatus to PAR, UVAR, and in particular UVBR, since the seaweeds acclimated to decreasing light conditions in the field and were therefore insufficiently protected against the high light treatment applied in the laboratory. However, in July, the recovery rates of PAR-exposed samples of *A. esculenta* and *L. digitata* further increased. This was because in shallow waters these species remained exposed to relatively high irradiances of PAR, despite of reduced water transparency. Hence, *A. esculenta* and *L. digitata* retained a high tolerance for PAR while in parallel their UVBR-sensitivity increased. The high photosynthetic susceptibility to radiation in September, observed in all species, was due acclimation to low ambient radiation in the field. In addition, shorter daylengths in September combined with lower temperatures and normally low levels of inorganic nitrogen have been show to be important cues that led to sorus formation and new blade formation in several kelp species and might also have a trigger function for changing the metabolic activity to brace for the dark period in winter (Wiencke et al. 2006). Thus, besides a trade-off between growth and storage of carbohydrate reserves (see below), the algae may also trade energy demands for protective and repair mechanisms off against energy conservation.

A high capability of *A. esculenta* and *S. latissima* to acclimate to increased PAR and UVR was previously reported for adult sporophytes by Bischof et al. (1998a, 1999) and Hanelt (1998). The same seasonal pattern in the susceptibility of F_v/F_m to artificial UVR-exposure was found in a long-term study on various field-collected Arctic macroalgae (Bischof et al. 2002). The changes in the UVR-tolerance of these species has been related to photoacclimation processes, resulting in a lower Chl *a* content, and in red and green algae, in an accumulation of UVR-absorbing mycosporine-like amino acids (MAAs) and increased antioxidative enzyme activities of the superoxide dismutase (SOD) and catalase (CAT) during periods of higher underwater radiation in the field (Aguilera et al. 2002b). In contrast to the present study no clear seasonal pattern of the UVR-sensitivity of F_v/F_m was observed in *S. latissima*, possibly due to the use of older individuals, which were proven to be significantly less sensitive to high irradiances (Hanelt et al. 1997a). The results of the present study are also consistent with the findings of Gévaert et al. (2002) showing that the photosynthetic performance of a spring population of cold temperate *S. latissima*, which was acclimated to high irradiances in the field, was less affected by an artificial high PAR treatment than it was in a low light acclimated winter population. This was attributed to the fact that *S. latissima* responded to high light conditions in spring by developing photoprotective mechanisms (i.e. higher pool size of the xanthophyll cycle pigments) and was therefore able to dissipate excess energy during the artificial light treatment.

Several molecular mechanisms may be involved in the observed photoacclimation. In all four species studied, the degree of recovery of F_v/F_m in PAR-exposed samples was positively correlated with the VAZ/Chl *a* ratio and negatively with the Chl *c*/Chl *a* ratio and α value (Table 11), suggesting that all species mainly protect their photosynthetic apparatus against photodamage, caused by high irradiances of PAR, by increasing the xanthophyll cycle capacity and reducing light absorption capability. In general, the higher sensitivity of shade plants to photoinhibition is usually attributed to a smaller pool size of xanthophyll cycle carotenoids, a larger photosynthetic unit size, a lower photosynthetic capacity, and a limited PS II repair cycle (Demmig-Adams 1990, Young 1991, Tyystjärvi et al. 1992, Demmig-Adams and Adams 1996, Rodrigues et al. 2000). Thus, at high irradiances, shade plants would be more prone to photodamage, since too many photons are absorbed and the excess excitation could not be properly dissipated via the xanthophyll cycle or be trapped via photochemistry, due to a limitation of the carbon fixation cycle enzymes, especially RUBISCO (Cunningham et al. 1992, Walker 1992). That the xanthophyll cycle plays an

important role in dynamic photoinhibition and recovery of brown macroalgae has been previously shown for *Dictyota dichotoma* and *Sargassum natans* (Uhrmacher et al. 1995, Schofield et al. 1998).

Accumulation of UVR-absorbing substances might be an additional means of photoprotection against the damaging effects of UVBR. At least in PAB-exposed samples of *S. latissima*, the degree of inhibition was negatively correlated with the relative content of UVR-absorbing compounds (Table 11). This might originate from an accumulation of phlorotannins, which possess the capability of screening UVBR and/or scavenging reactive oxygen species (ROS), such as superoxide anions (O_2^-) produced by harmful UVBR (Foti et al. 1994). However, the presence of the UVR-absorbing substances alone cannot explain the seasonality of UVBR-sensitivity observed in the species studied, since they were, e.g., always present in high amounts in *L. digitata*, although this species showed a noticeable seasonality in its UVBR-resistance. Therefore, there must be additional protection mechanisms against UVR. For instance, the sensitivity of juvenile sporophytes of Arctic *L. digitata*, *S. latissima* and *L. solidungula* for UVBR-induced DNA damage has been shown to be related to the thallus morphology (i.e. thallus thickness) of the species (Roleda et al. 2006b). An increase in the UVR-tolerance with increasing thallus thickness is an optical effect caused by a longer pathlength for UVR-absorption, thereby, the outer cell layers shade the inner cells (Franklin and Forster 1997). In general, a reduction in the degree of photoinhibition caused by UVR- and PAR-exposure, as well as an increase in the rate of recovery, might be also achieved by the activation of antioxidative defence systems, e.g. by the expression of a stress-specific bromoperoxidase catalyzing the reduction of hydrogen peroxide (H_2O_2), by increased gene expression or activity of repair processes, e.g. turnover rates of D1 and D2 reaction center subunits of PS II and DNA repair by photolyase, even though the molecular mechanisms are still unknown in macroalgae (Andersson et al. 1992, Tyystjärvi et al. 1992, Aro et al. 1993, Britt 1995, Kim and Sancar 1995, Campbell et al. 1998, Máté et al. 1998, Roeder et al. 2005). Furthermore, chloroplast displacement, which causes a decrease in absorption cross-section and is induced by blue light and UVA radiation, is also able to protect against photodamage in brown algae (Hanelt and Nultsch 1991).

5.3. Life strategy, adaptation and acclimation

The seasonal optima of photosynthetic capacities ($rETR_{max}$) found in summer, complementary to optimum growth rates in late winter and spring reported for wild and cultivated *A. esculenta*, *L. digitata*, *S. latissima* and *L. solidungula*, may indicate a programmed seasonal sequence (Dunton 1985, Dunton 1990, Makarov et al. 1999). All species studied have been classified as season anticipators in the sense of Kain (1989) and their seasonal development is based on photoperiodism and circannual rhythms (Lüning 1988, 1991, 1994, Lüning and tom Dieck 1989, Makarov et al. 1999). In this group of species, also photosynthetic performance and pigment content are finely adapted to the annually repeating periodic changes of abiotic factors, especially of the radiation conditions. Endogenous rhythmicity enables the algae to anticipate unfavorable winter conditions, and to respond immediately to improving light conditions in spring. However, the genetically fixed adaptation within different species or ecotypes sets the frame in which acclimation to actual irradiance, nutrient levels, and temperature conditions may occur. In general, adaptation to environmental factors is the result of evolutionary processes over long time periods (up to thousands of millions of years) whereas acclimation is achieved within hours to weeks and the physiological regulation processes take place within seconds to minutes. For example, in May, *A. esculenta*, *L. digitata* and *S. latissima* were still covered by sea ice and thus exposed to dim light for more than half a year. Therefore, the considerably high tolerance of their photosynthetic efficiency (F_v/F_m) to PAR and UVR (Fig. 10a, f, k) reflects their genetically fixed ability for dynamic photoinhibition, which was modified during the study period by acclimation processes to the strongly changing underwater irradiances at their natural growth sites.

Generally, polar macroalgae are regarded as low light adapted organisms typically characterized by high photosynthetic efficiencies and very low light compensation and saturation points (Kirst and Wiencke 1995, Brouwer 1996, Eggert and Wiencke 2000). In addition, the light requirements of polar macroalgae, especially of Antarctic species, are lower than those of cold temperate species (Gómez et al. 1997). For example, the annual light demand for growth of Antarctic Desmarestiales is 31.4 mol m^{-2} $year^{-1}$ of PAR only and for Arctic *L. solidungula* a minimum annual quantum demand of 49 mol m^{-2} $year^{-1}$ has been determined (Chapman and Lindley 1980, Wiencke 1990). In contrast minimum light

requirement of cold temperate *L. hyperborea* in the North Sea is 71.2 mol m^{-2} $year^{-1}$ (Lüning and Dring 1979).

However, *A. esculenta* and *L. digitata* from the upper sublittoral were able to acclimate to temporary high underwater irradiances. During spring and summer, these species were frequently exposed to photoinhibitory irradiances in the field (Table 6) and possessed, in the laboratory experiment, a higher capability for photoprotection than the species from deeper waters, since they were less inhibited by artificial UVR and recovered faster and more efficiently from photoinhibition (Fig. 10a - j, Table 8). This indicates more efficient photoprotective mechanisms active in these species. Indeed, on a seasonal average, the relative content of UVR-screening compounds and the proportion of *β*-Car and VAZ was inversely proportional to the depth distribution of the species investigated (Table 1). At Kongsfjorden, *L. digitata* and *A. esculenta* grow predominantly in the upper and mid sublittoral and are found between 1.5 and 13.5 m, *S. latissima* is common at depths between 1.5 and 16.5 m and *L. solidungula* occurs at the lower sublittoral between 7.5 and 19.5 m (Wiencke et al. 2004a). Thus, *S. latissima* from the mid sublittoral and, in particular, *L. solidungula* from the lower sublittoral are strongly shade-adapted and, therefore, exhibit a lower ability to down regulate photosynthesis by protective mechanisms, since the low rates of reduction and recovery of photosynthetic efficiency in September (Fig. 10o, t) were probably caused by photodamage of the PS II due to degradation of the D1 protein and slow repair via D1 turnover (Andersson et al. 1992). That a species susceptibility to artificial PAR and UVR is related to its position at the shore was previously reported by Hanelt et al. (1997c) and Hanelt (1998). In addition, the amplitude of seasonal variations in the PAR- and UVR-tolerance of the species was related to their vertical depth distribution at the shore. This is, because the irradiances applied in the laboratory mean severe light stress to low light acclimated algae such as *L. solidungula*, whereas do not necessarily mean a threat to shallow-water species. Furthermore, environmental conditions are more stable in deeper waters, even though the relative seasonal changes in the light conditions might be more pronounced in greater water depths. Therefore, deep water species, which are acclimated to rather constant abiotic factors, react more sensitive to any kind of changes in abiotic factors.

The finding that photosynthesis was saturated at lower irradiances in species from deeper waters (lower E_k values, Fig. 7) than in species inhabiting the upper parts of the shore, is in line with the previously reported relationship between E_k values of species and their position on the shore (Gómez et al. 2004). Thus, lowest E_k and high α values in *L. solidungula* are

presumably adaptations of this Arctic endemic species to low light availability caused by polar night and ice cover periods in winter and early spring as well as by high water turbidity in summer. Another feature characterizing the dark adaptation of *L. solidungula* is the reported low compensation point (E_c) for growth close to 0.6 µmol m^{-2} s^{-1} (Chapman and Lindley 1980). Nevertheless, photosynthesis in *A. esculenta* and *L. digitata* was light-saturated from June to September and in *S. latissima* in June, August and September, while *L. solidungula* achieved light saturation only in May, according to the measured values of E_k and monthly means of underwater PAR (Table 6, Fig. 7). This is, of course, a rough estimation only, since, e.g., the diurnal amplitude of PAR intensities is not considered. The great ecological success of *L. solidungula* in low light habitats of the Arctic is probably related to light-independent carbon fixation (LICF) and ability to retain several metabolically active annual blades that can store carbohydrate reserves to support meristem activity through the winter. Thus, *L. solidungula* produces most of its new frond tissue in winter by allocating food reserves stored from the previous year (Dunton and Schell 1986). In this species, cessation of linear growth occurs in early summer followed by storage of photosynthates (Chapman and Lindley 1980, Dunton et al. 1982). Mannitol and storage polysaccharides have been shown to fuel LICF reactions in kelps and probably support the non-photosynthetic carboxylation in *L. solidungula* (Kremer 1984). Dunton (1990) showed that the annual linear growth in *L. solidungula* in the Alaskan Beaufort Sea was not related to PAR received in the same year but to the light energy absorbed the previous summer and stored as carbohydrate reserves. The accumulation of photosynthates, in turn, was rather correlated with the duration of exposure to saturating levels of PAR (H_{sat}) than with the total amount of photons received (annual quantum budget). It is likely that such an alternative carboxylating mechanism as LICF is advantageous for species that have to endure prolonged conditions of reduced photosynthetic potential (low photon flux density, low temperature) in the Arctic (Küppers and Kremer 1978). In contrast, little accumulation of reserve carbohydrate occurs in cold temperate *L. digitata* which exhibits rapid, sustained summer growth in the North Sea near Helgoland (Lüning 1979, Drew 1983). Even though laminarin and mannitol are synthesized by *S. latissima* during summer, carbon fixation and growth in this species rather depend on active photosynthesis than on stored photosynthates. (Johnston et al. 1977, Lüning 1979, Drew 1983, Henley and Dunton 1995). Thus, winter growth in *L. solidungula* allows the plant to utilize the high nutrient availability during the dark period of ice cover, instead of delaying tissue expansion until early summer when nutrients are depleted, as it is done e.g. by

S. latissima (Henley and Dunton 1995). Hence, this species was best suited for a life in a habitat which is characterized by low light availability.

6. Conclusion and outlook

The findings of the present study demonstrate the strong adaptation of four common kelp species to Arctic light conditions and evaluate the species-specific acclimation potential and the underlying strategy over season and depth. Thereby, new aspects of the seasonality and life strategy of theses perennial Arctic kelps are provided and data on the genetically fixed adaptation of dynamic photoinhibition as well as on the physiological basis of photoacclimation processes are supplied.

6.1. Ecological implications of the findings for prospective changes in Arctic marine environments

Drastic losses of European kelp populations during the last century have been reported and an ongoing disappearance of kelps is expected in the future (Airoldi and Beck 2007). Possible climatic changes might additionally pose a threat to seaweeds. However, prospective rising temperatures, due to the greenhouse effect, would decrease the sea ice cover extent and thickness, thereby opening up new areas for primary production (Hassol 2005). An increase in the open-water period in Arctic fjords would prolong the period for net carbon assimilation in habitats characterized by a shortage of light availability (Parkinson et al. 1999, Vinnikov et al. 1999, Stroeve et al. 2005). Photosynthesis in species from polar regions, especially from the Arctic, is less strongly adapted to the ambient temperature regime as it is in warm temperate and tropical species. Stenothermal species from the Arctic, where the water temperature rarely exceeds 5 °C, exhibit optima of photosynthetic capacities at around 20 °C (Healey 1972), whereas highest growth rates are achieved at water temperatures between 10 and 15 °C (Wiencke et al. 1994). Thus, the predicted increase in temperature *per se* will not negatively affect Arctic macroalgae. However, low ambient temperature may be an advantage or even a prerequisite for survival in the long dark period, as it keeps respiration costs low (Kirst and Wiencke 1995, Eggert and Wiencke 2000).

At the same time, the detrimental effect of high light intensities might induce damage to organisms in an environment where life is usually rather adapted to low light conditions. Thus, seaweeds might be affected by an ozone-related increase of harmful

UVBR, resulting from the thinning of the stratospheric ozone layer, coinciding with an earlier sea ice break-up in spring (Müller et al. 1997, Rex et al. 1997, Rigor et al. 2000, Solomon et al. 2007). Therefore, the time course and the potential of algal photoacclimation are of high ecological relevance. There is evidence in the present study, that juvenile *S. latissima* could not prevent photodamage to its photosynthetic apparatus under conditions as extreme as those experienced during the sea ice break-up. In June, most of the very thin and translucent thalli of *S. latissima* were partly or completely bleached in the field, indicating that light stress exceeded the capacity for photoprotection and repair (Fig. 14).

Fig. 14: Bleached sporophyte of young *S. latissima* at its natural growth site at a water depth of 4 m in June. Picture was taken by Stephan Kremb.

Moreover, even in well pigmented sporophytes, chosen for the laboratory experiment, the initial F_v/F_m value was considerably low in June, probably because photoinhibition precedes photooxidation of pigments (Table 7, Powles 1984). Therefore, the observed decline in the photosynthetic pigment content (Fig. 11a) in parallel to strongly increased irradiances might rather result from photooxidation due to light stress exceeding the protective capacity than from acclimation to high light (Björkman 1981, Krause 1988). Thus, enhanced UVB radiation, penetrating deeper into the water column, may result in a shift of the upper distribution limit of UVBR-sensitive species to greater water depths, since the upper distribution limit of macroalgae is determined by their ability to resist high radiation stress (Hanelt et al. 1997a, b, c, Bischof et al. 1998a, b, 2000, Hanelt 1998, Karsten et al. 2001).

In contrast, highest acclimation potential of the species studied, over a wide range of light intensities on a short-time scale, was found in *A. esculenta*, particularly when compared to *L. digitata* which experienced the same environmental conditions. In fact, in *A. esculenta*, e.g., the E_k, α, and Chl *a* values were best correlated with the actual PAR intensity throughout the season, even shortly after the sea ice break-up, when irradiances changed dramatically within a short time (Fig. 7, 9, 11a). In *A. esculenta* and *L. digitata*, the xanthophyll cycle appears to be more operative than in the *S. latissima* and *L. solidungula*, effectively protecting them against high irradiances of PAR. In May, *A. esculenta* and *L. digitata* achieved a similar PAR-tolerance as *S. latissima* and *L. solidungula* despite of 25 % and 35 % lower VAZ/Chl *a* ratios, respectively. Non-photochemical dissipation of excess excitation energy has been shown to be species-specific and more efficient in shallow water species such as *L. digitata* and *Pelvetia canaliculata* compared to *Laminaria abyssalis* and *S. latissima* from deeper growth sites, respectively (Harker et al. 1999, Rodrigues et al. 2002). This was owned, beside to a larger xanthophyll cycle pool, to a higher efficiency of de-epoxidation of violaxanthin in the shallow water species. With regard to environmental changes in the Arctic adult sporophytes and zoospores of *A. esculenta* were proven to be tolerant and adaptable to interactive effects of elevated temperature and UVR as well as to reduced salinity possibly occurring due to global warming and ozone depletion and faster melting of glaciers (Fredersdorf et al. 2009). Additionally, the susceptibility to UVR has been shown to be lowest in the zoospores of *A. esculenta*, followed by *L. digitata*, *S. latissima* and finally *L. solidungula* (Wiencke et al. 2004b). Thus, *A. esculenta* might benefit from global warming and ozone depletion in the future due to a repression of other resource-competing kelp species.

On the other hand, the benthic macroflora might experience a decrease in underwater light intensities, caused by an increased influx of riverine dissolved organic matter (DOM) in Arctic costal waters due to melting of the inland ice and glaciers and lengthening of the melt season as observed for the eastern Arctic (Gibson et al. 2000, Rigor et al. 2000, Solomon et al. 2007). As a consequence, light shortage might become more severe, affecting the lower limit of macroalgal distribution, which is determined by the metabolic carbon balance (Gómez et al. 1997). The base of the euphotic zone is the light compensation depth, which is defined as the depth where gross photosynthetic carbon fixation balances respiratory losses (frequently taken as the depth corresponding to 1 % of surface PAR) (Falkowski and Raven

2007). Low light availability is the prevailing situation in the inner and turbid part of Kongsfjorden today, where virtually less macroalgae are present (Hop et al. 2002).

All together, the expected drastic changes in radiation conditions, temperature, and salinity in Arctic marine environments will result very likely in major changes in the ecosystem structure and function, in the ecological interactions of the species and in a shift in the geographical range of the species, with strong negative consequences for the biodiversity (Solomon et al. 2007, World Meteorological Organization 2007). However, to this day, the consequences of expected climatic changes for growth conditions of the species studied in Kongsfjorden and in other fjords of the Arctic cannot be predicted with any certainty, since, e.g., the interactive effects of various abiotic factors are rarely investigated and the irradiances and doses which exceed the acclimation capacity of the species are still unknown and must be clarified before possible changes in depth distribution due to enhanced UVBR could be reliably predicted for kelps.

6.2. Future experiments

With respect to future experiments it should be emphasized that the degree of algal acclimation to the respective environmental conditions, determined by season and water depth, has to be taken into account when results from short-term studies and laboratory experiments are extrapolated to the situation in the field.

Apart from a few studies on the seasonal growth of *S. latissima* and *L. solidungula*, the physiological performance of Arctic kelps in winter is widely unknown (Chapman and Lindley 1980, Dunton 1985). Only baseline field studies are available together with a few data based on laboratory studies. Growth, photosynthesis, reproduction, pigment content, nutritional composition, enzyme activities etc. need to be monitored over the entire year to understand the life strategy of species more detailed. All these studies need to be complemented by a detailed monitoring of the environmental conditions to understand the physiological bases of plant life in extreme environments.

There is a multitude of abiotic factors potentially causing stress to seaweeds such as degraded water quality, grazing pressure, excessive irradiance, suboptimal temperatures, desiccation, and low nutrient concentrations, making physiological field, mesocosms and

controlled laboratory studies on the interaction of various abiotic (stress) factors indispensable. These studies should include, beside the macroscopic sporophytes, also the haploid microscopic algal life stages such as unicellular zoospores and multicellular gametophytes. The obtained knowledge of these studies would also substantially improve the predictability of how, for example, increased UVBR and temperature may shape seaweed communities and thus rocky coastal ecosystems in the future.

Gene expression, biosynthetic pathways and metabolic regulations ensuring efficient acclimation, homeostasis, and functional integrity, are widely unexplored in polar seaweeds. Therefore, the application of molecular tools also in seaweed physiology will be a major step forward to elucidate the underlying molecular bases of effective protective and repair mechanisms contributing to the remarkable stress tolerance of kelps. A comparison of the gene expression of sensitive and tolerant kelp species under abiotic stresses by microarrays and quantitative real-time polymerase chain reaction (RT-PCR) might give insight into the different adaptive mechanisms regulating, e.g., chloroplast composition and facilitating acclimation. Virtually nothing is known about the biochemistry of signal transduction into gene expression and pigment synthesis (Anderson et al. 1995). Even though there is strong evidence that redox signalling, sugar levels, energy status, and photoreceptors are indirectly involved in the regulation of acclimational processes, it still has to be established which (if any) of these factors significantly determine the chloroplast composition (Walters 2005).

References

AALDERINK, R. H. and JOVIN, R. (1997) Estimation of the photosynthesis/irradiance (P/I) curve parameters from light and dark bottle experiments. Journal of Plankton Research 19: 1713-1742.

AGUILERA, J., DUMMERMUTH, A., KARSTEN, U., SCHRIEK, R. and WIENCKE, C. (2002a) Enzymatic defences against photooxidative stress induced by ultraviolet radiation in Arctic marine macroalgae. Polar Biology 25: 432-441.

AGUILERA, J., BISCHOF, K., KARSTEN, U., HANELT, D. and WIENCKE, C. (2002b) Seasonal variation in ecophysiological patterns in macroalgae from an Arctic fjord. II. Pigment accumulation and biochemical defence systems against high light stress. Marine Biology 140: 1087-1095.

AGUIRRE VON WOBESER, E., FIGUEROA, F. L. and CABELLO-PASINI, A. (2000) Effect of UV radiation on photoinhibition of marine macrophytes in culture systems. Journal of Applied Phycology 12: 159-168.

AIROLDI, L. and BECK, M. W. (2007) Loss, status and trends for coastal marine habitats of Europe. Oceanography and Marine Biology: An Annual Review 45: 345-405.

ALFONSO, M., MONTOYA, G., CASES, R., RODRIGUEZ, R. and PICOREL, R. (1994) Core antenna complexes, CP43 and CP47, of higher plant photosystem II. Spectral properties, pigment stoichiometry, and amino acid composition. Biochemistry 33: 10494-10500.

ALTAMIRANO, M., FLORES-MOYA, A., CONDE, F. and FIGUEROA, F. L. (2000) Growth seasonality, photosynthetic pigments, and carbon and nitrogen content in relation to environmental factors: a field study of *Ulva olivascens* (Ulvales, Chlorophyta). Phycologia 39: 50-58.

AMSLER, C. D., ROWLEY, R. J., LAUR, D. R., QUETIN, L. B. and ROSS, R. M. (1995) Vertical distribution of Antarctic peninsular macroalgae: cover, biomass and species composition. Phycologia 34: 424-430.

ANDERSON, J. M. (1986) Photoregulation of the composition, function, and structure of thylakoid membranes. Annual Review of Plant Physiology 37: 93-136.

ANDERSON, J. M. and ANDERSSON, B. (1988) The dynamic photosynthetic membrane and regulation of solar energy conversion. Trends in Biochemical Sciences 13: 351-355.

ANDERSON, J. M., CHOW, W. S. and PARK, Y. I. (1995) The grand design of photosynthesis: acclimation of the photosynthetic apparatus to environmental cues. Photosynthesis Research 46: 129-139.

ANDERSSON, B., SALTER, A. H., VIRGIN, I., VASS, I. and STYRING, S. (1992) Photodamage to photosystem II - primary and secondary events. Journal of Photochemistry and Photobiology B: Biology 15: 15-31.

APT, K. E., CLENDENNEN, S. K., POWERS, D. A. and GROSSMAN, A. R. (1995) The gene family encoding the fucoxanthin chlorophyll proteins from the brown alga *Macrocystis pyrifera*. Molecular and General Genetics 246: 455-464.

ARO, E. M., VIRGIN, I. and ANDERSSON, B. (1993) Photoinhibition of photosystem II. Inactivation, protein damage and turnover. Biochimica et Biophysica Acta 1143: 113-134.

AROLA, A., LAKKALA, K., BAIS, A., KAUROLA, J., MELETI, C. and TAALAS, P. (2003) Factors affecting short- and long-term changes of spectral UV irradiance at two European stations. Journal of Geophysical Research-Atmospheres 108: 4549.

BABU, T. S., JANSEN, M. A. K., GREENBERG, B. M., GABA, V., MALKIN, S., MATTOO, A. K. and EDELMAN, M. (1999) Amplified degradation of photosystem II D1 and D2 proteins under a mixture of photosynthetically active radiation and UVB radiation: dependence on redox status of photosystem II. Photochemistry and Photobiology 69: 553-559.

BALDWIN, M. P., DAMERIS, M. and SHEPHERD, T. G. (2007) Atmosphere - How will the stratosphere affect climate change? Science 316: 1576-1577.

BARBER, J., MALKIN, S. and TELFER, A. (1989) The origin of chlorophyll fluorescence in vivo and its quenching by the photosystem II reaction centre. Philosophical Transactions of the Royal Society of London Series B: Biological Sciences 323: 227-239.

BARTSCH, I., WIENCKE, C., BISCHOF, K., BUCHHOLZ, C. M., BUCK, B. H., EGGERT, A., FEUERPFEIL, P., HANELT, D., JACOBSEN, S., KAREZ, R., KARSTEN, U., MOLIS, M., ROLEDA, M. Y., SCHUBERT, H., SCHUMANN, R., VALENTIN, K., WEINBERGER, F. and WIESE, J. (2008) The genus *Laminaria* sensu lato: recent insights and developments. European Journal of Phycology 43: 1-86.

BEER, S. and AXELSSON, L. (2004) Limitations in the use of PAM fluorometry for measuring photosynthetic rates of macroalgae at high irradiances. European Journal of Phycology 39: 1-7.

BEER, S., VILENKIN, B., WEIL, A., VESTE, M., SUSEL, L. and ESHEL, A. (1998) Measuring photosynthetic rates in seagrasses by pulse amplitude modulated (PAM) fluorometry. Marine Ecology Progress Series 174: 293-300.

BEER, S., LARSSON, C., PORYAN, O. and AXELSSON, L. (2000) Photosynthetic rates of *Ulva* (Chlorophyta) measured by pulse amplitude modulated (PAM) fluorometry. European Journal of Phycology 35: 69-74.

BISCHOF, K., HANELT, D., TÜG, H., KARSTEN, U., BROUWER, P. E. M. and WIENCKE, C. (1998a) Acclimation of brown algal photosynthesis to ultraviolet radiation in Arctic coastal waters (Spitsbergen, Norway). Polar Biology 20: 388-395.

BISCHOF, K., HANELT, D. and WIENCKE, C. (1998b) UV-radiation can affect depth-zonation of Antarctic macroalgae. Marine Biology 131: 597-605.

BISCHOF, K., HANELT, D. and WIENCKE, C. (1999) Acclimation of maximal quantum yield of photosynthesis in the brown alga *Alaria esculenta* under high light and UV radiation. Plant Biology 1: 435-444.

BISCHOF, K., HANELT, D. and WIENCKE, C. (2000) Effects of ultraviolet radiation on photosynthesis and related enzyme reactions of marine macroalgae. Planta 211: 555-562.

BISCHOF, K., HANELT, D., AGUILERA, J., KARSTEN, U., VÖGELE, B., SAWALL, T. and WIENCKE, C. (2002) Seasonal variation in ecophysiological patterns in macroalgae from an Arctic fjord. I. Sensitivity of photosynthesis to ultraviolet radiation. Marine Biology 140: 1097-1106.

BJÖRKMAN, O. (1981) Responses to different quantum flux densities, pp 57-107. In: Lange, O. L., Nobel, P. L., Osmond, C. B. and Ziegler, H. (eds.), Physiological Plant Ecology I. Encyclopedia of Plant Physiology, NS, 12A. Axel Springer Verlag, Berlin, Heidelberg, New York.

BORNMAN, J. F. (1989) Target sites of UV-B radiation in photosynthesis of higher plants. Journal of Photochemistry and Photobiology B: Biology 4: 145-158.

BORUM, J., PEDERSEN, M. F., KRAUSE-JENSEN, D., CHRISTENSEN, P. B. and NIELSEN, K. (2002) Biomass, photosynthesis and growth of *Laminaria saccharina* in a high-arctic fjord, NE Greenland. Marine Biology 141: 11-19.

BRINKHUIS, B. H. (1977) Seasonal variations in salt-mash macroalgae photosynthesis II. *Fucus vesiculosus* and *Ulva lactuca*. Marine Biology 44: 177-186.

BRITT, A. B. (1995) Repair of DNA-damage induced by ultraviolet-radiation. Plant Physiology 108: 891-896.

BROUWER, P. E. M. (1996) In situ photosynthesis and estimated annual production of the red macroalga *Myriogramme mangin*i in relation to underwater irradiance at Signy Island (Antarctica). Antarctic Science 8: 245-252.

BÜCHEL, C. and WILHELM, C. (1993) In-vivo analysis of slow chlorophyll fluorescence induction kinetics in algae - progress, problems and perspectives. Photochemistry and Photobiology 58: 137-148.

CAMPBELL, D., ERIKSSON, M. J., ÖQUIST, G., GUSTAFSSON, P. and CLARKE, A. K. (1998) The cyanobacterium *Synechococcus* resists UV-B by exchanging photosystem II reaction-center D_1 proteins. Proceedings of the National Academy of Sciences, USA 95: 364-369.

CAMPBELL, S. J., BITÉ, J. S. and BURRIFGE, T. R. (1999) Seasonal patterns in the photosynthetic capacity, tissue pigment and nutrient content of different developmental stages of *Undaria pinnatifida* (Phaeophyta: Laminariales) in Port Phillip Bay, south-eastern Australia. Botanica Marina 42: 231-241.

CHAPMAN, A. R. O. and CRAIGIE, J. S. (1977) Seasonal growth in *Laminaria longicruris*: relations with dissolved inorganic nutrients and internal reserves of nitrogen. Marine Biology 40: 197-205.

CHAPMAN, A. R. O. and LINDLEY, J. E. (1980) Seasonal growth of *Laminaria solidungula* in the Canadian High Arctic in relation to irradiance and dissolved nutrient concentrations. Marine Biology 57: 1-5.

CLAYTON, M. N., WIENCKE, C., SCHOENWAELDER, M. E. A., ROLEDA, M. Y. and LÜDER, U. (2005) UV-screening compounds in spores of Arctic Laminariales. Phycologia 44: 51.

CLELAND, R. E., MELIS, A. and NEALE, P. J. (1986) Mechanism of photoinhibition: photochemical reaction center inactivation in system II of chloroplasts. Photosynthesis Research 9: 79-88.

COLOMBO-PALLOTTA, M. F., GARCIA-MENDOZA, E. and LADAH, L. B. (2006) Photosynthetic performance, light absorption, and pigment composition of *Macrocystis pyrifera* (Laminariales, Phaeophyceae) blades from different depths. Journal of Phycology 42: 1225-1234.

CONOLLY, N. J. and DREW, E. A. (1985) Physiology of *Laminaria*. IV. Nutrient supply and daylength, major factors affecting growth of *Laminaria digitata* and *Laminaria saccharina*. Marine Ecology 6: 299-320.

CRITCHLEY, C. and RUSSELL, A. W. (1994) Photoinhibition of photosynthesis in vivo: the role of protein-turnover in photosystem II. Physiologia Plantarum 92: 188-196.

CUNNINGHAM, F. X., VONSHAK, A. and GANTT, E. (1992) Photoacclimation in the red alga *Porphyridium cruentum*. Changes in photosynthetic enzymes, electron carriers, and light-saturated rate of photosynthesis as a function of irradiance and spectral quality. Plant Physiology 100: 1142-1149.

DAHLBACK, A. (2002) Recent changes in surface ultraviolet solar radiation and stratospheric ozone at a high Arctic site, pp 1-20. In: Hessen, D. O. (ed.), UV radiation and Arctic ecosystems. Ecological Studies, vol 153. Axel Springer Verlag, Berlin, Heidelberg.

DAVIES, B.H. (1965) Analysis of carotenoid pigments, pp 489-532. In: Goodwin, T.W. (ed.), Chemistry and biochemistry of plant pigments. Academic Press, London, New York

DAVISON, I. R. (1987) Adaptation of photosynthesis in *Laminaria saccharina* (Phaeophyta) to changes in growth temperature. Journal of Phycology 23: 273-283.

DAVISON, I. R. (1991) Environmental effects on algal photosynthesis: temperature. Journal of Phycology 27: 2-8.

DAVISON, I. R. and DAVISON, J. O. (1987) The effect of growth temperature on enzyme activities in the brown alga *Laminaria saccharina*. British Phycological Journal 22: 77-87.

DAVISON, I. R., GREENE, R. M. and PODOLAK, E. J. (1991) Temperature acclimation of respiration and photosynthesis in the brown alga *Laminaria saccharina*. Marine Biology 110: 449-454.

DE MARTINO, A., DOUADY, D., QUINET-SZELY, M., ROUSSEAU, B., CREPINEAU, F., APT, K. and CARON, L. (2000) The light-harvesting antenna of brown algae. Highly homologous proteins encoded by a multigene family. European Journal of Biochemistry 267: 5540-5549.

DEMMIG-ADAMS, B. (1990) Carotenoids and photoprotection in plants: a role for the xanthophyll zeaxanthin. Biochimica et Biophysica Acta 1020: 1-24.

DEMMIG-ADAMS, B. and ADAMS III, W. W. (1992) Photoprotection and other responses of plants to high light stress. Annual Review of Plant Physiology and Plant Molecular Biology 43: 599-626.

DEMMIG-ADAMS, B. and ADAMS, W. W. (1996) The role of xanthophyll cycle carotenoids in the protection of photosynthesis. Trends in Plant Science 1: 21-26.

DEMMIG-ADAMS, B., WINTER, K., WINKELMANN, E., KRÜGER, A. and CZYGAN, F. C. (1989) Photosynthetic characteristics and the ratios of chlorophyll, *β*-carotene, and the components of the xanthophyll cycle upon a sudden increase in growth light regime in several plant species. Botanica Acta 102: 319-325.

DOUADY, D., ROUSSEAU, B. and BERKALOFF, C. (1993) Isolation and characterization of PSII core complexes from a brown alga, *Laminaria saccharina*. FEBS Letters 324: 22-26.

DREW, E. A. (1983) Physiology of *Laminaria*. II. Seasonal variation of photosynthesis and respiration in *Laminaria digitata* Lamour., *L. hyperborea* (Gunn.) Fosl. and *L. saccharina*, (L.) Lamour and a model for calculation of annual carbon budgets. Marine Ecology 4: 227-250.

DREW, E. A. and HASTINGS, R. M. (1992) A year-round ecophysiological study of *Himantothallus grandifolius* (Desmarestiales, Phaeophyta) at Signy Island, Antarctica. Phycologia 31: 262-277.

DRING, M. J. (1986) Pigment composition and photosynthetic action spectra of sporophytes of *Laminaria* (Phaeophyta) grown in different light qualities and irradiances. British Phycological Journal 21: 199-207.

DRING, M. J., MAKAROV, V., SCHOSCHINA, E., LORENZ, M. and LÜNING, K. (1996) Influence of ultraviolet-radiation on chlorophyll fluorescence and growth in different life-history stages of three species of *Laminaria* (Phaeophyta). Marine Biology 126: 183-191.

DRING, M. J., WAGNER, A., FRANKLIN, L. A., KUHLENKAMP, R. and LÜNING, K. (2001) Seasonal and diurnal variations in ultraviolet-B and ultraviolet-A irradiances at and below the sea surface at Helgoland (North Sea) over a 6-year period. Helgoland Marine Research 55: 3-11.

DUNTON, K. H. (1985) Growth of dark-exposed *Laminaria saccharina* (L.) Lamour. and *Laminaria solidungula* J. Ag. (Laminariales: Phaeophyta) in the Alaskan Beaufort Sea. Journal of Experimental Marine Biology and Ecology 94: 181-189.

DUNTON, K. H. (1990) Growth and production in *Laminaria solidungula*: relation to continuous underwater light levels in the Alaskan High Arctic. Marine Biology 106: 297-304.

DUNTON, K. H. and JODWALIS, C. M. (1988) Photosynthetic performance of *Laminaria solidungula* measured in situ in the Alaskan High Arctic. Marine Biology 98: 277-285.

DUNTON, K. H. and SCHELL, D. M. (1986) Seasonal carbon budget and growth of *Laminaria solidungula* in the Alaskan High Arctic. Marine Ecology Progress Series 31: 57-66.

DUNTON, K. H., REIMNITZ, E. and SCHONBERG, S. (1982) An Arctic kelp community in the Alaskan Beaufort Sea. Arctic 35: 465-484.

EGGERT, A. and WIENCKE, C. (2000) Adaptation and acclimation of growth and photosynthesis of five Antarctic red algae to low temperatures. Polar Biology 23: 609-618.

EILERS, P. H. C. and PEETERS, J. C. H. (1988) A model for the relationship between light-intensity and the rate of photosynthesis in phytoplankton. Ecological Modelling 42: 199-215.

EILERTSEN, H. C., TAASEN, J. P. and WESLAWSKI, J. M. (1989) Phytoplankton studies in the fjords of West Spitsbergen: physical environment and production in spring and summer. Journal of Plankton Research 11: 1245-1260.

EL NAGGAR, S., GUSTAT, H., MAGISTER, H. and ROCHLITZER, R. (1995) An electronic personal UV-B-dosimeter. Journal of Photochemistry and Photobiology B: Biology 31: 83-86.

ENRÍQUEZ, S., AGUSTI, S. and DUARTE, C. M. (1994) Light-absorption by marine macrophytes. Oecologia 98: 121-129.

FAIRHEAD, V. A. and CHESHIRE, A. C. (2004) Seasonal and depth related variation in the photosynthesis-irradiance response of *Ecklonia Radiata* (Phaeophyta, Laminariales) at West Island, South Australia. Marine Biology 145: 415-426.

FALKOWSKI, P. G. and LAROCHE, J. (1991) Acclimation to spectral irradiance in algae. Journal of Phycology 27: 8-14.

FALKOWSKI, P. G. and OWENS, T. G. (1980) Light-shade adaptation: two strategies in marine phytoplankton. Plant Physiology 66: 592-595.

FALKOWSKI, P. G. and RAVEN, J. A. (2007) Aquatic photosynthesis. 2nd edition. Princeton University Press, Princeton, Oxford.

FALKOWSKI, P. G., OWENS, T. G., LEY, A. C. and MAUZERALL, D. C. (1981) Effects of growth irradiance levels on the ratio of reaction centers in two species of marine phytoplankton. Plant Physiology 68: 969-973.

FARMAN, J. C., GARDINER, B. G. and SHANKLIN, J. D. (1985) Large losses of total ozone in Antarctica reveal seasonal ClOx/NOx interaction. Nature 315: 207-210.

FILLIT, M. (1995) Seasonal changes in the photosynthetic capacities and pigment content of *Ulva rigida* in a Mediterranean coastal lagoon. Botanica Marina 38: 271-280.

FLORES-MOYA, A., FERNANDÉZ, J. A. and NIELL, F. X. (1995) Seasonal variations of photosynthetic pigments, total C, N, and P content, and photosynthesis in *Phyllariopsis purpurascens* (Phaeophyta) from the Strait of Gibraltar. Journal of Phycology 31: 867-874.

FOTI, M., PIATTELLI, M., AMICO, V. and RUBERTO, G. (1994) Antioxidant activity of phenolic meroditerpenoids from marine algae. Journal of Photochemistry and Photobiology B: Biology 26: 159-164.

FOYER, C. H., LELANDAIS, M. and KUNERT, K. J. (1994) Photooxidative stress in plants. Physiologia Plantarum 92: 696-717.

FRANK, H. A., CUA, A., CHYNWAT V., YOUNG, A., GOSZTOLA, D. and WASIELEWSKI, M. R. (1994) Photophysics of the carotenoids associated with the xanthophyll cycle in photosynthesis. Photosynthesis Research 41: 389-395.

FRANKLIN, L. A. and FORSTER, R. M. (1997) The changing irradiance environment: consequences for marine macrophyte physiology, productivity and ecology. European Journal of Phycology 32: 207-232.

FRANKLIN, L. A., OSMOND, C. B. and LARKUM, A. W. D. (2003) Photoinhibition, UV-B and algal photosynthesis, pp 351-384. In: Larkum, A. W. D., Douglas, S. E. and Raven, J. A. (eds.), Photosynthesis in Algae. Advances in Photosynthesis and Respiration, vol 14. Kluwer Academic Publishers, Dordrecht, Boston, London.

FREDERSDORF, J., MÜLLER, R., BECKER, S., WIENCKE, C. and BISCHOF, K. (2009) Interactive effects of radiation, temperature and salinity on different life history stages of the Arctic kelp *Alaria esculenta* (Phaeophyceae). Oecologia 160: 483-492.

FRENETTE, J. J., DEMERS, S., LEGENDRE, L. and DODSON, J. (1993) Lack of agreement among models for estimating the photosynthetic parameters. Limnology and Oceanography 38: 679-687.

GENTY, B., BRIANTAIS, J. M. and BAKER, N. R. (1989) The relationship between the quantum yield of photosynthetic electron transport and quenching of chlorophyll fluorescence. Biochimica et Biophysica Acta, Bioenergetics 990: 87-92.

GERLAND, S., WINTHER, J.-G., ØRBÆBK, J. B. and IVANOV, B. V. (1999) Physical properties, spectral reflectance and thickness development of first year fast ice in Kongsfjorden, Svalbard. Polar Research 18: 275-282.

GÉVAERT, F., CREACH, A., DAVOULT, D., HOLL, A. C., SEURONT, L. and LEMOINE, Y. (2002) Photo-inhibition and seasonal photosynthetic performance of the seaweed *Laminaria saccharina* during a simulated tidal cycle: chlorophyll fluorescence measurements and pigment analysis. Plant Cell and Environment 25: 859-872.

GIBSON, J. A. E., VINCENT, W. F., NIEKE, B. and PIENITZ, R. (2000) Control of biological exposure to UV radiation in the Arctic Ocean: comparison of the roles of ozone and riverine dissolved organic matter. Arctic 53: 372-382.

GORDILLO, F. J. L., AGUILERA, J. and JIMENEZ, C. (2006) The response of nutrient assimilation and biochemical composition of Arctic seaweeds to a nutrient input in summer. Journal of Experimental Botany 57: 2661-2671.

GROSS, C., TÜG, H. and SCHREMS, O. (2001) Three years spectral resolved UV-measurements at Koldewey-Station 1997-1999. National Institute of Polar Research 113-123.

GÓMEZ, I. (2001) Ecophysiology of Antarctic macroalgae: effects of environmental light conditions on photosynthesis metabolism. Revista Chilena de Historia Natural 74: 251-271.

GÓMEZ, I. and WIENCKE, C. (1997) Seasonal growth and photosynthetic performance of the Antarctic macroalga *Desmarestia menziesii* (Phaeophyceae) cultivated under fluctuating Antarctic daylengths. Botanica Acta 110: 25-31.

GÓMEZ, I., WIENCKE, C. and WEYKAM, G. (1995) Seasonal photosynthetic characteristics of *Ascoseira mirabilis* (Ascoseirales, Phaeophyceae) from King George Island, Antarctica. Mar. Biol. 123: 167-172.

GÓMEZ, I., WEYKAM, G., KLÖSER, H. and WIENCKE, C. (1997) Photosynthetic light requirements, metabolic carbon balance and zonation of sublittoral macroalgae from King George Island (Antarctica). Marine Ecology Progress Series 148: 281-293.

GÓMEZ, I., LÓPEZ-FIGUEROA, F., ULLOA, N., MORALES, V., LOVENGREEN, C., HUOVINEN, P. and HESS, S. (2004) Patterns of photosynthesis in 18 species of intertidal macroalgae from Southern Chile. Marine Ecology Progress Series 270: 103-116.

HÄDER, D.-P. (1999) Photosynthese. Georg Thieme Verlag, Stuttgart, New York.

HÄDER, D.-P. and FIGUEROA, F. L. (1997) Photoecophysiology of marine macroalgae. Photochemistry and Photobiology 66: 1-14.

HAGER, A. and MEYER-BERTENRATH, T. (1966) Die Isolierung und quantitative Bestimmung der Carotinoide und Chlorophylle von Blättern, Algen und isolierten Chloroplasten mit Hilfe dünnschichtchromatographischer Methoden. Planta 69: 189-217.

HANELT, D. (1998) Capability of dynamic photoinhibition in Arctic macroalgae is related to their depth distribution. Marine Biology 131: 361-369.

HANELT, D. and NULTSCH, W. (1991) The role of chromatophore arrangement in protecting the chromatophores of the brown alga *Dictyota dichotoma* against photodamage. Journal of Plant Physiology 138: 470-475.

HANELT, D. and NULTSCH, W. (1995) Field studies of photoinhibition show non-correlations between oxygen and flourescence measurements in the Arctic red alga *Palmaria palmata*. Journal of Plant Physiology 145: 31-38.

HANELT, D., HUPPERTZ, K. and NULTSCH, W. (1992) Photoinhibition of photosynthesis and its recovery in red algae. Botanica Acta 105: 278-284.

HANELT, D., UHRMACHER, S. and NULTSCH, W. (1995) The effect of photoinhibition on photosynthetic oxygen production in the brown alga *Dictyota dichotoma*. Botanica Acta 108: 99-105.

HANELT, D., WIENCKE, C., KARSTEN, U. and NULTSCH, W. (1997a) Photoinhibition and recovery after high light stress in different developmental and life-history stages of *Laminaria saccharina* (Phaeophyta). Journal of Phycology 33: 387-395.

HANELT, D., WIENCKE, C. and NULTSCH, W. (1997b) Influence of UV radiation on the photosynthesis of Arctic macroalgae in the field. Journal of Photochemistry and Photobiology B: Biology 38: 40-47.

HANELT, D., MELCHERSHEIM, B., WIENCKE, C. and NULTSCH, W. (1997c) Effects of high light stress on photosynthesis of polar macroalgae in relation to depth distribution. Marine Ecology Progress Series 149: 255-266.

HANELT, D., TÜG, H., BISCHOF, K., GROSS, C., LIPPERT, H., SAWALL, T. and WIENCKE, C. (2001) Light regime in an Arctic fjord: a study related to stratospheric ozone depletion as a basis for determination of UV effects on algal growth. Marine Biology 138: 649-658.

HARKER, M., BERKALOFF, C., LEMOINE, Y., BRITTON, G., YOUNG, A. J., DUVAL, J. C., RMIKI, N. E. and ROUSSEAU, B. (1999) Effects of high light and desiccation on the operation of the xanthophyll cycle in two marine brown algae. European Journal of Phycology 34: 35-42.

HARRIS, N. R. P., KYRO, E., STAEHELIN, J., BRUNNER, D., ANDERSEN, S. B., GODIN-BEEKMANN, S., DHOMSE, S., HADJINICOLAOU, P., HANSEN, G., ISAKSEN, I., JRRAR, A., KARPETCHKO, A., KIVI, R., KNUDSEN, B., KRIZAN, P., LASTOVICKA, J., MAEDER, J., ORSOLINI, Y., PYLE, J. A., REX, M., VANICEK, K., WEBER, M., WOHLTMANN, I., ZANIS, P. and ZEREFOS, C. (2008) Ozone trends at northern mid- and high latitudes - a European perspective. Annales Geophysicae 26: 1207-1220.

HASSOL, S. J. (2005) ACIA – Der Arktis Klimareport. Convent Verlag, Hamburg

HAUGAN, J. A. and LIAAEN-JENSEN, S. (1989) Improved isolation procedure for fucoxanthin. Phytochemistry 28: 2797-2798.

HEALEY, F. P. (1972) Photosynthesis and respiration of some Arctic seaweeds. Phycologia 11: 267-271.

HENLEY, W. J. and DUNTON, K. H. (1995) A seasonal comparison of carbon, nitrogen, and pigment content in *Laminaria solidungula* and *L. saccharina* (Phaeophyta) in the Alaskan Arctic. Journal of Phycology 31: 325-331.

HENLEY, W. J. and RAMUS, J. (1989) Optimization of pigment content and the limits of photoacclimation for *Ulva rotundata* (Chlorophyta). Marine Biology 103: 267-274.

HENRY, B. E. and VAN ALSTYNE, K. L. (2004) Effects of UV radiation on growth and phlorotannins in *Fucus gardneri* (Phaeophyceae) juveniles and embryos. Journal of Phycology 40: 527-533.

HOP, H., PEARSON, T., HEGSETH, E. N., KOVACS, K. M., WIENCKE, C., KWASNIEWSKI, S., EIANE, K., MEHLUM, F., GULLIKSEN, B., WLODARSKA-KOWALEZUK, M., LYDERSEN, C., WESLAWSKI, J. M., COCHRANE, S., GABRIELSEN, G. W., LEAKEY, R. J. G., LONNE, O. J., ZAJACZKOWSKI, M., FALK-PETERSEN, S., KENDALL, M., WANGBERG, S. A., BISCHOF, K., VORONKOV, A. Y., KOVALTCHOUK, N. A., WIKTOR, J., POLTERMANN, M., DI PRISCO, G., PAPUCCI, C. and GERLAND, S. (2002) The marine ecosystem of Kongsfjorden, Svalbard. Polar Research 21: 167-208.

HORTON, P., RUBAN, A. V. and WALTERS, R. G. (1996) Regulation of light harvesting in green plants. Annual Review of Plant Physiology and Plant Molecular Biology 47: 655-684.

HSIAO, S. I. C. (1990) Photosynthesis of two Arctic intertidal seaweeds. Sarsia 75: 43-52.

ISLER, O., LINDLAR, H., MONTAVON, M., RÜEGG, R. and ZELLER, P. (1956) Synthesen in der Carotinoid-Reihe. 1. Mitteilung. Die technische Synthese von *β*-Carotin. Helvetica Chimica Acta 39: 249-259.

ITO, H. and KUDOH, S. (1997) Characteristics of water in Kongsfjorden, Svalbard. Proceedings of the NIPR Symposium in Polar Meteorology and Glaciology 11: 211-232.

IWANZIK, W., TEVINI, M., DOHNT, G., VOSS, M., WEISS, W., GRABER, P. and RENGER, G. (1983) Action of UV-B radiation on photosynthetic primary reactions in spinach chloroplasts. Physiologia Plantarum 58: 401-407.

JACKSON, G. A. and WINANT, C. D. (1983) Effect of a kelp forest on coastal currents. Continental Shelf Research 2: 75-80.

JANSEN, M. A. K., GREENBERG, B. M., EDELMAN, M., MATTOO, A. K. and GABA, V. (1996) Accelerated degradation of the D2 protein of photosystem II under ultraviolet radiation. Photochemistry and Photobiology 63: 814-817.

JEFFREY, S. W. (1972) Preparation and some properties of crystalline chlorophyll c_1 and c_2 from marine algae. Biochimica et Biophysica Acta 279: 15-33.

JEFFREY, S. W. and HUMPHREY, G. F. (1975) New spectrophotometric equations for determining chlorophylls a, b, c_1 and c_2 in higher plants, algae and natural phytoplankton. Biochemie und Physiologie der Pflanzen 167: 191-194.

JERLOV, N. G. (1976) Marine Optics. 2nd edition. In: Elsevier Oceanography Series, vol 14. Elsevier Scientific Publishing Company, Amsterdam, Oxford, New York.

JOHNSTON, C. S., JONES, R. G. and HUNT, R. D. (1977) A seasonal carbon budget for a laminarian population in a Scottish sea-loch. Helgoländer Wissenschaftliche Meeresuntersuchungen 30: 527-545.

JONES, B. L. and PORTER, J. W. (1986) Biosynthesis of carotenes in higher plants. Critical Reviews in Plant Sciences 3: 295-324.

JONES, L. W. and KOK, B. (1966) Photoinhibition of chloroplast reactions. I. Kinetics and action spectra. Plant Physiology 41: 1037-1043.

JORDAN, B. R., HE, J., CHOW, W. S. and ANDERSON, J. M. (1992) Changes in messenger-RNA levels and polypeptide subunits of ribulose 1,5-bisphosphate carboxylase in response to supplementary ultraviolet-B radiation. Plant Cell and Environment 15: 91-98.

KAIN, J. M. (1979) A view of the genus *Laminaria*. Oceanography and Marine Biology: an Annual Review 17: 101-161.

KAIN, J. M. (1989) The seasons in the subtidal. British Phycological Journal 24: 203-215.

KAIN, J. M. (2006) Photoperiodism in *Delesseria sanguinea* (Ceramiales, Rhodophyta). 2. Daylengths are shorter underwater. Phycologia 45: 624-631.

KARSTEN, U., BISCHOF, K. and WIENCKE, C. (2001) Photosynthetic performance of Arctic macroalgae after transplantation from deep to shallow waters. Oecologia 127: 11-20.

KENDALL, M. A. and ASCHAN, M. (1993) Latitudinal gradients in the structure of macorbenthic communities - a comparison of Arctic, temperate and tropical sites. Journal of Experimental Marine Biology and Ecology 172: 157-169.

KIM, S. T. and SANCAR, A. (1995) Photorepair of nonadjacent pyrimidine dimers by DNA photolyase. Photochemistry and Photobiology 61: 171-174.

KING, R. J. and SCHRAMM, W. (1976) Photosynthetic rates of benthic marine algae in relation to light intensity and seasonal variations. Marine Biology 37: 215-222.

KIRK, J. T. O. (1994) Light and photosynthesis in aquatic ecosystems. 2nd edition. Cambridge University Press, Cambridge.

KIRST, G. O. and WIENCKE, C. (1995) Ecophysiology of polar algae. Journal of Phycology 31: 181-199.

KONDRATJEV, K. Y. (1954) Radiant solar energy. [In Russ.] Leningrad. Cited after Dunton K. H. (1990)

KRAUSE, G. H. (1988) Photoinhibition of photosynthesis - an evaluation of damaging and protective mechanisms. Physiologia Plantarum 74: 566-574.

KRAUSE, G. H. and WEIS, E. (1991) Chlorophyll fluorescence and photosynthesis - the basics. Annual Review of Plant Physiology and Plant Molecular Biology 42: 313-349.

KREMER, B. P. (1984) Carbohydrate reserve and dark carbon fixation in the brown macroalga *Laminaria hyperborea*. Journal of Plant Physiology 117: 233-242.

KÜPPERS, U. and KREMER, B. P. (1978) Longitudinal profiles of carbon dioxide fixation capacities in marine macroalgae. Plant Physiol 62: 49-53.

KÜPPERS, U. and WEIDNER, M. (1980) Seasonal variation of enzyme activities in *Laminaria hyperborea*. Planta 148: 222-230.

LANE, C. E., MAYES, C., DRUEHL, L. D. and SAUNDERS, G. W. (2006) A multi-gene molecular investigation of the kelp (Laminariales, Phaeophyceae) supports a substantial taxonomic re-organization. Journal of Phycology 42: 493-512.

LAO, K. Q. and GLAZER, A. N. (1996) Ultraviolet-B photodestruction of a light-harvesting complex. Proceedings of the National Academy of Sciences of the United States of America 93: 5258-5263.

LEWEY, S. A. and GORHAM, J. (1984) Pigment composition and photosynthesis in *Sargassum muticum*. Marine Biology 80: 109-115.

LONG, S. P., HUMPHRIES, S. and FALKOWSKI, P. G. (1994) Photoinhibition of photosynthesis in nature. Annual Review of Plant Physiology and Plant Molecular Biology 45: 633-662.

LÜDER, U. H., KNOETZEL, J. and WIENCKE, C. (2001) Acclimation of photosynthesis and pigments to seasonally changing light conditions in the endemic Antarctic red macroalga *Palmaria decipiens*. Polar Biology 24: 598-603.

LÜNING, K. (1971) Seasonal growth of *Laminaria hyperborea* under recorded underwater light conditions near Helgoland, pp 347-361. In: Crisp, D.J. (ed.), Fourth European Marine Biology Symposium. Cambridge University Press, Cambridge.

LÜNING, K. (1979) Growth strategies of three *Laminaria* species (Phaeophytceae) inhabiting different depth zones in the sublittoral region of Helgoland (North Sea). Marine Ecology Progress Series 1: 195-207.

LÜNING, K. (1988) Photoperiodic control of sorus formation in the brown alga *Laminaria saccharina*. Marine Ecology Progess Series 45: 137-144.

LÜNING, K. (1990) Seaweeds. Their environment, biogeography, and ecophysiology. Yarish, C. and Kirkman, H. (eds.). John Wiley and Sons, New York, Chichester, Brisbane, Toronto, Singapore.

LÜNING, K. (1991) Circannual growth rhythm in a brown alga *Pterygophora californica*. Botanica Acta 104: 157-162.

LÜNING, K. (1994) Circadian growth rhythm in juvenile sporophytes of Laminariales (Phaeophyta). Journal of Phycology 30: 193-199.

LÜNING, K. and DRING, M. J. (1979) Continuous underwater light measurement near Helgoland (North Sea) and its significance for characteristic light limits in the sublittoral region. Helgoländer Meeresuntersuchungen 32: 403-424.

LÜNING, K. and KADEL, P. (1993) Daylength range for circannual rhythmicity in *Pterygophora californica* (Alariaceae, Phaeophyta) and synchronization of seasonal growth by daylength cycles in several other brown algae. Phycologia 32: 379-387.

LÜNING, K. and TOM DIECK, I. (1989) Environmental triggers in algal seasonality. Botanica Marina 32: 389-397.

LÜTZ, C., SEIDLITZ, H. K. and MEINDL, U. (1997) Physiological and structural changes in the chloroplast of the green alga *Micrasterias denticulata* induced by UV-B simulation. Plant Ecology 128: 54-64.

MACHALEK, K. M., DAVISON, I. R. and FALKOWSKI, P. G. (1996) Thermal acclimation and photoacclimation of photosynthesis in the brown alga *Laminaria saccharina*. Plant Cell and Environment 19: 1005-1016.

MACKERNESS, S. A. H., BUTT, P. J., JORDAN, B. R. and THOMAS, B. (1996) Amelioration of ultraviolet-B-induced down-regulation of mRNA levels for chloroplast proteins, by high irradiance, is mediated by photosynthesis. Journal of Plant Physiology 148: 100-106.

MADRONICH, S., MCKENZIE, R. L., BJÖRN, L. O. and CALDWELL, M. M. (1995) Changes in ultraviolet radiation reaching the Earth´s surface. Ambio 24: 143-152.

MAKAROV, V. N., MAKAROV, M. V. and SCHOSCHINA, E. V. (1999) Seasonal dynamics of growth in the Barents Sea seaweeds: endogenous and exogenous regulation. Botanica Marina 42: 43-49.

MALANGA, G. and PUNTARULO, S. (1995) Oxidative stress and antioxidant content in *Chlorella vulgaris* after exposure to ultraviolet-B radiation. Physiologia Plantarum 94: 672-679.

MARKAGER, S. (1993) Light-absorption and quantum yield for growth in 5 species of marine macroalgae. Journal of Phycology 29: 54-63.

MARKAGER, S. and SAND-JENSEN, K. (1992) Light requirements and depth zonation of marine macroalgae. Marine Ecology Progress Series 88: 83-92.

MARQUARDT, J. and HANELT, D. (2004) Carotenoid composition of *Delesseria lancifolia* and other marine red algae from polar and temperate habitats. European Journal of Phycology 39: 285-292.

MAUZERALL, D. and GREENBAUM, N. L. (1989) The absolute size of a photosynthetic unit. Biochimica et Biophysica Acta 974: 119-140.

MAYKUT, G. A. and GRENFELL, T. C. (1975) The spectral distribution of light beneath first-year ice in the Arctic Ocean. Limnology and Oceanography 20: 554-563.

MCGUINNESS, K. A. (2002) Of rowing boats, ocean liners and tests of the Anova homogeneity of variance assumption. Austral Ecology 27: 681-688.

MCKENZIE, R. L., AUCAMP, P. J., BAIS, A. F., BJORN, L. O. and ILYAS, M. (2007) Changes in biologically-active ultraviolet radiation reaching the Earth's surface. Photochemical and Photobiological Sciences 6: 218-231.

MCKINLEY A. F. and Diffey, B. L. (1987) A reference action spectrum for ultraviolet induced erythema in human skin. CIE Research Note, CIE-Journal 6: 17-22.

MEHLUM, F. (1991) Breeding population size of the common eider *Somateria mollissima* in Kongsfjorden, Svalbard, 1981-1987. Norsk Polarinstitut Skrifter 195: 21-29.

MORISON, J., AAGAARD, K. and STEELE, M. (2000) Recent environmental changes in the Arctic: a review. Arctic 53: 359-371.

MÁTÉ, Z., SASS, L., SZEKERES, M., VASS, I. and NAGY, F. (1998) UV-B-induced differential transcription of psbA genes encoding the D1 protein of photosystem II in the cyanobacterium *Synechocystis* 6803. Journal of Biological Chemistry 273: 17439-17444.

MÜLLER, P., LI, X. P. and NIYOGI, K. K. (2001) Non-photochemical quenching. A response to excess light energy. Plant Physiology 125: 1558-1566.

MÜLLER, R., CRUTZEN, P. J., GROOSS, J. U., BRÜHL, C., RUSSELL, J. M., GERNANDT, H., MCKENNA, D. S. and TUCK, A. F. (1997) Severe chemical ozone loss in the Arctic during the winter of 1995-96. Nature 389: 709-712.

NEALE, P. J., CULLEN, J. J., LESSER, M. P. and MELIS, A. (1993) Physiological bases for detecting and predicting photoinhibition of aquatic photosynthesis by PAR and UV radiation, pp 61-77. In: Yamamoto, H. Y. and Smith, C. M. (eds.), Photosynthetic responses to the environment. American Society of Plant Physiologists, Rockville, Maryland.

NIYOGI, K. K. (1999) Photoprotection revisited: genetic and molecular approaches. Annual Review of Plant Physiology and Plant Molecular Biology 50: 333-359.

NOGUÉS, S. and BAKER, N. R. (1995) Evaluation of the role of damage to photosystem II in the inhibition of CO_2 assimilation in pea leaves on exposure to UV-B radiation. Plant Cell and Environment 18: 781-787.

OLAIZOLA, M., LAROCHE, J., KOLBER, Z. and FALKOWSKI, P. G. (1994) Nonphotochemical fluorescence quenching and the diadinoxanthin cycle in a marine diatom. Photosynthesis Research 41: 357-370.

ØRBÆK, J. B., HISDAL, V. and SVAASAND, L. E. (1999) Radiation climate variability in Svalbard: surface and satellite observations. Polar Research 18: 127-134.

OSMOND, C. (1994) Photoinhibition of photosynthesis from molecular mechanisms to the field, pp 1-24. In: Baker, N. R. and Bowyer, J. R. (eds.), What is photoinhibition? Insights from comparisons of shade and sun plants. BIOS Scientific Publishers, Oxford.

PALMISANO, A. C., SOOHOO, J. B., MOE, R. L. and SULLIVAN, C. W. (1987) Sea ice microbial communities. VII. Changes in under-ice spectral irradiance during the development of Antarctic sea ice microalgal communities. Marine Ecology Progress Series 35: 165-173.

PARK, Y. I., CHOW, W. S., ANDERSON, J. M. and HURRY, V. M. (1996) Differential susceptibility of photosystem II to light stress in light-acclimated pea leaves depends on the capacity for photochemical and non-radiative dissipation of light. Plant Science 115: 137-149.

PARKINSON, C. L., CAVALIERI, D. J., GLOERSEN, P., ZWALLY, H. J. and COMISO, J. C. (1999) Arctic sea ice extents, areas, and trends, 1978-1996. Journal of Geophysical Research 104: 20837-20856.

PASSAQUET, C., THOMAS, J. C., CARON, L., HAUSWIRTH, N., PUEL, F. and BERKULOFF, C. (1991) Light-harvesting complexes of brown algae. Biochemical characterization and immunological relationships. FEBS Letters 280: 21-26.

PAVIA, H. and BROCK, E. (2000) Extrinsic factors influencing phlorotannin production in the brown alga *Ascophyllum nodosum*. Marine Ecology Progress Series 193: 285-294.

PAVIA, H., CERVIN, G., LINDGREN, A. and ABERG, P. (1997) Effects of UV-B radiation and simulated herbivory on phlorotannins in the brown alga *Ascophyllum nodosum*. Marine Ecology Progress Series 157: 139-146.

PETERS, K. J., AMSLER, C. D., AMSLER, M. O., MCCLINTOCK, J. B., DUNBAR, R. B. and BAKER, B. J. (2005) A comparative analysis of the nutritional and elemental composition of macroalgae from the western Antarctic peninsula. Phycologia 44: 453-463.

PFANNSCHMIDT, T., NILSSON, A. and ALLEN, J. F. (1999) Photosynthetic control of chloroplast gene expression. Nature 397: 625-628.

PFANNSCHMIDT, T., SCHUTZE, K., BROST, M. and OELMULLER, R. (2001) A novel mechanism of nuclear photosynthesis gene regulation by redox signals from the chloroplast during photosystem stoichiometry adjustment. Journal of Biological Chemistry 276: 36125-36130.

POWLES, S. B. (1984) Photoinhibition of photosynthesis induced by visible light. Annual Review of Plant Physiology 35: 15-44.

QUAIL, P. H. (2002) Photosensory perception and signalling in plant cells: new paradigms? Current Opinion in Cell Biology 14: 180-188.

RAGAN, M. A. and GLOMBITZA, K. W. (1986) Phlorotannins, brown algal polyphenols. Progress in Phycological Research 4: 129-241.

RAMUS, J. (1978) Seaweed anatomy and photosynthetic performance: the ecological significance of light guides, heterogeneous absorption and multiple scatter. Journal of Phycology 14: 352-362.

RAMUS, J. (1990) A form-function analysis of photon capture for seaweeds. Hydrobiologia 204: 65-71.

RAMUS, J., BEALE, S. I., MAUZERALL, D. and HOWARD, K. L. (1976a) Changes in photosynthetic pigment concentration in seaweeds as a function of water depth. Marine Biology 37: 223-229.

RAMUS, J., BEALE, S. I. and MAUZERALL, D. (1976b) Correlation of changes in pigment content with photosynthetic capacity of seaweeds as a function of water depth. Marine Biology 37: 231-238.

RAMUS, J., LEMONS, F. and ZIMMERMANN, C. (1977) Adaptation of light-harvesting pigments to downwelling light and the consequent photosynthetic performance of the eulittoral rockweeds *Ascophyllum nodosum* and *Fucus vesiculosus*. Marine Biology 42: 293-303.

RAVEN, J. A. (1984) A cost-benefit analysis of photon absorption by photosynthetic unicells. New Phytologist 98: 593-625.

RAVEN, J. A. and GEIDER, R. J. (2003) Adaptation, acclimation and regulation in algal photosynthesis, pp 385-412. In: Larkum, A. W. D., Douglas, S. E. and Raven, J. A. (eds.), Photosynthesis in Algae. Advances in Photosynthesis and Respiration, vol 14. Kluwer Academic Publishers, Dordrecht, Boston, London.

RENGER, G., VÖLKER, M., ECKERT, H. J., FROMME, R., HOHMVEIT, S. and GRÄBER, P. (1989) On the mechanism of photosystem II deterioration by UV-B irradiation. Photochemistry and Photobiology 49: 97-105.

REX, M., HARRIS, N. R. P., VON DER GATHEN, P., LEHMANN, R., BRAATHEN, G. O., REIMER, E., BECK, A., CHIPPERFIELD, M. P., ALFIER, R., ALLAART, M., OCONNOR, F., DIER, H., DOROKHOV, V., FAST, H., GIL, M., KYRO, E., LITYNSKA, Z., MIKKELSEN, I. S., MOLYNEUX, M. G., NAKANE, H., NOTHOLT, J., RUMMUKAINEN, M., VIATTE, P. and WENGER, J. (1997) Prolonged stratospheric ozone loss in the 1995-96 Arctic winter. Nature 389: 835-838.

REX, M., SALAWITCH, R. J., DECKELMANN, H., VON DER GATHEN, P., HARRIS, N. R. P., CHIPPERFIELD, M. P., NAUJOKAT, B., REIMER, E., ALLAART, M., ANDERSEN, S. B., BEVILACQUA, R., BRAATHEN, G. O., CLAUDE, H., DAVIES, J., DE BACKER, H., DIER, H., DOROKHOV, V., FAST, H., GERDING, M., GODIN-BEEKMANN, S., HOPPEL, K., JOHNSON, B., KYRO, E., LITYNSKA, Z., MOORE, D., NAKANE, H., PARRONDO, M. C., RISLEY, A. D., SKRIVANKOVA, P., STUBI, R., VIATTE, P., YUSHKOV, V. and ZEREFOS, C. (2006) Arctic winter 2005: implications for stratospheric ozone loss and climate change. Geophysical Research Letters 33: L23808

RIGOR, I. G., COLONY, R. L. and MARTIN, S. (2000) Variations in surface air temperature observations in the Arctic, 1979-97. Journal of Climate 13: 896-914.

RIJSTENBIL, J. W., COELHO, S. M. and EIJSACKERS, M. (2000) A method for the assessment of light-induced oxidative stress in embryos of fucoid algae via confocal laserscan microscopy. Marine Biology 137: 763-774.

RODRIGUES, M. A., DOS SANTOS, C. P., YONESHIGUE-VALENTIN, Y., STRBAC, D. and HALL, D. O. (2000) Photosynthetic light-response curves and photoinhibition of the deep-water *Laminaria abyssalis* and the intertidal *Laminaria digitata* (Phaeophyceae). Journal of Phycology 36: 97-106.

RODRIGUES, M. A., DOS SANTOS, C. P., YOUNG, A. J., STRBAC, D. and HALL, D. O. (2002) A smaller and impaired xanthophyll cycle makes the deep sea macroalgae *Laminaria abyssalis* (Phaeophyceae) highly sensitive to daylight when compared with shallow water *Laminaria digitata.* Journal of Phycology 38: 939-947.

ROEDER, V., COLLÉN, J., ROUSVOAL, S., CORRE, E., LEBLANC, C. and BOYEN, C. (2005) Identification of stress sene transcripts in *Laminaria digitata* (Phaeophyceae) protoplast cultures by expressed sequence tag analysis. Journal of Phycology 41: 1227-1235.

ROLEDA, M. Y., CLAYTON, M. N. and WIENCKE, C. (2006a) Screening capacity of UV-absorbing compounds in spores of Arctic Laminariales. Journal of Experimental Marine Biology and Ecology 338: 123-133.

ROLEDA, M. Y., WIENCKE, C. and HANELT, D. (2006b) Thallus morphology and optical characteristics affect growth and DNA damage by UV radiation in juvenile Arctic *Laminaria* sporophytes. Planta 223: 407-417.

ROSENBERG, G. and RAMUS, J. (1982) Ecological growth strategies in the seaweeds *Gracilaria foliifera* (Rhodophyceae) and *Ulva* sp. (Chlorophyceae): photosynthesis and antenna composition. Marine Ecology Progress Series 8: 233-241.

ROWLAND, F. S. (2006) Stratospheric ozone depletion. Philosophical Transactions of the Royal Society B: Biological Sciences 361: 769-790.

ROY, C. R., GIES, H. P. and ELLIOTT, G. (1990) Ozone depletion. Nature 347: 235-236.

RUNCIE, J. W. and RIDDLE, M. J. (2006) Photosynthesis of marine macroalgae in ice-covered and ice-free environments in East Antarctica. European Journal of Phycology 41: 223-233.

RYSGAARD, S., ARENDT, K., FREDERIKSEN, M. S., EGEVANG, C., LABANSEN, A., MORTENSEN, J., SIMON, M., PEDERSEN, L. T., WITTING, L., BERGSTROM , B. and MIKKELSEN, D. M. (2008) Nuuk Basic: The Marine Basic Program 2005-2006, pp 38-73. In: Jensen, L. M. and Rasch, M. (eds.), Nuuk Ecological Research Operations, 1st Annual Report, 2007. Danish Polar Center, Danish Agency for Science, Technology and Innovation, Ministry of Science, Technology and Innovation, Copenhagen.

SAKSHAUG, E. and SLAGSTAD, D. (1991) Light and productivity of phytoplankton in polar marine ecosystems: a physiological view. Polar Research 10: 69-86.

SAROUSSI, S. and BEER, S. (2007) Alpha and quantum yield of aquatic plants derived from PAM fluorometry: uses and misuses. Aquatic Botany 86: 89-92.

SAVITCH, L. V., MASSACCI, A., GRAY, G. R. and HUNER, N. P. A. (2000) Acclimation to low temperature or high light mitigates sensitivity to photoinhibition: roles of the Calvin cycle and the Mehler reaction. Australian Journal of Plant Physiology 27: 253-264.

SCHAEFFELKE, B. and LÜNING, K. (1994) A circannual rythm controls seasonal growth in the kelps *Laminaria hyperbore*a and *L. digitata* from Helgoland. European Journal of Phycology 29: 49-56.

SCHIEL, D. R. and FOSTER, M. S. (2006) The population biology of large brown seaweeds: ecological consequences of multiphase life histories in dynamic coastal environments. Annual Review of Ecology Evolution and Systematics 37: 343-372.

SCHIERMEIER, Q. (2007) Chemists poke holes in ozone theory. Nature 449: 382-383.

SCHOENWAELDER, M. E. A. (2002a) The occurrence and cellular significance of physodes in brown algae. Phycologia 41: 125-139.

SCHOENWAELDER, M. E. A. (2002b) Physode distribution and the effect of 'thallus sunburn' in *Hormosira banksii* (Fucales, Phaeophyceae). Botanica Marina 45: 262-266.

SCHOENWAELDER, M. E. A. and WIENCKE, C. (2000) Phenolic compounds in the embryo development of several Northern Hemisphere fucoids. Plant Biology 2: 24-33.

SCHOFIELD, O., KROON, B. M. A. and PREZELIN, B. B. (1995) Impact of ultraviolet-B radiation on photosystem II activity and its relationship to the inhibition of carbon fixation rates for Antarctic ice algae communities. Journal of Phycology 31: 703-715.

SCHOFIELD, O., EVENS, T. J. and MILLIE, D. F. (1998) Photosystem II quantum yields and xanthophyll-cycle pigments of the macroalga *Sargassum natans* (Phaeophyceae): responses under natural sunlight. Journal of Phycology 34: 104-112.

SCHREIBER, U., BILGER, W. and NEUBAUER, C. (1994) Ecophysiology of photosynthesis, pp 49-70. In: Schulze, E.-D. and Caldwell, M. M. (eds.), Chlorophyll fluorescence as a non-intrusive indicator for rapid assessment of in vivo photosynthesis. Ecological studies: analysis and synthesis, vol 100. Axel Springer Verlag, Heidelberg.

SCOUT-O3 (2005) Press release 25 April 2005. This report is available on the World Wide Web at http://ec.europa.eu/research/environment/pdf/press-release-apr-2005.pdf

SEJR, M. K., RYSGAARD, S., MIKKELSEN, D., FREDERIKSEN, M., FRANDSEN, E. R., LENNERT, K. and JUUL-PEDERSEN, T. (2008) Zackenberg Basic: The MarinBasic programme, pp 57-69. In: Jensen, L. M. and Rasch, M. (eds.), Zackenberg Ecological Research Operations, 13th Annual Report, 2007. Danish Polar Center, Danish Agency for Science, Technology and Innovation, Ministry of Science, Technology and Innovation, Copenhagen.

SHINDELL, D. T., RIND, D. and LONERGAN, P. (1998) Increased polar stratospheric ozone losses and delayed eventual recovery owing to increasing greenhouse-gas concentrations. Nature 392: 589-592.

SILVA, J., SANTOS, R., SERODIO, J. and MELO, R. A. (1998) Light response curves for *Gelidium sesquipedale* from different depths, determined by two methods: O_2 evolution and chlorophyll fluorescence. Journal of Applied Phycology 10: 295-301.

SMITH, S. V. (1981) Marine macrophytes as a global carbon sink. Science 211: 838-840.

SOKAL, R. R. and ROHLF, F. J. (1981) Biometry. The principles and practice of statistics in biological research. 2nd edition. W. H. Freeman and Company, San Francisco.

SOLOMON, S., QIN, D., MANNIN, M., CHEN, Z., MARQUIS, M., AVERYT, K. B., TIGNOR, M. and MILLER, H. L. (2007) Climate Change 2007: The Physical Science Basis. Contribution of Working Group I to the Fourth Assessment Report of the Intergovernmental Panel on Climate Change (IPPC). Cambridge University Press, Cambridge, New York. This report is available on the World Wide Web at http://www.ipcc.ch/ipccreports/ar4-wg1.htm

STENECK, R. S., GRAHAM, M. H., BOURQUE, B. J., CORBETT, D., ERLANDSON, J. M., ESTES, J. A. and TEGNER, M. J. (2002) Kelp forest ecosystems: biodiversity, stability, resilience and future. Environmental Conservation 29: 436-459.

STENGEL, D. B. and DRING, M. J. (1998) Seasonal variation in the pigment content and photosynthesis of different thallus regions of *Ascophyllum nodosum* (Fucales, Phaeophyta) in relation to position in the canopy. Phycologia 37: 259-268.

STRAIN, H. H. (1938) Leaf xanthophylls. Carnegie Institution of Washington, Washington D.C.

STRID, A., CHOW, W. S. and ANDERSON, J. M. (1990) Effects of supplementary ultraviolet-B radiation on photosynthesis in *Pisum sativum*. Biochimica et Biophysica Acta 1020: 260-268.

STRID, A., CHOW, W. S. and ANDERSON, J. M. (1994) UV-B damage and protection at the molecular level in plants. Photosynthesis Research 39: 475-489.

STROEVE, J. C., SERREZE, M. C., FETTERER, F., ARBETTER, T., MEIER, W., MASLANIK, J. and KNOWLES, K. (2005) Tracking the Arctic's shrinking ice cover: another extreme September minimum in 2004. Geophysical Research Letters 32: L04501.

STROEVE, J., HOLLAND, M. M., MEIER, W., SCAMBOS, T. and SERREZE, M. (2007) Arctic sea ice decline: faster than forecast. Geophysical Research Letters 34: L09501

SUKENIK, A., BENNETT, J. and FALKOWSKI, P. (1987) Light-saturated photosynthesis - limitation by electron-transport or carbon fixation. Biochimica et Biophysica Acta 891: 205-215.

SUNDBY, C. and ANDERSSON, B. (1985) Temperature-induced reversible migration along the thylakoid membrane of photosystem II regulates it association with LHC-II. FEBS Letters 191: 24-28.

SVENDSEN, H., BESZCZYNSKA-MOLLER, A., HAGEN, J. O., LEFAUCONNIER, B., TVERBERG, V., GERLAND, S., ØRBÆK, J. B., BISCHOF, K., PAPUCCI, C., ZAJACZKOWSKI, M., AZZOLINI, R., BRULAND, O., WIENCKE, C., WINTHER, J. G. and DALLMANN, W. (2002) The physical environment of Kongsfjorden-Krossfjorden, an Arctic fjord system in Svalbard. Polar Research 21: 133-166.

SWANSON, A. K. and DRUEHL, L. D. (2002) Induction, exudation and the UV protective role of kelp phlorotannins. Aquatic Botany 73: 241-253.

SWANSON, A. K. and FOX, C. H. (2007) Altered kelp (Laminariales) phlorotannins and growth under elevated carbon dioxide and ultraviolet-B treatments can influence associated intertidal food webs. Global Change Biology 13: 1696-1709.

TARGETT, N. M. and ARNOLD, T. M. (1998) Predicting the effects of brown algal phlorotannins on marine herbivores in tropical and temperate oceans. Journal of Phycology 34: 195-205.

TEDETTI, M. and SÉMPERÉ, R. (2006) Penetration of ultraviolet radiation in the marine environment. A review. Photochemistry and Photobiology 82: 389-397.

TILMES, S., MÜLLER, R. and SALAWITCH, R. (2008) The sensitivity of polar ozone depletion to proposed geoengineering schemes. Science 320: 1201-1204.

THAYER, S. S. and BJÖRKMAN, O. (1990) Leaf xanthophyll content and composition in sun and shade determined by HPLC. Photosynthesis Research 23: 331-343.

TOM DIECK, I. (1991) Circannual growht rhythm and photoperiodic sorus induction in the kelp *Laminaria setchellii* (Phaeophyta). Journal of Phycology 27: 341-350.

TRISSL, H.-W. (2003) Modelling the excitation energy capture in thylakoid membranes, pp 245–276. In: Larkum, A. W. D., Douglas, S. E. and Raven, J. A. (eds.), Photosynthesis in Algae. Advances in Photosynthesis and Respiration, vol 14. Kluwer Academic Publishers, Dordrecht, Boston, London.

TYYSTJÄRVI, E., ALI-YRKKÖ, K., KETTUNEN, R. and ARO E. (1992) Slow degradation of the D1 protein is related to the susceptibility of low-light-grown pumpkin plants to photoinhibition. Plant Physiology 100: 1310-1317.

UHRMACHER, S., HANELT, D. and NULTSCH, W. (1995) Zeaxanthin content and the degree of photoinhibition are linearly correlated in the brown alga *Dictyota dichotoma*. Marine Biology 123: 159-165.

UNDERWOOD, A. J. (1997) Experiments in ecology: their logical design and interpretation using analysis of variance. Cambridge University Press, Cambridge

VAN DE POLL, W. H., EGGERT, A., BUMA, A. G. J. and BREEMAN, A. M. (2001) Effects of UV-B-induced DNA damage and photoinhibition on growth of temperate marine red macrophytes: habitat-related differences in UV-B tolerance. Journal of Phycology 37: 30-37.

VASS, I., KIRILOVSKY, D. and ETIENNE, A. L. (1999) UV-B radiation-induced donor- and acceptor-side modifications of photosystem II in the cyanobacterium *Synechocystis sp.* PCC 6803. Biochemistry 38: 12786-12794.

VINNIKOV, K. Y., ROBOCK, A., STOUFFER, R. J., WALSH, J. E., PARKINSON, C. L., CAVALIERI, D. J. , MITCHELL, J. F. B., GARRETT, D. and ZAKHAROV, V. F. (1999) Global warming and Northern Hemisphere sea ice extent. Science 286: 1934-1937.

WALKER D. (1992) Excited leaves. New Phytologist 121: 325-345.

WALTERS, R. G. (2005) Towards an understanding of photosynthetic acclimation. Journal of Experimental Botany 56: 435-447.

WEATHERHEAD, E. C. and ANDERSEN, S. B. (2006) The search for signs of recovery of the ozone layer. Nature 441: 39-45.

WEYKAM, G., GÓMEZ, I., WIENCKE, C., IKEN, K. and KLÖSER, H. (1996) Photosynthetic characteristics and C:N ratios of macroalgae from King George Island (Antarctica). Journal of Experimental Marine Biology and Ecology 204: 1-22.

WHEELER, P. A. and NORTH, W. J. (1981) Nitrogen supply, tissue composition and frond growth rates for *Macrocystis pyrifera* off the coast of Southern California. Marine Biology 64: 59-69.

WIENCKE, C. (1990) Seasonality of brown macroalgae from Antarctica: a long-term culture study under fluctuating Antarctic daylengths. Polar Biology 10: 589-600.

WIENCKE, C., RAHMEL, J., KARSTEN, U., WEYKAM, G. and KIRST, G. O. (1993) Photosynthesis of marine macroalga from Antarctica: Light and temperature requirements. Botanica Acta 106: 78-87.

WIENCKE, C., BARTSCH, I., BISCHOF, K., PETERS, A. F. and BREEMAN, A. M. (1994) Temperature requirements and biogeography of Antarctic, Arctic and amphiequatorial seaweeds. Botanica Marina 37: 247-259.

WIENCKE, C., VÖGELE, B., KOVALTCHOUK, N. and HOP, H. (2004a) Species composition and zonation of marine benthic macroalgae at Hansneset in Kongsfjorden, Svalbard, pp 55-62. In: Wiencke, C. (ed.), The coastal ecosystem of Kongsfjorden, Svalbard. Synopsis of biological research performed at the Koldewey Station in the years 1991-2003. Reports on Polar and Marine Research, vol 492. Alfred Wegener Institute for Polar and Marine Research, Bremerhaven.

WIENCKE, C., CLAYTON, M. N. and SCHOENWAELDER, M. (2004b) Sensitivity and acclimation to UV radiation of zoospores from five species of Laminariales from the Arctic. Marine Biology 145: 31-39.

WIENCKE, C., CLAYTON, M. N., GÓMEZ, I., IKEN, K., LÜDER, U. H., AMSLER, C. D., KARSTEN, U., HANELT, D., BISCHOF, K. and DUNTON, K. (2006) Life strategy, ecophysiology and ecology of seaweeds in polar waters. Reviews in Environmental Science and Biotechnology 6: 95-126.

WISE, R. R. and NAYLOR, A. W. (1987) Chilling-enhanced photooxidation. Evidence for the role of singlet oxygen and superoxide in the breakdown of pigments and endogenous antioxidants. Plant Physiology 83: 278-282.

WOOD, W. F. (1987) Effect of solar ultraviolet radiation on the kelp *Ecklonia radiata*. Marine Biology 96: 143-150.

WORLD METEOROLOGICAL ORGANIZATION (2007) Scientific Assessment of Ozone Depletion: 2006. Global Ozone Research and Monitoring Project - Report No. 50. World Meterological organization, Geneva. This report is available on the World Wide Web at http://ozone.unep.org/Assessment_Panels/SAP/Scientific_Assessment_2006/index.asp

YOUNG, A. J. (1991) The photoprotective role of carotenoids in higher plants. Physiologia Plantarum 83: 702-708.

Acknowledgements

It is a pleasure to thank the many people who supported my work in numerous ways:

First of all, I wish to express my warm and sincere thanks to my supervisor Prof. Dr. Christian Wiencke for his continuous and solid support giving me the opportunity to accomplish my research work.

I am also especially grateful to Prof. Dr. Kai Bischof for supervising my work and for his valuable advices, friendly help and encouragement.

I warmly thank Dr. Ralf Rautenberger for thorough proofreading and constructive comments.

I am very grateful to Dr. Jürgen Marquardt for the productive collaboration during establishing the HPLC protocols and for sharing his technical know-how with me.

Dr. Nelson Valdivia and Dr. Katharina Zacher are thanked for their valuable comments on statistical analysis.

I wish to thank the scientific diving team for seaweed collection and technical assistance with the underwater light measurements as well as the staff at the AWIPEV Arctic Research Base and Kings Bay AS at Ny-Ålesund for facilitating a comfortable working environment.

All colleagues and friends are thanked for the great time I had, for the numerous stimulating discussions, for the help with the experimental setup, for general advices and great encouragement.

I also thank Dr. Sigrid Wuttke and Siegrid Debatin for providing the data on surface UVR and air temperature.

Lastly, and most importantly, I wish to thank my family for their faith, loving care, and encouragement when it was needed most. To them I dedicate this thesis.

Funding by the Helmholtz Society of German Research Centers (Project VH-NG-059) is gratefully acknowledged.